Thymic interferons and protein O-GlcNAcylation in regulatory T cells: two tales of T cell tolerance

A DISSERTATION
SUBMITTED TO THE FACULTY OF THE
UNIVERSITY OF MINNESOTA
BY

Oscar Camilo Salgado Barrero

IN PARTIAL FULFILLMENT OF THE REQUIREMENTS
FOR THE DEGREE OF
DOCTOR OF PHILOSOPHY

Advisor: Kristin Ann Hogquist, Ph.D.

MARCH 2021

Acknowledgements

I am truly grateful to so many people that participated in these research projects and to all the people that supported me to get to this point.

Thank you to all members of the Hogquist, Jameson, and Hamilton-Hart labs for creating a comfortable and supportive work environment. The same is true to all the members of the Center for Immunology, a place where collaboration meets excellence. Chapter 2 of this thesis was a collaborative endeavor with the lab of Dr. Hai-Bin Ruan. I am very thankful to him and Dr. Bing Liu for their commitment and support to this exciting research project.

Special thanks to my thesis committee members, Dr. Bryce Binstadt, Dr. Vaiva Vezys and Dr. Ryan Langlois for their discussions, suggestions and encouragement during all these years. Thank you Dr. Juan Abrahante Lloréns for his bioinformatic analyses.

I want to thank all the members of the MICaB program, especially the DGSs Dr. Steve Jameson and Dr. Wade Bresnahan for all their work to make this a wonderful training environment. And I would like to thank Louise Shand and Megan Ruf for all their amazing work to make sure that everything runs smoothly and for their support.

I am extremely grateful to the most wonderful of all advisors, Kris Hogquist. Her decision to welcome me to her lab has changed my life and I am happy she gave me this opportunity to grow as a scientist and as a person. Week after week she instilled her optimism and curiosity in me, lifted me up during rough moments, and always treated me with the highest respect and kindness. Every day I strive to be better, a strive to be a bit more like her.

I'm eternally grateful to my parents, who under every circumstance put our well-being on top of their priorities and provided us with the most amazing and loving environment.

Finally, to the person who I had the fortune to team up with for this journey of life, Andrea. My wife has been next to me since the day this doctorate project was only an idea. Ever since, she has been encouraging and motivating me to continue and to give my best every single day, even when difficulties arose. This has been a very challenging life project and I could not have made it without her continuous support and love. As our projects together and our family grows, I feel lucky and happy to have her by my side.

Abstract

Immune tolerance mechanisms prevent the development of immune responses directed to the host. This is especially important for the adaptive immune system, whose potent and long-lasting responses would be extremely deleterious to the host if misguided. This work explores two aspects of immune tolerance: the role of protein O-GlcNAcylation in regulatory T (Treg) cells and the importance of interferons during T cell tolerance development in the thymus.

In chapter 2 of this document, we show that the posttranslational modification by O-linked N-Acetylglucosamine (O-GlcNAc) stabilizes FOXP3 and activates STAT5, thus integrating these critical signaling pathways. O-GlcNAc-deficient Treg cells developed normally but displayed modestly reduced FOXP3 expression, strongly impaired lineage stability and effector function, and ultimately fatal autoimmunity in mice. Moreover, deficiency in protein O-GlcNAcylation attenuated IL-2/STAT5 signaling, while overexpression of a constitutively active form of STAT5 partially ameliorated Treg cell dysfunction and systemic inflammation in O-GlcNAc deficient mice. These data demonstrate that protein O-GlcNAcylation is essential for lineage stability and effector function in Treg cells.

In chapter 3, we characterize the expression of interferons in the thymus. We found that developing thymocytes displayed a type I IFN signature that was mainly dependent on IFN-β. Using *Ifnb* tdtomato and luciferase reporter mouse strains, we found expression in a small population of medullary thymic epithelial cells (mTEC), which was AIRE dependent and peaked at 2-3 weeks of age. To study the cellular response to thymic interferon, we used an *Mx1*^{gfp} reporter mouse strain and report that numerous thymic cell populations respond constitutively to IFN *in vivo*. The response in some cell populations was not abrogated unless both IFNαR and IFNλR, or STAT1 were deficient, suggesting that both type I and type III IFNs are at play. Indeed, single cell RNA sequencing analysis revealed dramatic transcriptional changes in all thymic APCs in IFNαR/ IFNλR deficient mice. These results show that steady state type I and type III IFN signaling drives a gene-expression program in thymic APCs that shapes the thymic microenvironment.

Table of Contents

List of Figures

Chapter 1 Introduction

1.1 T cell tolerance

The immune system provides a powerful defense against infections and cancer. However, there are mechanisms of immune tolerance in place to prevent immune responses against the body's own cells. When these mechanisms fail, disorders like autoimmune diseases may develop.

In vertebrates, which have a highly specific adaptive immune system, immune tolerance mechanisms are complex and involve the control of lymphocyte responses against healthy host cells. The expression of antigen receptors - which are randomly generated by recombination - in lymphocytes represents a particular challenge for the development of tolerance by the adaptive immune system. Specifically in T lymphocytes, the somatic gene rearrangements of T-cell antigen receptors (TCRs) afford protection against a vast number of pathogens but also generate some TCRs that are either useless or have the potential to recognize self-antigens. Tolerance mechanisms ensure that potentially autoreactive TCRs do not cause any damage.

T cell tolerance guarantees that the T cell repertoire remains unresponsive to every self-antigen expressed in the body. This includes not only ubiquitously expressed self-antigens but also self-antigens that have different expression patterns. For instance, tolerance should develop to self-antigens that are normally expressed in specific peripheral tissues, or during a specific stage of the development of the organism, or during transient processes like inflammation or tissue repair.

When T cell tolerance mechanisms operate during T cell development in the thymus they are referred to as "central tolerance, whereas if they occur during circulation on mature T cells, they are termed "peripheral tolerance".

1.1.1 Central Tolerance

T cell progenitors develop in the bone marrow and migrate to the thymus, where they randomly rearrange their TCR α and β genes. Once expressing a functional TCR on their surface, CD4 and CD8 double-positive (DP) thymocytes interact with self-peptide-major histocompatibility complexes (MHC) displayed on cortical thymic

epithelial cells (cTEC). If there is a low-affinity interaction, thymocytes receive survival signals and differentiate into CD4- and CD8-single positive (SP) cells – a process known as positive selection [1].

1.1.1.1 Clonal Deletion

Thymocytes with TCRs that interact strongly with self-peptide-MHC complexes are potentially autoreactive and could cause damage if allowed in the periphery, thus many of these clones are removed from the repertoire through a mechanism known as clonal deletion, whereby cell death is induced by apoptosis. Most deletion events take place in the cortex at the DP stage, and during the SP stage, thymocytes migrate to the medullary region, where their interactions with an extensive network of different antigen-presenting cells (APCs) can also result in clonal deletion [2].

Among the APCs that mediate clonal deletion, medullary thymic epithelial cells (mTEC) are critical. This is because of their exceptional capacity to express tissue-restricted antigens (TRAs), a process mediated mainly by specialized transcriptional factors such as the autoimmune regulator (AIRE) [3] and Fezf2 [4].
Dendritic cells (DC) also mediate clonal deletion in the thymus [5]. Three main subsets of thymic DCs have been described: plasmacytoid DC (pDCs), XCR1+ cDC1, and SIRPα+ cDC2 [6]. The relative contribution of DCs to clonal deletion is large since they are distributed both in the cortex and the medulla, can “cross present” antigens, and express high amounts of co-stimulatory molecules.

Thymic B cells, located mainly in the medulla and the cortico-medullary region, have also been shown to contribute to clonal deletion [7–9]. They express high amounts of MHC and co-stimulatory molecules, which likely results in a greater ability to present antigens. Some thymic B cells also express Aire [10], which allows them to present a diverse set of self-antigens, while others present antigens that have been acquired with their B cell receptor (BCR) [11].

Although numerous thymic APCs can mediate clonal deletion, not all self-reactive T cell clones are removed from the repertoire. Some of these T cells with autoreactive potential can differentiate into regulatory T (Treg) cells, which mediate tolerance mainly through the suppression of other cells. The factors that determine

whether a self-reactive T cell clone is deleted or becomes a Treg cell are complex and will be discussed below.

1.1.1.2 Regulatory T cell differentiation

Recognition of self-antigens during T cell development can also result in the differentiation of forkhead box protein P3 $(FOXP3)^+$ Treg cells. Treg cells are essential to maintaining immune tolerance and homeostasis [12,13]. As opposed to the cell-intrinsic recessive tolerance mediated by mechanisms like clonal deletion, the tolerance provided by Treg cells is dominant, meaning that they actively exert suppressive and regulatory functions on other cells. The specific signals and conditions that determine a Treg cell fate will be discussed in the sections below.

Most of the thymic APCs that mediate clonal deletion, are also involved in delivering signals for Treg differentiation. In mTECs, Aire plays an important role in the development of tissue-specific Treg cells [14]. Both cDC1 and cDC2 also contribute to Treg cell induction by providing antigens and cytokines to self-specific T cell clones [15,16]. Finally, B cells have recently been involved in Treg cell differentiation through their expression of MHC and co-stimulatory molecules [17,18].

Although most self-reactive T cells are either eliminated or become Treg cells in the thymus, some are not controlled by central tolerance mechanisms and make it out of the thymus into the circulation. To limit the expansion and reactivity of these T cells in peripheral tissues, there are mechanisms of peripheral tolerance in place.

1.1.2 Peripheral Tolerance

Several peripheral tolerance checkpoints exist to regulate the self-reactive potential of T cells within lymphoid and non-lymphoid tissues. Some of them are cell-intrinsic and operate directly within the responding T cells and some are T cell-extrinsic and involve other cell populations acting on the self-reactive T cells [19].

1.1.2.1 Cell-intrinsic tolerance mechanisms

Numerous cell-intrinsic mechanisms maintain mature self-reactive T cells in an unresponsive state. For instance, quiescence [20–22] and ignorance [23] operate on naïve T

cells and make sure that they maintain a G0 stage of the cell cycle or just fail to get activated by avoiding getting in contact with the cognate antigen, respectively.

Anergy is a very well-studied mechanism that results in a state of hyporesponsiveness after TCR stimulation. This occurs when co-stimulation is deficient during TCR engagement [24]. Anergy is regulated at the epigenetic [25] and post-translational [26] levels and can be reversed under certain conditions [27,28].

T cell exhaustion is an additional non-deletional mechanism that operates on T cells during their effector stage, well after undergoing productive activation. This mechanism tends to occur in the context of chronic TCR stimulation [29] and results in T cells with strongly reduced responses to antigen encounters [30].

Finally, tolerance can be mediated through senescence, a state where the replicative potential of the T cell is lost. This can occur under certain circumstances such as repeated TCR stimulation, stimulation by certain cytokines [31], or simply with aging [32]. Senescence can be explained by telomere erosion but there might be other telomer-independent mechanisms at play [19].

1.1.2.2 Cell-extrinsic tolerance mechanisms

In some cases, peripheral cells can actively induce and maintain tolerance in T cells. An example of this is DC-mediated tolerance, in which tolerogenic immature DCs present antigens to T cells without delivering proper co-stimulation. These DC populations express low levels of both MHC and costimulatory molecules but have an increased capacity for endocytosis and phagocytosis [33]. They also produce several immunosuppressive factors such as TGF-β, IL-10, and corticosteroids, which promote T cell anergy [34–36], Treg differentiation [37–40], or even T cell apoptosis [33].

The other main cell population that maintains peripheral immune tolerance is Treg cells. As mentioned in the previous sections, most Treg cells develop in the thymus. However, under specific circumstances, some Treg cells can arise in the periphery – these are called pTreg cells. The presence of TGF-β during the activation

of naïve T cells is a critical factor for pTreg cell induction. This occurs mainly in the gastrointestinal tract but can happen in other tissues such as the skin and the liver [41].

Regardless of their origin, Treg cells are functionally diverse and versatile in the periphery. Some populations of Treg cells, called central Treg (cTreg) cells populate, lymphoid tissues and are more quiescent, whereas effector Treg (eTreg) cells seem to be further differentiated, express activation markers, and have a higher suppressive capacity. Furthermore, eTreg cells acquire specific functions and characteristics that are specific to the tissues that they reside [42].

1.2 Clonal deletion versus Treg cell differentiation

Self-reactive T cell fate after cognate antigen encounter is determined by several factors. One of them is the nature of the TCR-peptide-MHC interaction, which is determined by its affinity and/or avidity. However, other variables influence the outcome such as the modality of the self-antigen expression and presentation, the presence of co-stimulation and additional cytokine signals, and even the developmental stage of the T cell at the moment of TCR engagement [43].

1.2.1 T cell developmental stage

T cells move through several stages of development in a well-regulated manner, and it is thought that each stage influences the susceptibility to undergo either clonal deletion or Treg cell differentiation. DP thymocytes are extremely sensitive to antigen and seem to have a lower threshold to elicit clonal deletion compared to SP thymocytes, despite their comparatively low levels of TCR expression [44,45]. At the same time, the susceptibility to become a Treg cell might come around the time of CD4+ lineage commitment and might be mediated by cell-intrinsic signals occurring after the DP stage, and extrinsic signals present only in the medulla, where SP thymocytes are predominant [43].

1.2.2 Nature of the TCR stimulus

Both the strength (affinity) and the number of interactions (avidity) between the TCR and the self-antigen-MHC complex are important for the outcome of the T cell.

Stronger interactions and increasing antigen density tend to favor clonal deletion over Treg cell differentiation. Recent evidence from tetramer-based studies on polyclonal populations suggests that ubiquitously expressed self-antigens elicit clonal deletion, whereas less abundant self-antigens, like TRAs, favor the development of Treg cells [46,47]. In support of this, Treg cells are important players in the tolerance developed to AIRE-dependent TRAs [5,48]. Interestingly, these experiments also indicate that clonal deletion and Treg cell differentiation can occur in parallel for the same self-antigen.

Self-antigen expression patterns might also influence the number of interactions that a single T cell has with APCs, thus impacting the outcome. Highly expressed self-antigens might promote a single and sustained interaction that likely results in apoptotic signals being delivered to the T cell, whereas a TRA-like expression pattern might result in discontinuous TCR engagement with several APCs, which in turn will promote Treg cell differentiation [43].

1.2.3 Co-stimulation and soluble factors

Non-antigenic signals during TCR-self-peptide-MHC interactions can also impact how T tolerance is developed. They can come from co-stimulatory molecules or cytokines and will be described below.

1.2.3.1 IL-2

In addition to TCR stimulation, the availability of IL-2 is vital for Treg cell development. TCR-self-peptide-MHC interactions of intermediate strength initiate Treg cell commitment by either inducing the expression of CD25 (a chain of the high-affinity IL-2 receptor) or upregulating the transcription factor FOXP3 to generate CD25+ or $FOXP3^{lo}$ Treg cell precursors, respectively. Both of these precursors require IL-2/STAT5 survival signals to complete their differentiation into mature CD25+ FOXP3+ Treg cells [49].

The availability of IL-2 is determined by the cell sources and competition between developing Treg cells. Thymic DCs may provide some IL-2 but the main cell sources are T cells themselves, with CD4+ SP thymocytes or recirculating T cells being the most likely [50]. Competition for IL-2 can result in mature Treg cells limiting the

availability of IL-2 for Treg cell precursors, thus inhibiting de novo differentiation. Recently, recirculating Treg cells have also been proposed to limit Treg cell differentiation through the same mechanism [51].

1.2.3.2 CD28

The role of co-stimulation through CD28 in the type of tolerance induced in T cells is not completely understood. It is clear that the absence of CD28, or its ligands CD80 and CD86, results in a reduced compartment of Treg cells [52]. CD28 might negatively regulate death signals in Treg cell precursors, thus allowing an efficient development of the Treg cell compartment [53,54], however, the molecular mechanisms are not well defined. Interestingly, CD28 can also adopt a different role and favor clonal deletion. The requirement of CD28 for clonal deletion has been described in *in vitro* experiments [55], superantigen-mediated T cell death [56], and at the polyclonal level under physiologic conditions [2]. Recently, it has been proposed that the CD28 signaling domain requirements for Treg cell differentiation and clonal deletion are different and that these two outcomes can widely vary depending on the TCR specificity and the APC [57]. Nevertheless, the absence of co-stimulation results in defective T cell tolerance establishment.

1.2.3.3 TGF-β

Although the role of TGF-β for the conversion of naïve T cells into pTreg cells is relatively well-established, its importance during thymic Treg cell development is not as clear. TGF-β does appear to restrain clonal deletion in favor of Treg cell differentiation, but whether this is the result of merely pro-survival signals or differentiation cues, is not understood [43].

1.2.3.4 TNFR superfamily members (TNFRSF)

TCR engagement coupled with CD28 co-stimulatory signals also upregulate the expression of three TNFRSF members: OX40, GITR, and TNFR2. The level of expression of these receptors correlates with the strength of TCR stimulation and their engagement results in an increased IL-2 sensitivity by developing Treg cells, thereby enhancing Treg cell differentiation [58].

1.2.3.5 O-GlcNAcylation

Protein post-translational modifications regulate the signaling networks required for Treg cell differentiation and stability. Phosphorylation, acetylation, and ubiquitination are some of the modifications that occur in several signaling molecules that mediate Treg cell stability and function [59]. A novel modification consisting of the addition of O-linked N-Acetylglucosamine (O-GlcNAc) to serine and threonine residues has been described in numerous cell populations. O-GlcNAcylation modifies thousands of proteins, and we studied its role in the integration of important molecular signals for Treg cells [60]. Indeed, we found that O-GlcNAcylation was essential for the stability and function of both TCR-derived signals, like FOXP3, and IL-2-related mediators like STAT5. These findings are presented in chapter 2 of this dissertation.

1.3 Antigen presentation during T cell tolerance development

The efficiency of T cell tolerance is closely correlated with the availability of self-antigens during development. Thus, the way antigens are processed and presented in the context of MHC class I and MHC class II greatly influences the outcome of tolerance. This depends on a variety of variables like the type of APC delivering the antigen, the maturation status of the APC, and the presence of soluble factors. Indeed, there is no evidence that distinct APCs selectively promote either clonal deletion or Treg cell differentiation, instead, it is clear that most thymic APCs can induce both forms of tolerance [61] and that, for the establishment of optimal immune tolerance, they should all together present the entire repertoire of self-antigens (peptidome) that T cells are likely to encounter later in life. The major APC populations in the thymus will be described below.

1.3.1 Major APCs in the thymus

1.3.1.1 Medullary thymic epithelial cells (mTECs)

mTECs are highly specialized APCs that are vital for the development of T cell tolerance. They have a unique promiscuous gene expression that allows them to express numerous TRAs. As stated in previous sections, this is partly due to the expression of Aire and the recently described transcription factor Fezf2. In addition to TRAs, Aire drives the expression of co-stimulatory molecules like CD80 in mTECs. In fact, mutations in the *Aire* gene lead to autoimmune poly-endocrinopathy candidiasis

ectodermal dystrophy syndrome (APECED) in humans [62]. Furthermore, mTECs express CCL19 and CCL21, chemokine ligands that attract CCR7-expressing thymocytes to the medullary region [63].

AIRE-deficient animals have slightly higher numbers of CD4SP specific for a certain antigen, which suggests that mTEC can enable T cell tolerance through clonal deletion [62]. However, recent TCR repertoire analyses have shown that the expression pattern of TRAs in mTECs also promotes Treg cell differentiation [5,48].

1.3.1.2 Conventional dendritic cells (cDC)

Thymic DCs are ontogenically and functionally diverse. Conventional type I DCs (cDC1) express CD8a and XCR1 and get recruited to the medulla by XCL1-expressing mTECs in an AIRE-dependent manner [64]. This mTEC-cDC1 interaction may result in cross-presentation of mTEC-derived self-antigens by cDC1.

Thymic conventional type 2 DCs (cDC2) migrate from the periphery into the thymus as mature DCs. Their recruitment is mediated by their CCR2 expression and CCL8 expression by mTECs. Interestingly, cDC2s express SIRPα and can acquire and transport self-antigens into the thymus [65], which opens the possibility that they mediate tolerance to extrathymic antigens.

1.3.1.3 B cells

B cells localize to the medulla and the cortico-medullary junction, where they mediate T cell tolerance. Although their origin is still unclear, there is evidence that B cells could both develop in the thymus and recirculate from the periphery [61]. Compared to splenic B cells, thymic B cells have increased expression of MHC class II and co-stimulatory molecules [10,18], which suggests a higher antigen presentation capacity. Interestingly, some B cells, like mTECs, express Aire and some TRAs [10], but the exact role of Aire in B cells is still being investigated.

Thymic B cells interact with developing thymocytes and receive CD40 stimulation, which is required for their maintenance [7]. These cognate interactions are indeed important for tolerance development. The absence of B cells in the thymus

reduces the frequency of thymic Treg cells [17,18]. Furthermore, B cells can also promote clonal deletion to endogenous antigens and exogenous antigens acquired via their B cell receptor (BCR). Class switching, mediated by the activation-induced cytidine deaminase (AID), is also common in thymic B cells, and the absence of this enzyme increases the number of autoreactive T cells [66], which indicates that these class-switched B cells are important for T cell tolerance development.

1.3.1.4 Monocyte/Macrophages cells

Because of their heterogeneity and complex ontogeny, non-DC myeloid cells in the thymus have not been studied in detail. Regardless of their origin, it is clear that a subset of thymic macrophages plays an essential role in the clearance of the numerous apoptotic cells that result from positive and negative selection [67,68]. Additionally, monocytes and monocyte-derived cells, which together with macrophages can be referred to as mononuclear phagocytes [69], have been described in the thymus. As is the case in many tissues, there are LY6C^{hi} classical monocytes as well as LY6C^{low} non-classical monocytes in the thymus. Recently, a study identified a CD14^{+} monocyte-derived DC population that acquires mTEC-derived antigens and promotes T cell tolerance through Treg cell differentiation [70].

1.3.2 Maturation status of thymic APCs

Some thymic APCs can undergo maturation, which may provide signals that allow for a more efficient tolerance establishment. The best-described case is for cDC1, which undergo constant homeostatic maturation in the thymus characterized by the upregulation of the chemokine receptor CCR7, MHC class II, CD40, and co-stimulatory molecules. Mature cDC1 acquire the capacity to cross-present mTEC-derived antigens [71].

In humans, studies have shown the importance of thymic stromal lymphopoietin (TSLP), produced by epithelial cells of the Hassall's corpuscles, for the maturation of cDCs and pDCs [72,73]. This maturation was characterized by increased expression of co-stimulatory molecules and efficient Treg cell induction. Recent data from human single-cell RNA sequencing studies indicate that maturation occurs in both cDC1 and cDC2 and significantly changes gene expression, increases the expression of

chemokines and co-stimulatory molecules, and induces the expression of transcription factors like Aire and FOXD4 [74].

1.3.3 Interferon and antigen processing and presentation

Soluble factors like interferons (IFNs) can greatly affect antigen processing and presentation (as will be shown below), and if present in the thymus, could drastically influence T cell tolerance establishment. There are three major IFN families. Type I IFNs (IFN-I) bind to the IFN-α/β receptor (IFNAR) and are composed of 14 IFN-α subtypes in mice (13 in humans), one IFN-β, and other minor subtypes. Type II IFN (IFN-II) consists of IFN-γ only and binds to a specific receptor IFNGR. Type III IFNs (IFN-λ or IFN-III) are the most recently described; there can be 2 to 4 subtypes depending on the species, and they bind to the IFNLR (see Figure 1.1).

1.3.3.1 IFN gamma

The gene expression levels of MHC class II are tightly regulated mainly by the MHC class II transactivator (CIITA), which is constitutively expressed only in professional APCs, and its activity can respond to environmental cues [75]. It is well known that IFN-γ controls CIITA expression and thus the upregulation of MHC class II [76]. Analogously, the protein NLRC5 transcriptionally activates MHC class I genes and acts as an MHC class I transactivator (CITA) [77]. NLRC5 is highly responsive to IFN-γ. IFN-γ-treated APCs also display high levels of constitutive autophagy and efficient delivery of endogenous antigens to MHC class II-expressing compartments [78]. Several mechanisms have been proposed to explain this activation of autophagy [79]. Finally, IFN-γ plays an important role in the regulation of antigen processing and presentation by MHC class I. IFN-γ not only induces the expression of several proteasome subunits and modulates their activity, but also stimulates the expression of additional proteases, which together modulates the efficiency and quality of antigen processing and presentation [80–82].

1.3.3.2 Type I IFNs

There are numerous ways IFN-I may modulate antigen processing and presentation. For example, in immature DCs and monocytes, IFN-α/β stimulation, like

IFNγ, upregulates the expression of MHC molecules (class I and II) and co-stimulatory molecules CD80 and CD86 [83–85].

IFNs-I are also important for efficient cross-presentation by DCs, which allows them to load exogenous peptides into MHC class I molecules. This is important in both infections and cancer. The cross-presentation capacity of murine DCs lacking IFNAR is greatly reduced, which results in their inability to reject tumors [86,87]. The importance of IFN-I in cross-presentation has also been extensively assessed during viral infections in both mice and humans [88–91]. Furthermore, IFN-I can also modulate the expression of some proteasome subunits [92,93], and, similar to IFN-γ, can induce the expression of CITA [94].

The role of IFN-I is also key for antigen processing and presentation through MHC class II. For instance, IFN-α/β promotes a type of maturation in DCs that, unlike TLR-dependent maturation, results in continued MHC class II synthesis and antigen processing [95]. Additionally, IFN-I induce the production of CXC-chemokine ligand 9 (CXCL9) and CXCL10 by APCs, which can attract T cells and facilitate TCR-self-peptide-MHC interactions [96]. Finally, autophagy, which promotes MHC class II presentation of self-peptides, is induced by IFN-I [97,98].

IFN-I also have direct and indirect effects on B cells, which could modify the antigens they present. For instance, IFN-I induce the expression of B cell-activating factor (BAFF) and a proliferation-inducing ligand (APRIL) in DCs, molecules that enhance class switching in B cells [99,100]. IFN-I can also enhance antibody responses and subclass switching directly on B cells [101], which potentially results in the presentation of activation-dependent self-antigens.

1.3.3.3 Type III IFNs

While IFN-λs and IFN-α/β are induced by similar pathways and activate related gene expression programs, it is becoming clear that they also have non-redundant functions in mediating protection, especially in the context of mucosal and barrier surfaces [102]. Recent studies on the capacity of IFN-III to modulate immune responses

indicate that these molecules might also have strong effects on antigen processing and presentation.

The biological activity of IFN-λs in mice was initially thought to be restricted to epithelial cells, but numerous studies have shown potent effects on B cells, DCs, neutrophils, among others [103]. Studies on IFNLR-deficient bone marrow-derived DCs (BMDCs) suggest reduced maturation and antigen processing [104]. Interestingly, quantitative proteomics analyses of IFN-λ-stimulated cells indicate the upregulation of several molecules involved in antigen processing and presentation, including subunits of the immunoproteasome [105].

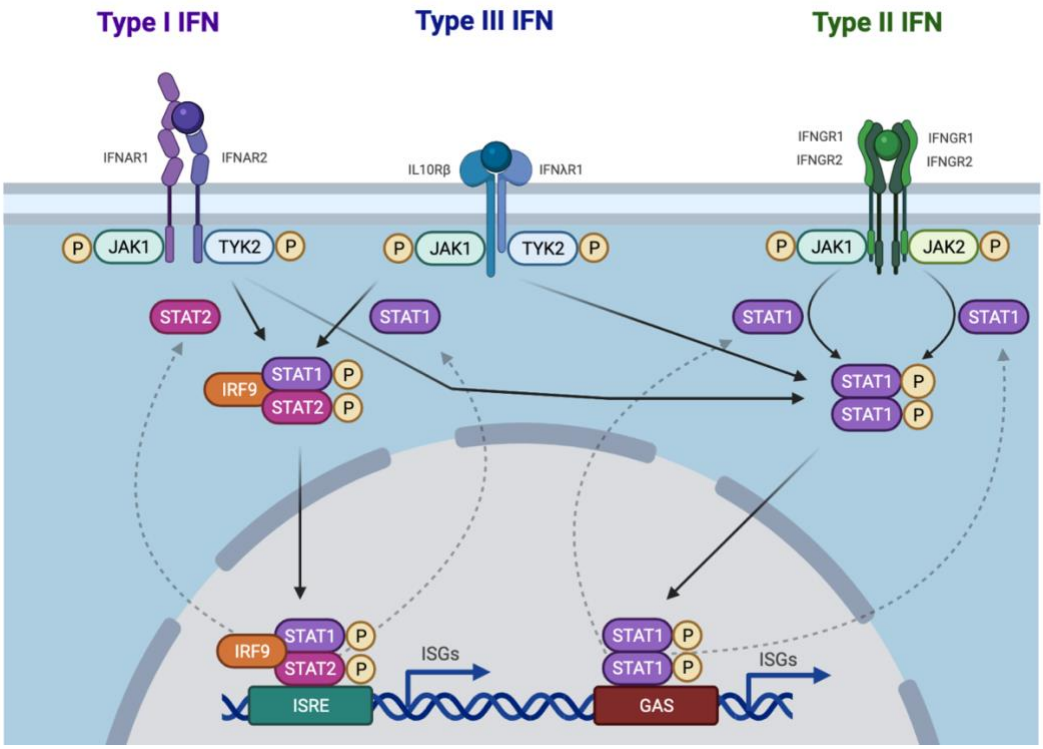

Figure 1.1. Canonical interferon signaling pathways.

The three different types of IFN bind to different receptors. IFN-I bind to IFNAR (IFNAR1 and IFNAR2) whereas IFN-III bind to IFNLR (IL10Rβ and IFNLR1); both of these receptors activate the tyrosine kinases JAK1 and TYK2, eventually leading to the recruitment of STAT1 and STAT2. Heterodimers of STAT1 and STAT2 can bind to IRF9 to form the interferon-stimulated gene factor 3 (ISGF3) complex, which bind to interferon-stimulated response elements (ISREs) in interferon stimulated genes (ISGs) to activate their transcription. Homodimers of STAT1 can translocate into the nucleus and bind γ-activated sequence (GAS) promoter elements in ISG to induce their transcription. IFN-II binds to the IFNGR (two chains of IFNGR1 and two of IFNGR2) to activate JAK1 and JAK2, leading to the recruitment and activation of homodimers of STAT1,

which will then bind GAS elements in the nucleus. These are the canonical pathways, but additional signaling pathways might get activated by IFNs. Created in BioRender.com.

Because some of the gene changes induced by IFN (like proteosome subunits and autophagy genes) alter the specificity of self-peptide processing and presentation, IFN treatment of APC not only increases, but changes, the displayed self-peptidome. For example, in cells responding to viral infection, there was a profound alteration of the displayed self-peptides, 40% of which were derived from interferon-stimulated genes (ISG) [106]. If such potent effects of IFNs on antigen processing/presentation were occurring during T cell development, this would have significant implications for the establishment of T cell tolerance. We made the discovery that IFN-I and IFN-III are constitutively produced in the thymus and activate all the major thymic APCs. The details of this study are presented in chapter 3 of this dissertation.

Chapter 2 The lineage stability and suppressive program of regulatory T cells require protein O-GlcNAcylation

2.1 Introduction

Regulatory T (Treg) cells are distinct T lymphocytes that control immunological self-tolerance and homeostasis [12,13]. The lineage-defining transcription factor Forkhead box P3 (FOXP3), together with other transcription regulators, induces Treg-cell development in the thymus. T-cell receptor (TCR)- and interleukin-2 receptor (IL-2R)-derived instructive signals act in two steps to induce the *Foxp3* gene expression in developing Treg cells [107–109]. Deleting or mutating the *Foxp3* gene leads to the scurfy phenotype characterized by multi-organ inflammation in mice [110–112]. In mature Treg cells, continued expression of FOXP3 maintains their lineage identity [113,114]; however, a small but significant population of Treg cells may lose FOXP3 expression and acquire effector T-cell activities in normal and particularly inflammatory settings [115–117]. Nevertheless, molecular mechanisms controlling FOXP3 protein stability under homeostatic and pathologic conditions are not well understood.

Effector Treg (eTreg) cells are the most biologically potent population of Treg cells [42,118]. Recent studies have demonstrated that pathways that regulate Treg-cell development are also required for the formation and function of eTreg cells. Continuous TCR signaling maintains the transcriptional program and suppressive function of eTreg cells, without affecting *Foxp3* gene expression [119,120]. IL-2R and downstream STAT5 signaling are also indispensable for eTreg-cell differentiation and function by controlling a distinct set of genes that are separable from those regulated by TCR signaling [121]. It is still unclear how Treg cells integrate these pathways to maintain the suppressive program.

Post-translational modification networks exist in Treg cells to rapidly integrate signals from diverse environmental stimuli to modulate Treg-cell function accordingly. In this regard, FOXP3 protein has been intensively investigated. FOXP3 can be regulated by phosphorylation, acetylation, and ubiquitination in response to environmental changes to modulate its protein stability and DNA-binding ability [59]. In recent years, a novel modification was discovered: O-linked N-Acetylglucosamine (O-GlcNAc) modifies intracellular proteins at serine or threonine residues [122]. O-GlcNAcylation is radically different from other types of glycosylation, and analogous to phosphorylation plays a central role in signaling pathways relevant to chronic human diseases including cardiovascular disease, diabetes, neurodegeneration, and cancer

[60,123]. The enzymes O-GlcNAc transferase (OGT) and O-GlcNAcase (OGA) mediate the addition and removal of O-GlcNAc, respectively. We and others have demonstrated that O-GlcNAc signaling acts as a hormone and nutrient sensor to control many biological processes such as gene transcription, protein stability, and cell signaling [124–127].

Earlier studies have shown that T cells express and upregulate O-GlcNAcylation upon immune activation [128]. T cell-specific ablation of OGT resulted in an increase of apoptotic T cells [129], and blocked T cell progenitor renewal, malignant transformation and peripheral T cell clonal expansion [130]. These data demonstrate that protein O-GlcNAcylation links TCR signaling to T cell differentiation and function; however, the role of O-GlcNAcylation in Treg cells has not been studied.

Here, we demonstrate that protein O-GlcNAcylation is abundant, and is functionally important in Treg cells by modifying FOXP3 and STAT5. Selective ablation of OGT in Treg cells leads to an aggressive autoimmune syndrome in mice as a result of Treg lineage instability and eTreg cell deficiency. On the other hand, pharmacological elevation of protein O-GlcNAcylation enhances the suppressive activity of human Treg cells, which will provide insights to help us better manipulate these cells in patients to treat diseases such as autoimmune disorders, transplant rejection and cancer.

2.2 Results

2.2.1 FOXP3 is modified and stabilized by O-GlcNAcylation

TCR-activated protein O-GlcNAcylation is critical for T-cell development and function [130]. We found that similar to $CD4^+CD25^-$ naïve T cells, $CD4^+CD25^+FOXP3^+$ Treg cells displayed abundant expression of OGT and global protein O-GlcNAcylation (Fig. 2.1A and B), implying a potential role of O-GlcNAcylation in Treg cells. Consistent with findings in T cells, TCR activation further promoted protein O-GlcNAcylation in Treg cells ex vivo (Fig. 2.1C). We also stimulated naïve T cells with TGFβ to generate induced Treg (iTreg) cells in vitro. Compared with cells only treated with anti-CD3/CD28 beads, iTreg cell showed increased levels of the *Ogt* gene expression and global protein O-GlcNAcylation (Fig. 2.2A and B). These data indicate that TCR activates protein O-GlcNAcylation in Treg cells.

The FOXP3 protein is subjected to various posttranslational modifications that are required for lineage maintenance and suppressive function [59]. Thus, we sought to test whether the FOXP3 protein itself could be modified by O-GlcNAcylation. FOXP3 O-GlcNAcylation could be detected when ectopically expressed in human embryonic kidney (HEK) 293 cells (Fig. 2.1.D). OGT overexpression increased levels of total and O-GlcNAcylated FOXP3, while OGA decreased FOXP3 protein expression and its O-GlcNAcylation (Fig. 2.1D). Similarly, levels of total and O-GlcNAcylated FOXP3 were increased when OGA was inhibited by Thiamet-G (TMG); in contrast, inhibition of OGT by ST045849 decreased both total and O-GlcNAcylated FOXP3 (Fig. 2.1E). FOXP3 protein degradation induced by the protein synthesis inhibitor cycloheximide (CHX) could be prevented by the proteasome inhibitor MG132 (Fig. 2.1F), indicating that FOXP3 was degraded through a ubiquitin/proteasome-dependent pathway. OGT overexpression or OGA inhibition increased FOXP3 stability (Fig. 2.1F-H), while OGA overexpression or OGT inhibition destabilized FOXP3 (Fig. 2.1G and I). The ubiquitin ligase STUB1 and the deubiquitinase USP7 have been reported to control FOXP3 polyubiquitination and degradation [131,132]. STUB1 overexpression reduced FOXP3 levels, which could not be further decreased by OGA. When USP7 was present, OGT could not further increase FOXP3 protein levels (Fig. 2.2C). These data suggest that O-GlcNAcylation may counteract ubiquitination to stabilize FOXP3 protein.

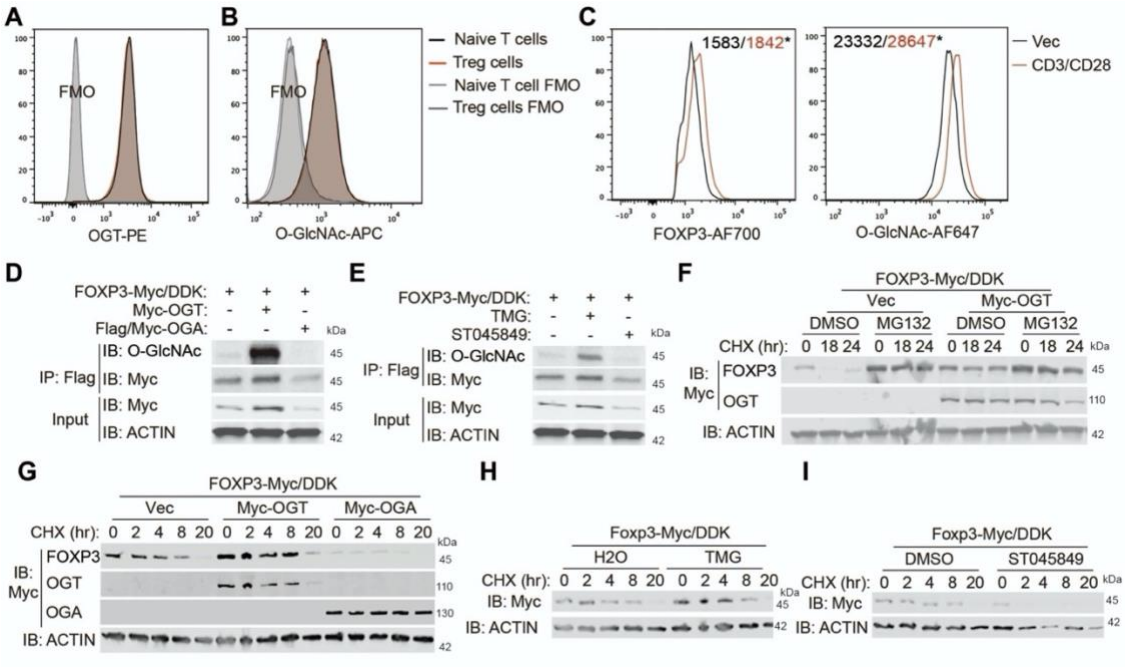

Figure 2.1. O-GlcNAc-cycling enzymes regulate FOXP3 stability in vitro.

(A, B) Mean fluorescence intensity (MFI) of OGT (A) and O-GlcNAcylation (B) in $CD4^{+}CD25^{-}$ naïve T cells, $CD4+CD25^{+}FOXP3^{+}$ Treg cells and corresponding Fluorescence Minus One (FMO) negative controls. (C) Treg cells isolated from wildtype mice were stimulated with or without anti-CD3/CD28 beads for 24h ex vivo (n = 3). MFI of FOXP3 and O-GlcNAcylation was analyzed in $CD4^{+}CD25^{+}$ $FOXP3^{+}$ Treg cells. (D, E) HEK 293 cells were transfected FOXP3 together with OGT or OGA (D) or treated with inhibitors of OGT (ST045849) or OGA (TMG) (E). FOXP3 O-GlcNAcylation was determined by immunoprecipitation followed by western blotting. (F) FOXP3 stability was determined by treatment of cycloheximide (CHX) in combination with MG132, DMSO was used as a control. (G-I) FOXP3 stability was determined in the presence of OGT/OGA overexpression (G), TMG (H), or ST045849 (I). Data are shown as mean ± s.e.m. * $p<0.05$ by unpaired student's t-test.

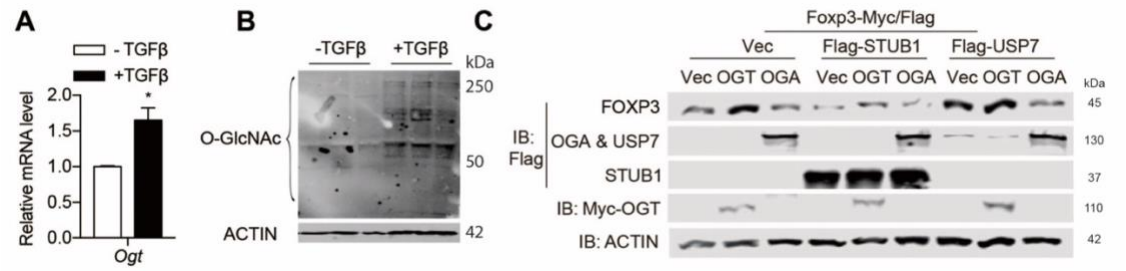

Figure 2.2. iTreg cells showed increased levels of the *Ogt* gene expression and global protein O-GlcNAcylation.

(A, B) $CD4^{+}CD25^{-}$ cells isolated from the LNs and spleen of wildtype mice were activated for 5-day with anti-CD3/CD28 beads in the presence of TGF-β to generate iTreg cells *ex vivo*. mRNA levels of *Ogt* (A, n = 3) and global protein O-GlcNAcylation (B) were measured. (C) Expression of FOXP3 protein in HEK 293 cells co-transfected with OGT or OGA and STUB1 or USP7. Data are shown as mean ± s.e.m. *$p<0.05$ by unpaired student's t-test.

We then sought to determine whether O-GlcNAcylation controls FOXP3 protein stability in Treg cells. $CD4^+CD25^+$ Treg cells from inducible OGT knockout (KO) mice (*Ubc-Cre/ERT2*$^+$*Ogt*$^{fl/Y}$) were isolated and expanded ex vivo in the presence of anti-CD3/CD28 antibodies and recombinant IL-2. 4-Hydroxytamoxifen (4-OHT) treatment in wildtype cells had no adverse effect on protein O-GlcNAcylation, FOXP3 expression, or Treg-cell number (Fig. 2.3A-C). In *Ubc-Cre/ERT2*$^+$*Ogt*$^{fl/Y}$ cells, however, 4-OHT reduced global O-GlcNAcylation (Fig. 2.3D), FOXP3 protein abundance on a per-cell basis (Fig. 2.4A and B), and frequencies of $CD4^+CD25^+$ (Fig. 2.3E) and $CD4^+FOXP3^+$ Treg cells (Fig. 2.4C and D), demonstrating that loss of O-GlcNAcylation destabilizes FOXP3 protein in Treg cells ex vivo.

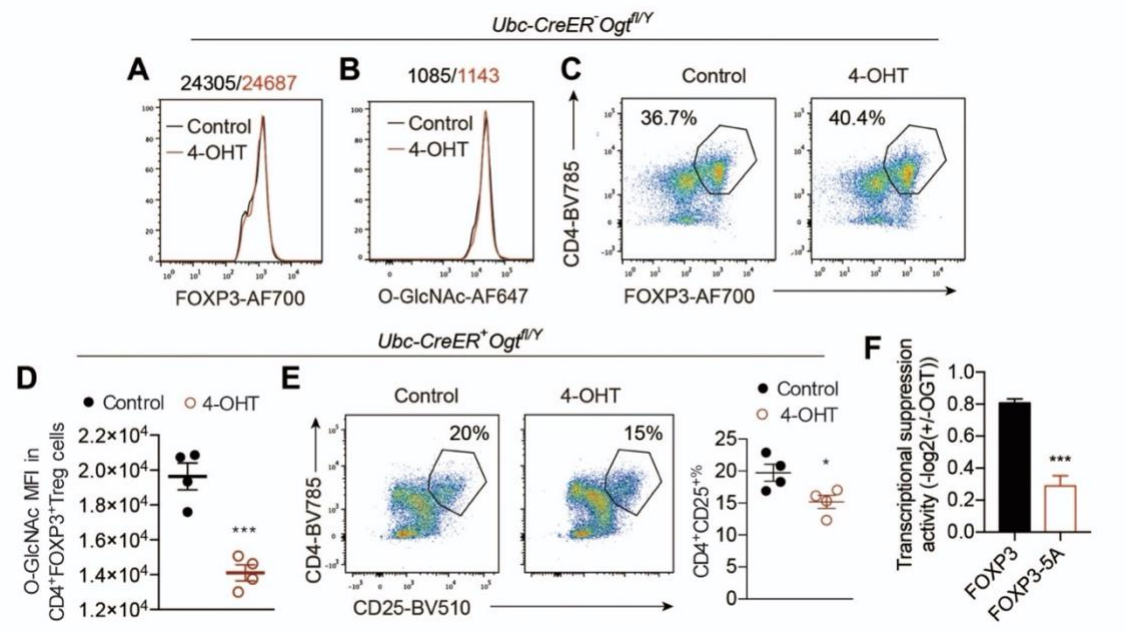

Figure 2.3. 4-Hydroxytamoxifen (4-OHT) treatment had no adverse effects in wildtype cells.

(A-C) Isolated Treg cells from *Ubc-CreER*$^-$*Ogt*$^{fl/Y}$ mice were treated for 3-day 4-OHT ex vivo. Ethanol was used as a control. MFI of O-GlcNAcylation (A) and FOXP3 (B) among $CD4^+FOXP3^+$ Treg cells. Frequencies of $CD4^+FOXP3^+$ Treg cells were shown in (C). (D) MFI of O-GlcNAcylation in $CD4^+FOXP3^+$ Treg cells from *Ubc-CreER*$^+$*Ogt*$^{fl/Y}$ mice that were treated with ethanol or 4-OHT, n = 4. (E) Representative flow cytometry and quantification of the frequencies of $CD4^+CD25^+$ Treg cells from *Ubc-CreER*$^+$*Ogt*$^{fl/Y}$ mice that were treated with ethanol or 4-OHT, n = 4. (F) Forkhead responsive element (FHRE)-luciferase assay in HEK 293 cells transfected with FOXP3 or FOXP3-5A in the presence/absence of OGT. pIS1-Rluc was co-transfected to control transfection efficiency. OGT-induced activation of FOXP3 suppressive activity on FHRE was plotted (n = 6). Data are shown as mean ± s.e.m. *p<0.05, ***p<0.001 by unpaired student's t-test.

To identify sites of FOXP3 O-GlcNAcylation, Flag-tagged FOXP3 was expressed in HEK 293 cells together with OGT, immunopurified with anti-Flag beads, trypsin digested, and analyzed by liquid chromatography with tandem mass spectrometry (LC-MS/MS) using electron transfer dissociation (ETD). Multiple O-GlcNAcylation sites were identified. Mutating 5 of these sites, including Thr38, Ser57, Ser58, Ser270, and Ser273, to alanine (5A) on the FOXP3 protein significantly blunted its O-GlcNAcylation level (Fig. 2.4E), reduced its stability (Fig. 2.4F), and ablated its transcriptional suppression activity induced by OGT (Fig. 2.3F). We then retrovirally transduced FOXP3 and FOXP3-5A into $CD4^+CD25^-$ conventional T cells and flow cytometric analyses of transduced cells showed that the protein expression level of FOXP3-5A was much lower than that of wildtype FOXP3 (Fig. 2.4G and H). These results indicate that O-GlcNAcylation is required to stabilize FOXP3.

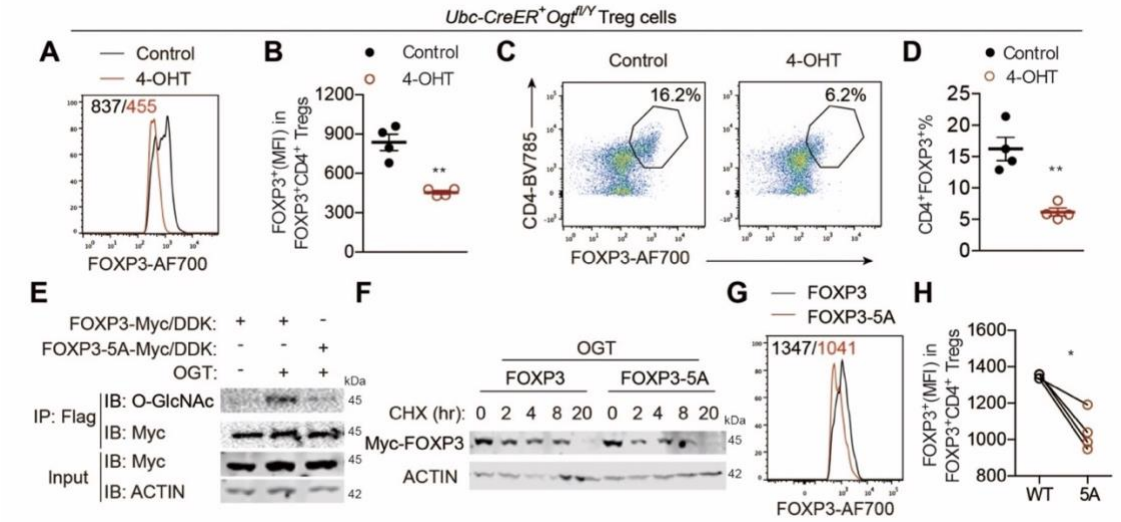

Figure 2.4. O-GlcNAcylation stabilizes the FOXP3 protein in Treg cells.

(A-D) Treg cells isolated from *Ubc-CreER*$^+$*Ogt*$^{fl/Y}$ mice were treated with 4-OHT for 3-day ex vivo, ethanol was used as the control, n = 4 each group. MFI of FOXP3 in $CD4^+FOXP3^+$ Treg cells was analyzed in (A) and quantified in (B). Representative flow cytometry of $CD4^+$ $FOXP3^+$Treg cells was plotted in (C) and the frequencies of Treg cells were shown in (D). (E) FOXP3 or FOXP3-5A were transfected in HEK 293 cells with or without OGT. FOXP3 O-GlcNAcylation was determined by immunoprecipitation followed by Western blotting. (F) FOXP3 and FOXP3-5A stability was determined in the presence of OGT overexpression. (G, H) $CD4^+CD25^-$ naïve T cells isolated from wildtype mice were infected with retroviruses expressing FOXP3 or FOXP3-5A in the presence of anti-CD3/CD28 beads (n = 4). MFI of FOXP3 was analyzed (G) and quantified (H) in $CD4^+FOXP3^+$ Treg cells. Data are shown as mean ± s.e.m. *p<0.05; **p<0.01 by unpaired student's t-test (B, D) and paired student's t-test (H).

2.2.2 OGT-deficiency in Treg cells leads to a scurfy phenotype

To directly examine whether OGT regulates mature Treg cell function in vivo, we generated mice with Treg cell-specific deletion of OGT by using Cre recombinase driven by the endogenous *Foxp3* locus (*Foxp3*$^{YFP\text{-}Cre}$) to delete the *lox*P-flanked *Ogt* gene after FOXP3 was expressed in Treg cells. Of note, the *Foxp3* and *Ogt* genes are located about 40 centimorgans apart on the X Chromosome; thus, we were able to successfully obtain KO mice. Protein O-GlcNAcylation was specifically diminished in Treg cells but not non-Treg CD4$^+$ T, CD8$^+$ T, B, or natural killer cells (Fig. 2.5A). Compared to *Foxp3*$^{YFP\text{-}Cre/Y}$*Ogt*$^{wt/Y}$ control mice, *Foxp3*$^{YFP\text{-}Cre/Y}$*Ogt*$^{fl/Y}$ male KO mice progressively developed systemic autoimmune lesions including conjunctivitis, dermatitis, hunched posture (Fig. 2.6A), extensive lymphadenopathy and splenomegaly (Fig. 2.6B), and loss of body weight (Fig. 2.6C). KO male mice became moribund at approximately 4 weeks of age (Fig. 2.6D), and massive lymphocytic infiltration could be seen in colon epithelium, skin epidermis, liver sinusoids, and lung interstitium (Fig. 2.6E).

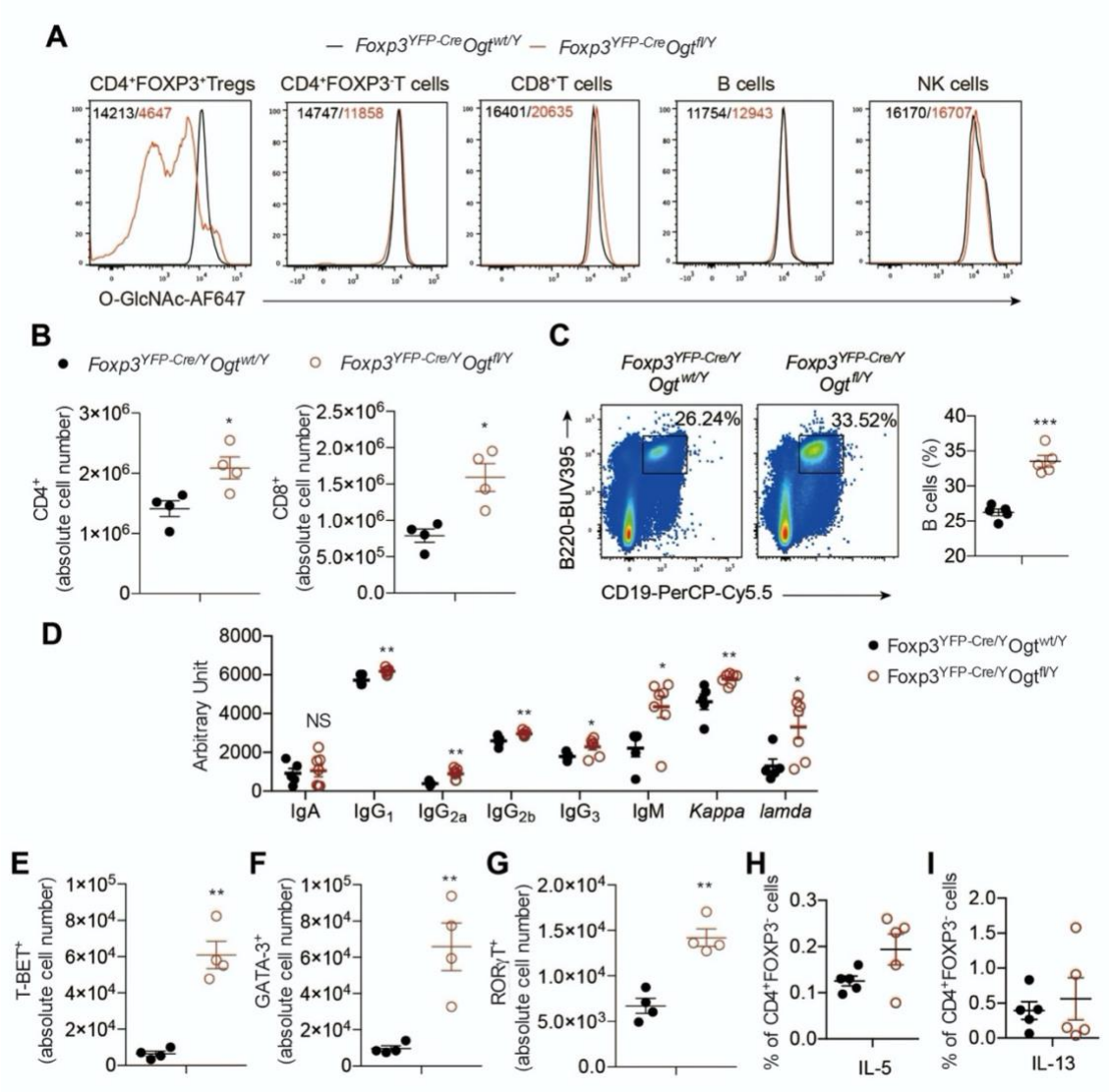

Figure 2.5. Protein O-GlcNAcylation deficiency and effects were specific to Treg cells.

(A) MFI of O-GlcNAcylation in indicated cell populations from *Foxp3*$^{YFP\text{-}Cre/Y}$ *Ogt*$^{wt/Y}$ and *Foxp3*$^{YFP\text{-}Cre/Y}$ *Ogt*$^{fl/Y}$ mice. (B) Total number of CD4$^+$ and CD8$^+$ T cells in the LNs from 2-week-old *Foxp3*$^{YFP\text{-}Cre/Y}$ *Ogt*$^{wt/Y}$ and *Foxp3*$^{YFP\text{-}Cre/Y}$ *Ogt*$^{fl/Y}$ mice, n = 4 each group. (C) Representative flow cytometry plot and quantification of the frequencies showing CD19$^+$B220$^+$ B cells among single cells in the LNs of 2-week-old *Foxp3*$^{YFP\text{-}Cre/Y}$ *Ogt*$^{wt/Y}$ and *Foxp3*$^{YFP\text{-}Cre/Y}$ *Ogt*$^{fl/Y}$ mice, n = 5 each group, n = 5. (D) Levels of IgA, IgG$_1$, IgG$_{2a}$, IgG$_{2b}$, IgG$_3$, IgM, *Kappa* and *lamda* in sera of *Foxp3*$^{YFP\text{-}Cre/Y}$ *Ogt*$^{wt/Y}$ (n = 5) and *Foxp3*$^{YFP\text{-}Cre/Y}$ *Ogt*$^{fl/Y}$ (n = 7) mice. (E-G) Total numbers of T-BET$^+$ (E), GATA-3$^+$ (F) and RORγT$^+$ (G) cells among CD4$^+$ T cells in the LNs from 2-week-old *Foxp3*$^{YFP\text{-}Cre/Y}$ *Ogt*$^{wt/Y}$ and *Foxp3*$^{YFP\text{-}Cre/Y}$ *Ogt*$^{fl/Y}$ mice, n=4 each group. (H, I) Frequencies of IL-5$^+$ (H) and IL-13$^+$ (I) cells in CD4$^+$FOXP3$^-$ T cells stimulated with PMA/Ionomycin in the LNs of 2-week-old *Foxp3*$^{YFP\text{-}Cre/Y}$ *Ogt*$^{wt/Y}$ and *Foxp3*$^{YFP\text{-}Cre/Y}$ *Ogt*$^{fl/Y}$ mice, n = 5. Data are shown as mean ± s.e.m. **p*<0.05; ***p*<0.01; ****p*<0.001 by unpaired student's *t*-test.

We then analyzed the lymphocyte compartment at the age of 2 weeks, before an autoimmune phenotype was overtly apparent. The absolute numbers of $CD4^+$ and $CD8^+$ T cells were increased in the lymph nodes (LNs) of *Foxp3*$^{YFP\text{-}Cre/Y}$ *Ogt*$^{fl/Y}$ mice (Fig. 2.5B). The percentage of effector/memory cells ($CD44^{hi}CD62L^{lo}$) within the $CD4^+$ and $CD8^+$ compartments were consistently higher in both the LNs and the spleen of *Foxp3*$^{YFP\text{-}Cre/Y}$ *Ogt*$^{fl/Y}$ KO mice than those in *Foxp3*$^{YFP\text{-}Cre/Y}$ *Ogt*$^{wt/Y}$ controls (Fig. 2.6F, G). B cell frequency in the LNs and levels of IgG, IgM, and free kappa and lambda chains in the serum were upregulated in KO mice (Fig. 2.5C and D). Moreover, the frequencies and absolute numbers of effector $CD4^+$ subsets including T helper (Th) 1, Th2, and Th17 were all increased (Fig. 2.6H-K and Fig. 2.5E-G). However, we could only observe significantly increased expression of interferon-γ (IFNγ) in $CD4^+FOXP3^-$ T cells in *Foxp3*$^{YFP\text{-}Cre/Y}$ *Ogt*$^{fl/Y}$ KO mice (Fig. 2.6L). Expression of IL-4, IL-5, IL-13, and IL-17 remained unchanged (Fig. 2.6L and Fig. 2.5H, I). These observations reveal an excessive Th1-dominant inflammatory response in *Foxp3*$^{YFP\text{-}Cre/Y}$ *Ogt*$^{fl/Y}$ mice.

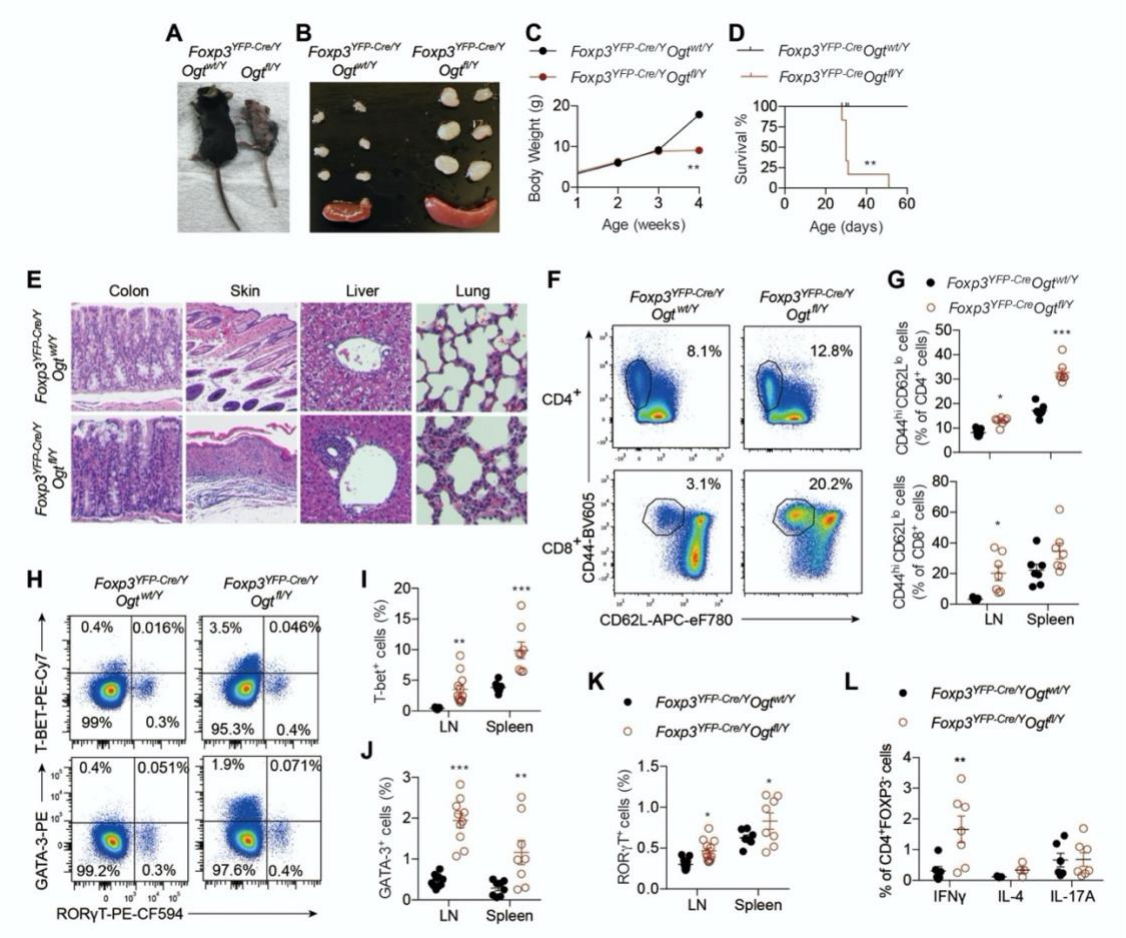

Figure 2.6. OGT-deficiency in Treg cells leads to a scurfy phenotype in mice.

(A, B) Representative images of 4-week-old *Foxp3*$^{YFP\text{-}Cre/Y}$ *Ogt*$^{wt/Y}$ and *Foxp3*$^{YFP\text{-}Cre/Y}$ *Ogt*$^{fl/Y}$ mice (A) and peripheral LNs and spleen (B). (C, D) Body weight curve (C, n = 5) and survival curve (D, n = 6) of *Foxp3*$^{YFP\text{-}Cre/Y}$ *Ogt*$^{wt/Y}$ and *Foxp3*$^{YFP\text{-}Cre/Y}$ *Ogt*$^{fl/Y}$ mice. (E) Representative images of H&E staining of the colon, skin, liver, and lung from 4-week-old *Foxp3*$^{YFP\text{-}Cre/Y}$ *Ogt*$^{wt/Y}$ and *Foxp3*$^{YFP\text{-}Cre/Y}$ *Ogt*$^{fl/Y}$ mice. (F, G) Representative flow cytometry plots showing CD44hiCD62Llo effector T cells among CD4^{+} (top) and CD8^{+} (bottom) T cells in the LNs (F) and quantification of the frequencies of CD44^{hi}CD62L^{lo} effector T cells in the LNs and spleen of 2-week-old *Foxp3*$^{YFP\text{-}Cre/Y}$ *Ogt*$^{wt/Y}$ and *Foxp3*$^{YFP\text{-}Cre/Y}$ *Ogt*$^{fl/Y}$ mice, at least n = 6 each group (G). (H-K) Representative flow cytometry plots showing T-BET^{+}, GATA3^{+} and RORγT^{+} cells among CD4^{+} T cells in the LNs (H) and quantification of the frequencies of T-BET^{+} cells (I), GATA3^{+} cells (J) and RORγT^{+} cells (K) in the LNs and spleen of 2-week-old *Foxp3*$^{YFP\text{-}Cre/Y}$ *Ogt*$^{wt/Y}$ and *Foxp3*$^{YFP\text{-}Cre/Y}$ *Ogt*$^{fl/Y}$ mice were shown, n = 8 each group. (L) Frequencies of IFNγ^{+}, IL-4^{+} and IL-17A^{+} cells in CD4^{+}FOXP3^{-} T cells stimulated with PMA/Ionomycin in the LNs of 2-week-old Foxp3$^{YFP\text{-}Cre/Y}$ Ogt$^{wt/Y}$ and *Foxp3*$^{YFP\text{-}Cre/Y}$ *Ogt*$^{fl/Y}$ mice, at least n = 3 each group. Data are shown as mean ± s.e.m. **p*<0.05; ***p*<0.01; ****p*<0.001 by unpaired student's t-test (C, G, and I-L) and Kaplan-Meier Analysis (D).

2.2.3 O-GlcNAcylation stabilizes the Treg-cell lineage

We then sought to characterize Treg cells directly. 2-week-old mice showed no difference in the Treg-cell frequency among CD4^{+}TCRβ^{+} cells in the LNs or spleen (Fig. 2.7A and B). The absolute number of Treg cells in the LNs of *Foxp3*$^{YFP\text{-}Cre/Y}$*Ogt*$^{fl/Y}$ mice even surpassed those in *Foxp3*$^{YFP\text{-}Cre/Y}$*Ogt*$^{wt/Y}$ controls (Fig. 2.8A and B). In the thymus, we did not observe any reduction in the frequency or number of Treg cells (Fig. 2.8C and D). In addition, there was no difference in Treg-cell proliferation or apoptosis between *Foxp3*$^{YFP\text{-}Cre/Y}$*Ogt*$^{fl/Y}$ and *Foxp3*$^{YFP\text{-}Cre/Y}$*Ogt*$^{wt/Y}$ mice, shown by Ki-67 and Annexin V staining, respectively (Fig. 2.8E and F). These data suggest that OGT is dispensable for the development of thymic Treg cells.

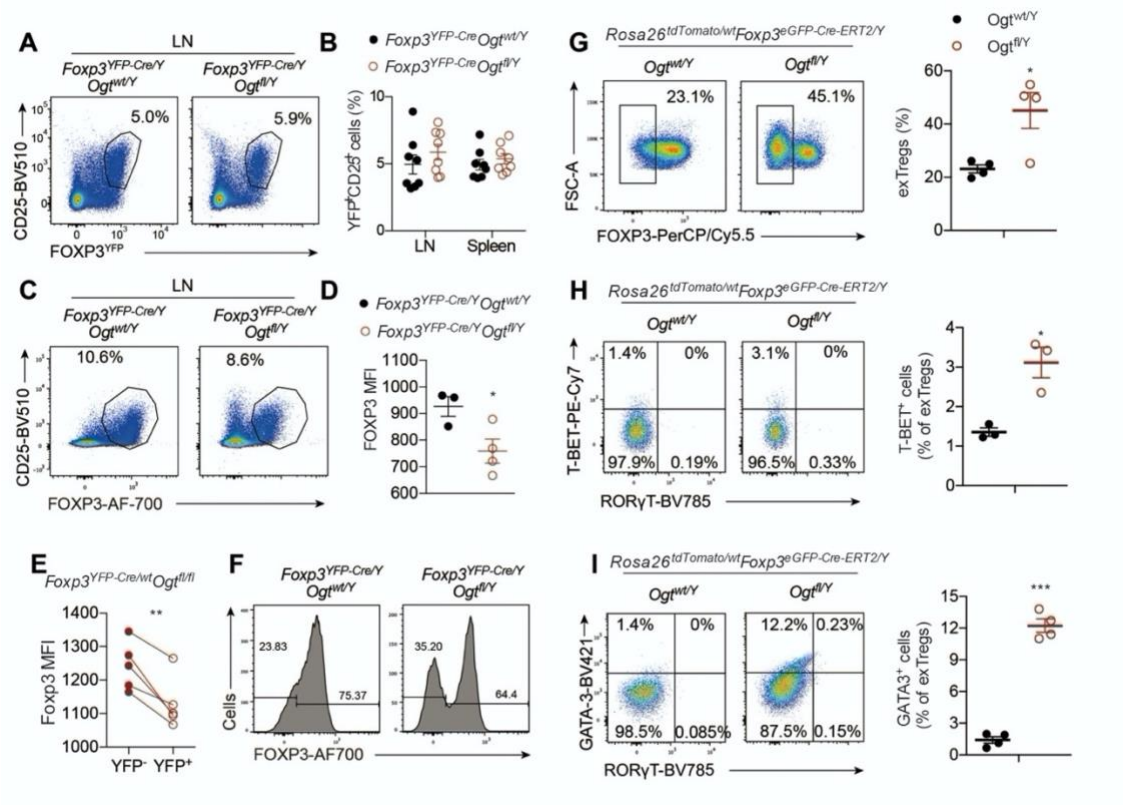

Figure 2.7. Protein O-GlcNAcylation stabilizes the Treg-cell lineage.

(A, B) Flow cytometry of YFP$^+$CD25$^+$ cells among CD4$^+$ T cells in the LNs (A) and frequencies of YFP$^+$CD25$^+$ cells in the LNs and spleen from 2-week-old *Foxp3*$^{YFP\text{-}Cre/Y}$ *Ogt*$^{wt/Y}$ and *Foxp3*$^{YFP\text{-}Cre/Y}$ *Ogt*$^{fl/Y}$ mice, n = 8 each group (B). (C, D) Flow cytometry of FOXP3$^+$CD25$^+$ cells among CD4$^+$ T cells (C) and MFI of FOXP3 in FOXP3$^+$CD25$^+$ Treg cells (D, n = 3-4) in the LNs from 2-week-old *Foxp3*$^{YFP\text{-}Cre/Y}$ *Ogt*$^{wt/Y}$ and *Foxp3*$^{YFP\text{-}Cre/Y}$ *Ogt*$^{fl/Y}$ mice. (E) MFI of FOXP3 in OGT-sufficient and -deficient Treg cells in the LNs from *Foxp3*$^{YFP\text{-}Cre/Y}$ *Ogt*$^{fl/fl}$ mice, n = 5. (F) Histogram of FOXP3 expression in CD4$^+$CD25$^+$YFP$^+$ Treg cells in the LNs from 2-week-old *Foxp3*$^{YFP\text{-}Cre/Y}$ *Ogt*$^{wt/Y}$ and *Foxp3*$^{YFP\text{-}Cre/Y}$ *Ogt*$^{fl/Y}$ mice, n = 6 each group. (G) Flow cytometry and quantification of the frequencies of Td-tomato$^+$GITR$^+$FOXP3$^-$ ex-Treg cells among CD4$^+$ T cells in the LNs from *Foxp3*$^{eGFP\text{-}Cre\text{-}ERT2/Y}$ *Ogt*$^{wt/Y}$ *Rosa26*$^{tdTomato/wt}$ and *Foxp3* $^{eGFP\text{-}Cre\text{-}ERT2/Y}$ *Ogt*$^{fl/Y}$ *Rosa26*$^{tdTomato/wt}$ mice, n = 4. (H, I) T-BET$^+$, GATA3$^+$ and RORγT$^+$ cells among ex-Treg cells in the LNs from *Foxp3*$^{eGFP\text{-}Cre\text{-}ERT2/Y}$ *Ogt*$^{wt/Y}$ *Rosa26*$^{tdTomato/wt}$ and *Foxp3* $^{eGFP\text{-}Cre\text{-}ERT2/Y}$ *Ogt*$^{fl/Y}$ *Rosa26*$^{tdTomato/wt}$ mice, n= 3-4. Data are shown as mean ± s.e.m. **p*<0.05; ***p*<0.01; ****p*<0.001 by unpaired (B, D, G-I) and paired (E) student's *t*-test.

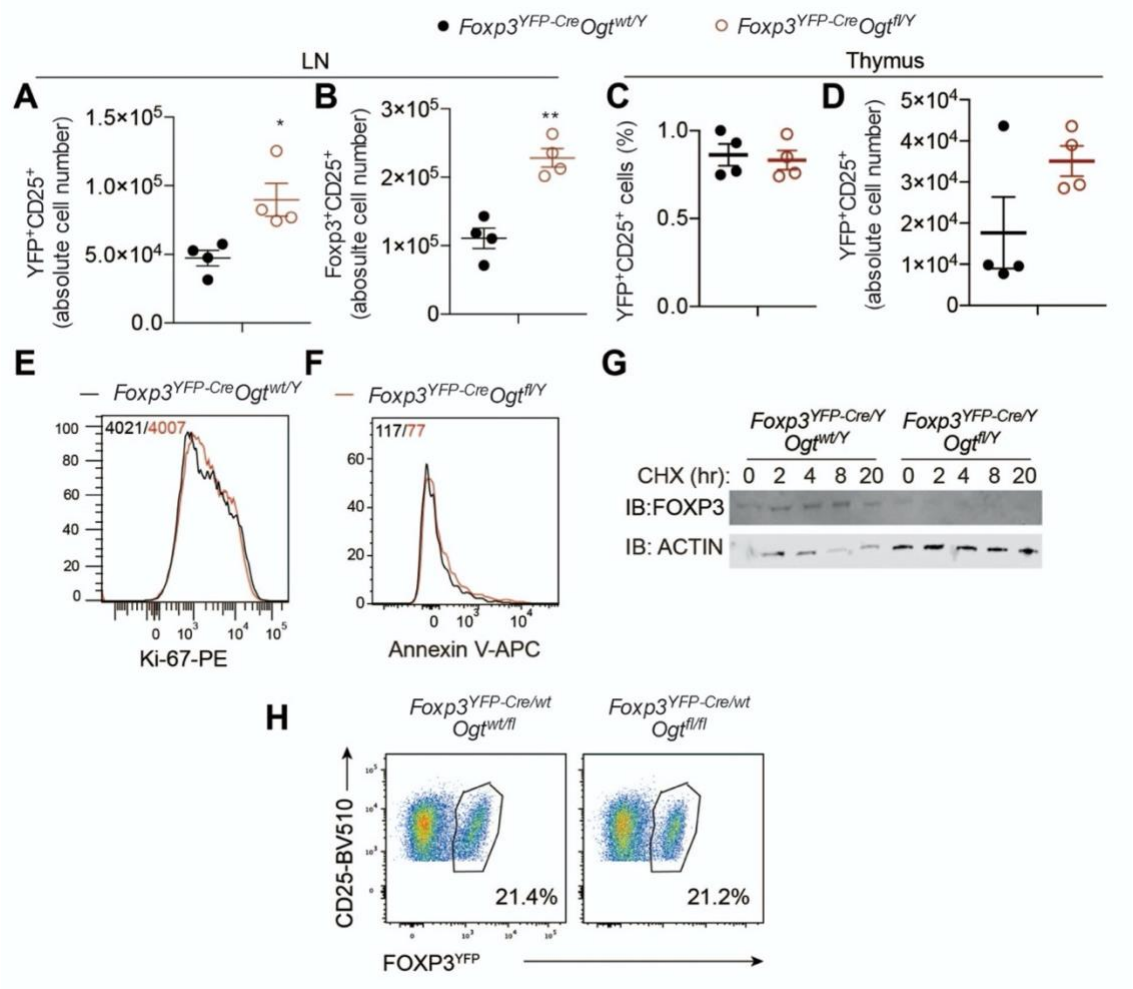

Figure 2.8. *Foxp3*$^{YFP\text{-}Cre/Y}$*Ogt*$^{fl/Y}$ characterization in 2-week-old mice and in the thymus.

(A, B) Total numbers of YFP$^+$CD25$^+$ (A) and FOXP3$^+$CD25$^+$ (B) Treg cells among CD4$^+$ T cells in the LNs from 2-week-old *Foxp3*$^{YFP\text{-}Cre/Y}$ *Ogt*$^{wt/Y}$ and *Foxp3*$^{YFP\text{-}Cre/Y}$ *Ogt*$^{fl/Y}$ mice, n = 4 each group. (C, D) Frequency (C) and total number (D) of YFP$^+$CD25$^+$ Treg cells among CD4$^+$ T cells in the thymus from 2-week-old *Foxp3*$^{YFP\text{-}Cre/Y}$ *Ogt*$^{wt/Y}$ and *Foxp3*$^{YFP\text{-}Cre/Y}$ *Ogt*$^{fl/Y}$ mice, n = 4 each group. (E, F) MFI of Ki-67 (E) and Annexin V (F) among YFP$^+$CD25$^+$ Treg cells in the LNs from 2-week-old *Foxp3*$^{YFP\text{-}Cre/Y}$ *Ogt*$^{wt/Y}$ and *Foxp3*$^{YFP\text{-}Cre/Y}$ *Ogt*$^{fl/Y}$ mice. (G) FOXP3 stability in Treg cells isolated from *Foxp3*$^{YFP\text{-}Cre/Y}$ *Ogt*$^{wt/Y}$ and *Foxp3*$^{YFP\text{-}Cre/Y}$ *Ogt*$^{fl/Y}$ mice was determined by CHX treatment. (H) Frequencies of YFP$^+$ Treg cells in the LNs from *Foxp3*$^{YFP\text{-}Cre/wt}$ *Ogt*$^{wt/fl}$ and *Foxp3*$^{YFP\text{-}Cre/wt}$ *Ogt*$^{fl/fl}$ female mice. Data are shown as mean ± s.e.m. *, p<0.05; **, p<0.01 by unpaired student's *t*-test.

Similar to findings in induced *Ubc-Cre/ERT2*$^+$*Ogt*$^{fl/Y}$ cells ex vivo (see Fig. 2.4A-D), Treg cells from 2-week-old *Foxp3*$^{YFP\text{-}Cre/Y}$*Ogt*$^{fl/Y}$ KO mice had less FOXP3 protein expression than those from control mice (Fig. 2.7C and D). Treating isolated Treg cells from *Foxp3*$^{YFP\text{-}Cre/Y}$*Ogt*$^{wt/Y}$ and *Foxp3*$^{YFP\text{-}Cre/Y}$*Ogt*$^{fl/Y}$ mice with CHX, we were able to find

decreased FOXP3 protein stability in OGT-deficient Treg cells (Fig. 2.8G). In adult *Foxp3*$^{YFP\text{-}Cre/wt}$*Ogt*$^{fl/fl}$ female mice, in which OGT-sufficient (YFP^{-}) and OGT-deficient (YFP^{+}) Treg cells co-existed because of random inactivation of the X chromosome, YFP^{+} OGT-deficient Treg cells displayed similar abundance as those YFP^{+} OGT-sufficient Treg cells in *Foxp3*$^{YFP\text{-}Cre/wt}$*Ogt*$^{wt/fl}$ females (Fig. 2.8H). In *Foxp3*$^{YFP\text{-}Cre/wt}$*Ogt*$^{fl/fl}$ females, FOXP3 expression was lower in OGT-deficient Treg cells than in OGT-sufficient Treg cells (Fig. 2.7E). These data demonstrate that OGT is required for FOXP3 protein stability in Treg cells.

Continuous expression of FOXP3 maintains the Treg-cell identity. In *Foxp3*$^{YFP\text{-}Cre/Y}$*Ogt*$^{fl/Y}$ KO mice, a significant proportion of YFP^{+}CD25^{+} cells lost FOXP3 expression when compared to their *Foxp3*$^{YFP\text{-}Cre/Y}$*Ogt*$^{wt/Y}$ counterparts (Fig. 2.7F), suggesting that OGT-deficient cells tend to become the so-called “ex-Treg” cells or “latent” Treg cells [116]. To directly trace the *Foxp3* lineage, we crossed inducible *Foxp3*$^{eGFP\text{-}Cre\text{-}ERT2/Y}$*Ogt*$^{fl/Y}$ mice to the *Rosa26*^{tdTomato} Cre-reporter line, in which a *loxP*-flanked STOP cassette preventing transcription of the tdTomato protein was inserted into the *Rosa26* locus [133]. Tamoxifen-containing diet feeding induced Treg cell-specific ablation of protein O-GlcNAcylation (Fig. 2.9A) and progressive systemic inflammation in *Foxp3*$^{eGFP\text{-}Cre\text{-}ERT2/Y}$ *Ogt*$^{fl/Y}$ *Rosa26*$^{tdTomato/wt}$ mice (Fig. 2.9B-E). Gating on the CD4^{+}GITR^{+}tdTomato^{+} population, we found that more FOXP3^{-}tdTomato^{+} ex-Treg cells emerged in *Foxp3*$^{eGFP\text{-}Cre\text{-}ERT2/Y}$*Ogt*$^{fl/Y}$ *Rosa26*$^{tdTomato/wt}$ KO mice than in *Foxp3*$^{eGFP\text{-}Cre\text{-}ERT2/Y}$ *Ogt*$^{wt/Y}$ *Rosa26*$^{tdTomato/wt}$ controls (Fig. 2.7G). These ex-Treg cells were prone to express the Th1 transcription factor T-BET and the Th2 transcription factor GATA3, but not the Th17 transcription factor RORγT (Fig. 2.7H and I). These results show that OGT-mediated protein O-GlcNAcylation contributes to the maintenance of Treg lineage stability.

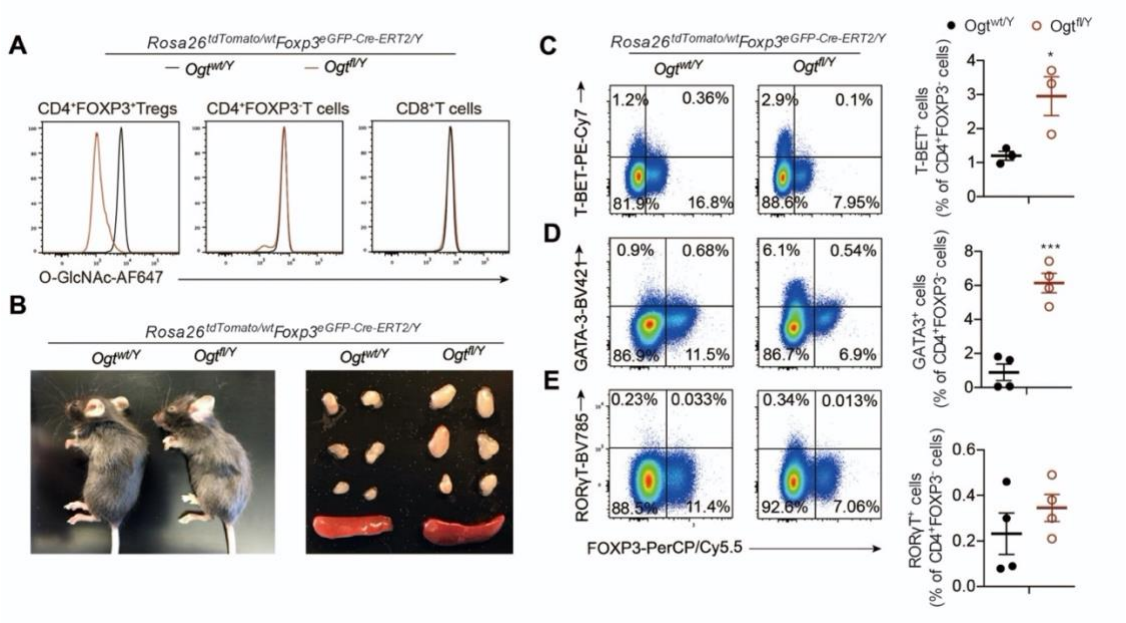

Figure 2.9. Tamoxifen-containing diet feeding induced Treg cell-specific ablation of protein O-GlcNAcylation.

(A) MFI of O-GlcNAcylation in indicated cell populations from *Foxp3*$^{eGFP\text{-}Cre\text{-}ERT2/Y}$ *Ogt*$^{wt/Y}$ *Rosa26*$^{tdTomato/wt}$ and *Foxp3* $^{eGFP\text{-}Cre\text{-}ERT2/Y}$ *Ogt*$^{fl/Y}$ *Rosa26*$^{tdTomato/wt}$ mice. (B) Representative images of 6-week-old *Foxp3*$^{eGFP\text{-}Cre\text{-}ERT2/Y}$ *Ogt*$^{wt/Y}$ *Rosa26*$^{tdTomato/wt}$ and *Foxp3* $^{eGFP\text{-}Cre\text{-}ERT2/Y}$ *Ogt*$^{fl/Y}$ *Rosa26*$^{tdTomato/wt}$ mice fed tamoxifen food for 3 weeks and peripheral LNs and spleen. (C-E) T-BET^{+} FOXP3^{-} cells (C), GATA3^{+} FOXP3^{-} cells (D) and RORγT^{+} FOXP3^{-} cells (E) among CD4^{+} T cells in LNs from *Foxp3*$^{eGFP\text{-}Cre\text{-}ERT2/Y}$ *Ogt*$^{wt/Y}$ *Rosa26*$^{tdTomato/wt}$ and *Foxp3* $^{eGFP\text{-}Cre\text{-}ERT2/Y}$ *Ogt*$^{fl/Y}$ *Rosa26*$^{tdTomato/wt}$ mice, n = 3-4. Data are shown as mean ± s.e.m. Data are shown as mean ± s.e.m. *p<0.05; ***p<0.001 by unpaired student's t-test.

2.2.4 O-GlcNAcylation is indispensable for the development of effector Treg cells

In mature Treg cells, IL-2 and TCR signaling are not only required for lineage stability, but also for suppressive function, partially via the AKT-mTOR axis [134]. The intensity of S6 phosphorylation but not AKT S473 phosphorylation was decreased in OGT-deficient Treg cells (Fig. 2.10A), suggesting a mTORC1-specific defect. In *Foxp3*$^{YFP\text{-}Cre/Y}$ *Ogt*$^{fl/Y}$ mice, we found that the abundance of CD44^{hi}CD62L^{lo} effector Treg (eTreg) cells was significantly lower than *Foxp3*$^{YFP\text{-}Cre/Y}$ *Ogt*$^{wt/Y}$ counterparts (Fig. 2.11A). Strikingly, eTreg cells that express signature effector molecules such as KLRG1 [135], PD-1 [136], and CD73 [137] were almost eliminated in *Foxp3*$^{YFP\text{-}Cre/Y}$ *Ogt*$^{fl/Y}$ mice (Fig. 2.11B-D).

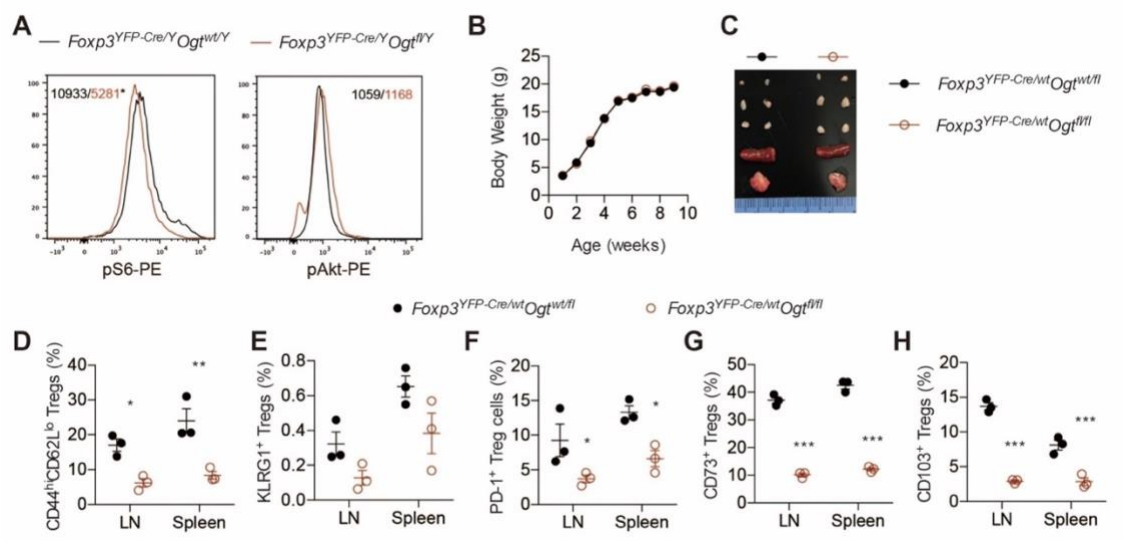

Figure 2.10. Treg characterization in *Foxp3*$^{YFP\text{-}Cre/wt}$ *Ogt*$^{fl/fl}$ female mice.

(A) MFI of pS6 and pS473-AKT among CD4$^+$FOXP3$^+$ Treg cells in LNs of 2-week-old *Foxp3*$^{YFP\text{-}Cre/Y}$ *Ogt*$^{wt/Y}$ and *Foxp3*$^{YFP\text{-}Cre/Y}$ *Ogt*$^{fl/Y}$ mice, n = 2. (B, C) Body weight (B, n = 12) and representative images of peripheral LNs, spleen and thymus (C) of *Foxp3*$^{YFP\text{-}Cre/wt}$*Ogt*$^{wt/fl}$ and *Foxp3*$^{YFP\text{-}Cre/wt}$*Ogt*$^{fl/fl}$ female mice. (D-H) Frequencies of indicated cell populations among YFP$^+$ Treg cells in the LNs and spleen from *Foxp3*$^{YFP\text{-}Cre/wt}$ *Ogt*$^{wt/fl}$ and *Foxp3*$^{YFP\text{-}Cre/wt}$ *Ogt*$^{fl/fl}$ female mice, n = 3 each group. Data are shown as mean ± s.e.m. **p*<0.05; ***p*<0.01; ****p*<0.001 by unpaired student's *t*-test.

Foxp3$^{YFP\text{-}Cre/wt}$ *Ogt*$^{fl/fl}$ female mice were devoid of autoimmune defects (Fig. 2.10B and C), since they possessed both OGT-sufficient (YFP$^-$) and OGT-deficient (YFP$^+$) Treg cells because of random inactivation of the X chromosome. Nevertheless, we could observe significant reductions in the abundance of CD44^{hi}CD62L^{lo}, KLRG1$^+$, PD-1$^+$, CD73$^+$, and CD103$^+$ eTreg cells when comparing YFP$^+$ OGT-deficient to YFP$^-$ OGT-sufficient cells in the same *Foxp3*$^{YFP\text{-}Cre/wt}$*Ogt*$^{fl/fl}$ mice (Fig. 2.11E-I). Similar reductions in eTreg signature molecules could be observed when comparing YFP$^+$ Treg cells between *Foxp3*$^{YFP\text{-}Cre/wt}$*Ogt*$^{fl/fl}$ and *Foxp3*$^{YFP\text{-}Cre/wt}$*Ogt*$^{wt/fl}$ mice (Fig. 2.10.D-H). These data indicate a cell-intrinsic loss of effector molecules in OGT-deficient Treg cells.

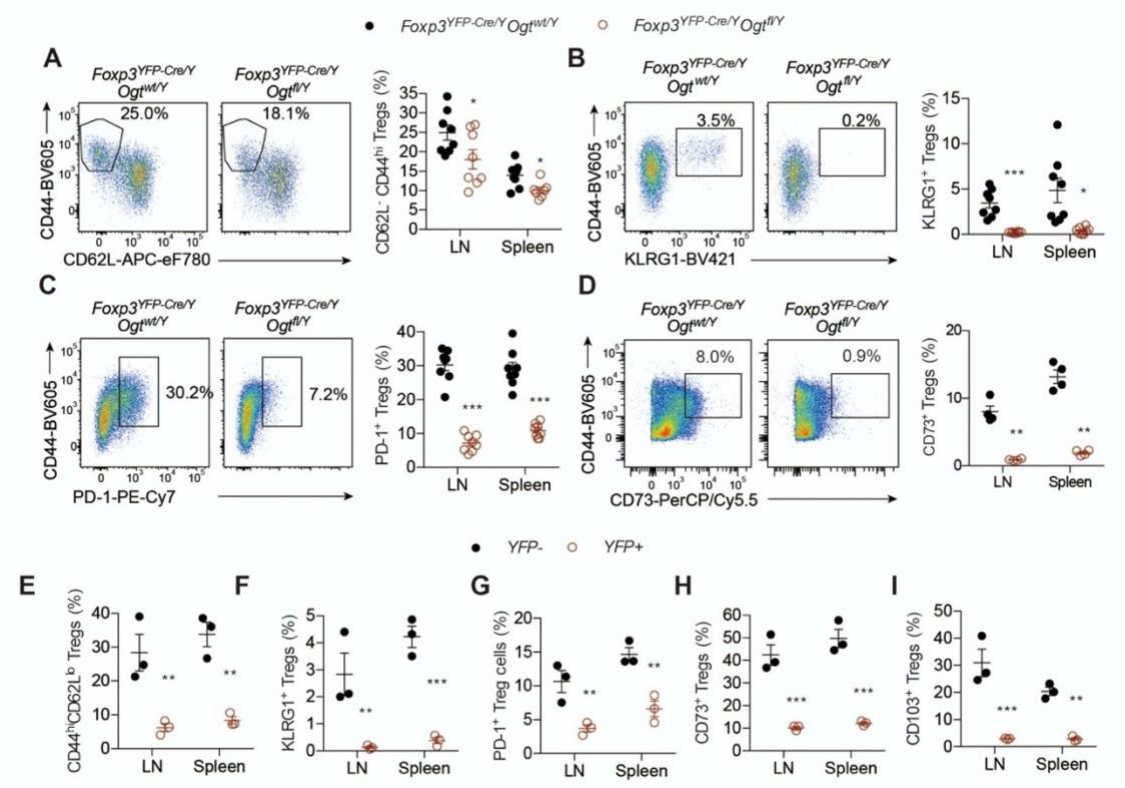

Figure 2.11. O-GlcNAcylation is required for the effector differentiation of Treg cells.

(A, D) Frequencies of $CD44^{hi}CD62L^{lo}$ (A), $CD44^{+}KLRG1^{+}$ (B), $CD44^{+}PD\text{-}1^{+}$ (C), and $CD44^{+}CD73^{+}$ (D) cells among $YFP^{+}CD25^{+}$ Treg cells in the LNs and spleen from 2-week-old *Foxp3*$^{YFP\text{-}Cre/Y}$ *Ogt*$^{wt/Y}$ and *Foxp3*$^{YFP\text{-}Cre/Y}$ *Ogt*$^{fl/Y}$ mice, at least n = 4 each group. (E-I) Frequencies of indicated cell populations among YFP^{-} OGT-sufficient and YFP^{+} OGT-deficient $CD4^{+}TCR\beta^{+}CD25^{+}GITR^{+}$ Treg cells in the LNs and spleen from *Foxp3*$^{YFP\text{-}Cre/wt}$ *Ogt*$^{fl/fl}$ mice, n = 3 each group. Data are shown as mean ± s.e.m. **p*<0.05; *p*<0.01; ****p*<0.001 by unpaired student's *t*-test.

2.2.5 Attenuated IL-2/STAT5 signaling in OGT-deficient Treg cells

It seemed unlikely to us that the mild downregulation of FOXP3 protein stability could account for the absence of eTreg-cell formation, as FOXP3 binds to the same set of regulatory elements in both resting Treg cells and eTreg cells [138]. To gain comprehensive insight into the OGT-dependent transcriptional program in Treg cells, we performed RNA-sequencing of isolated YFP^{+} Treg cells from *Foxp3*$^{YFP\text{-}Cre/wt}$*Ogt*$^{wt/fl}$ and healthy *Foxp3*$^{YFP\text{-}Cre/wt}$*Ogt*$^{fl/fl}$ females to avoid secondary changes in gene expression caused by inflammation. We were able to identify 269 differentially expressed genes including 154 downregulated and 115 upregulated with p values less

than 0.01 (Fig. 2.12A). eTreg-cell markers such as *klrg1*, *S100a4*, *Gzmb*, and *Ccr2* were downregulated by the loss of O-GlcNAcylation (Fig. 2.12A). The transcription factor B lymphocyte-induced maturation protein (BLIMP)-1 is common to all eTreg cells [139], and we found that BLIMP-1-upregulated genes were enriched in OGT-sufficient Treg cells, while BLIMP-1-downregulated genes were enriched in OGT-deficient Treg cells (Fig. 2.12B and C), suggesting that OGT maintains a transcriptional program similar to that of BLIMP-1$^+$ eTreg cells. Ingenuity Pathway Analysis (IPA) identified 9 potential upstream regulators which were all predicted to be inhibited, and the top one was IL-2 (Fig. 2.12D). To evaluate the responsiveness of Treg cells to IL-2, we treated mice with immune complexes consisting of mouse IL-2 and anti-IL-2 antibody to expand eTreg cells (Fig. 2.13A) [135,140]. IL-2 immune complex treatment moderately enlarged the LNs and spleen but did not change total protein O-GlcNAcylation in Treg cells (Fig. 2.13B, C), suggesting IL-2 does not directly regulate O-GlcNAc signaling. However, protein O-GlcNAcylation was required for IL-2-stimulated development of eTreg cells, as the expansion of KLRG1$^+$, GZMB$^+$, and BLIMP-1$^+$ eTreg populations was absent in OGT-deficient Treg cells (Fig. 2.12E-J and Fig. 2.13D). The increase in the expression of CD25 and IL-10 induced by IL-2 in OGT-sufficient cells was also inhibited when OGT was deleted (Fig. 2.13E and F).

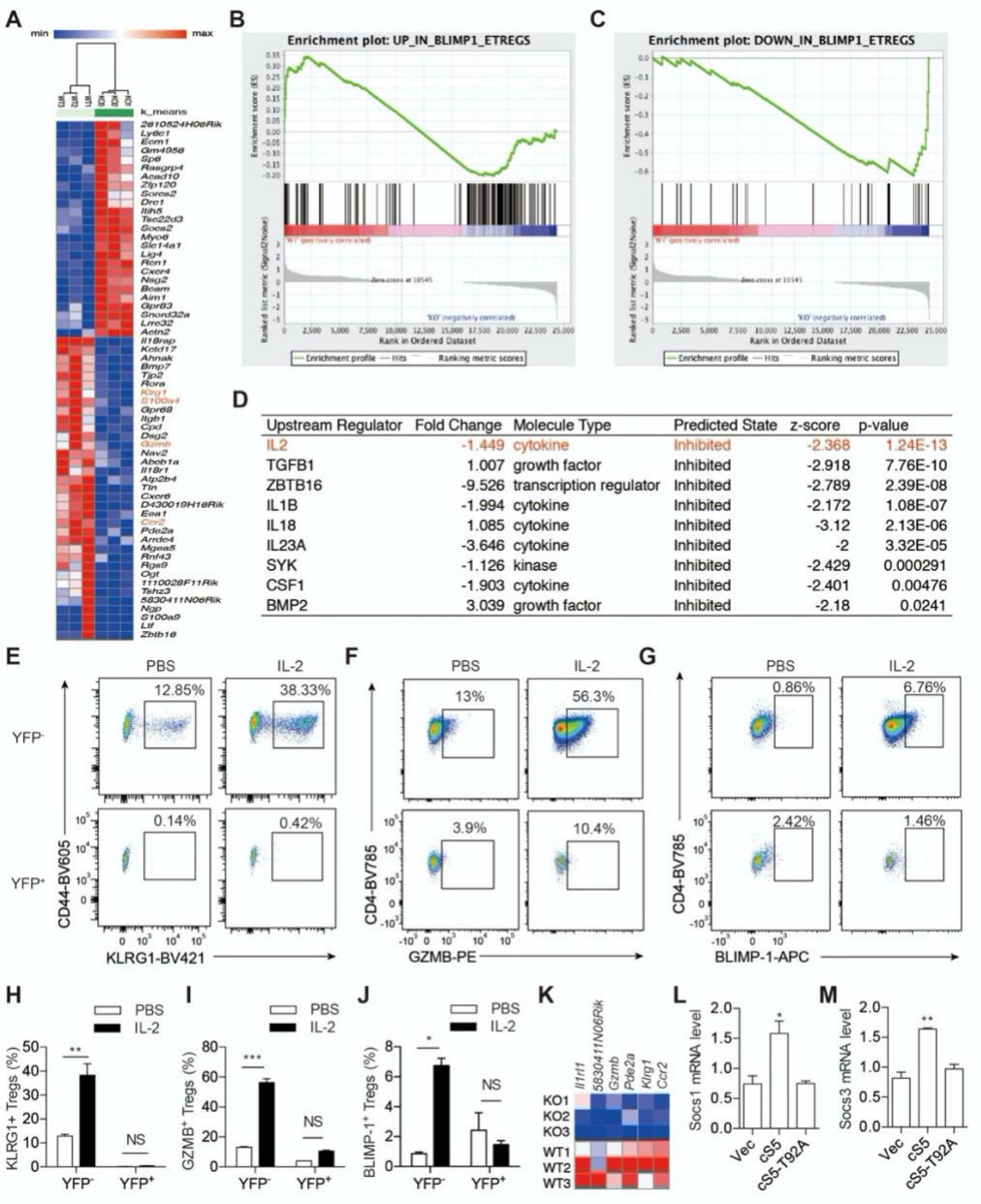

Figure 2.12. Attenuated IL-2/STAT5 signaling in OGT-deficient Treg cells.

(A) Hierarchical clustering of top differentially expressed genes (60 genes with FDR q values less than 0.1) between OGT-sufficient and -deficient Treg cells using Morpheus. (B, C) Enrichment plots for up- (B) and down-regulated (C) genes in Blimp1^{+} eTreg cells from the Gene Set Enrichment Analysis (GSEA) of differentially expressed genes between OGT-sufficient and -deficient Treg cells. (D) Ingenuity Pathway Analysis (IPA) of predicted upstream regulators for observed changes in gene expression. (E-J) *Foxp3*$^{YFP\text{-}Cre/wt}$ *Ogt*$^{fl/fl}$ female mice were injected with PBS or the IL-2 immune complex (n = 2-5) for 3 consecutive days. Flow cytometry of CD44^{+}KLRG1^{+}(E), CD4^{+}GZMB^{+} (F) and CD4^{+}BLIMP-1^{+} (G) Treg cells among YFP^{-} OGT-sufficient and YFP^{+} OGT-deficient Treg cells (CD4^{+}CD25^{+}GITR^{+}) in LNs and spleen and corresponding frequencies in (H-J). (K) Expression of STAT5-target genes in OGT-sufficient and -deficient Treg cells. (L-M) mRNA levels of *Socs1* (L) and *Socs3* (M) in OGT-sufficient Treg

cells after retrovirus infection as indicated, n = 3 each group. Data are shown as mean ± s.e.m. *p<0.05; **p<0.01; ***p<0.001 by two-way ANOVA (H-J) and one-way ANOVA (L, M).

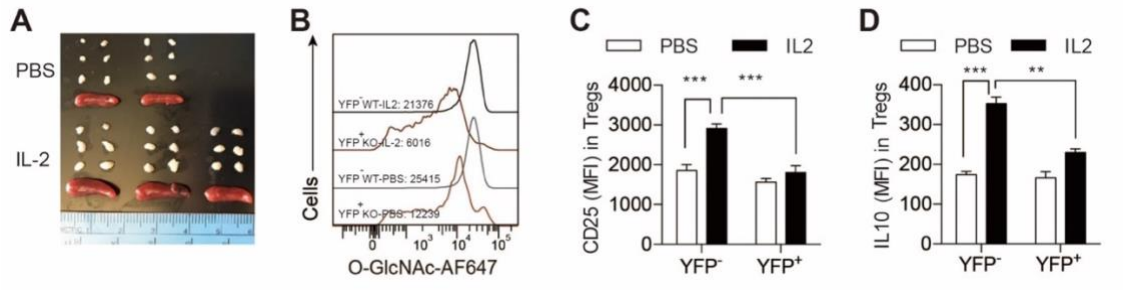

Figure 2.13. Treatment with IL-2 in *Foxp3*$^{YFP\text{-}Cre/wt}$ *Ogt*$^{fl/fl}$ female mice.

Foxp3$^{YFP\text{-}Cre/wt}$ *Ogt*$^{fl/fl}$ female mice were injected with PBS or the IL-2 immune complex for 3 consecutive days (A) Peripheral LNs and Spleen. (B) MFI of O-GlcNAcylation among YFP$^-$ OGT-sufficient or YFP$^+$OGT-deficient Treg cells (CD4$^+$CD25$^+$GITR$^+$). (C, D) MFI of CD25 (C) and IL10 (D) among YFP$^-$OGT-sufficient or YFP$^+$OGT-deficient Treg cells (CD4$^+$CD25$^+$GITR$^+$), n = 2-5. Data are shown as mean ± s.e.m. **p<0.01; ***p<0.001 by unpaired student's t-test.

STAT5, acting downstream of IL-2, is indispensable for the formation of KLRG1$^+$ terminally differentiated Treg cells and their suppressive function [121,135]. O-GlcNAcylation of STAT5 has been shown to promote its oligomerization and transcriptional activity in cooperation with tyrosine phosphorylation in neoplastic cells [141]. Consistent with the defective IL-2 response, many STAT5-target genes were downregulated in OGT-deficient Treg cells (Fig. 2.12K). However, the IL-2-activated tyrosine phosphorylation of STAT5 (pY-STAT5) in Treg cells was not affected by the loss of OGT (Fig. 2.14A and B), again supporting the notion that O-GlcNAcylation can act independently of tyrosine phosphorylation [141]. O-GlcNAcylation seemed not to regulate the cellular localization of STAT5 either (Fig. 2.14C). Retroviral expression of a constitutively active STAT5A (cS5) in Treg cells increased the expression of the STAT5-target gene *Socs1* and *Socs3*, whereas the O-GlcNAc-deficient cS5-T92A diminished such effect [141] (Fig. 2.12L, M). Moreover, in OGT-deficient Treg cells, reconstitution of cS5 but not cS5-T92A increased *Socs1* expression (Fig. 2.14D), suggesting that STAT5 O-GlcNAcylation is important for its transcriptional activity. Collectively, these data demonstrate that the deficiency in protein O-GlcNAcylation results in attenuated IL-2/STAT5 activity in Treg cells.

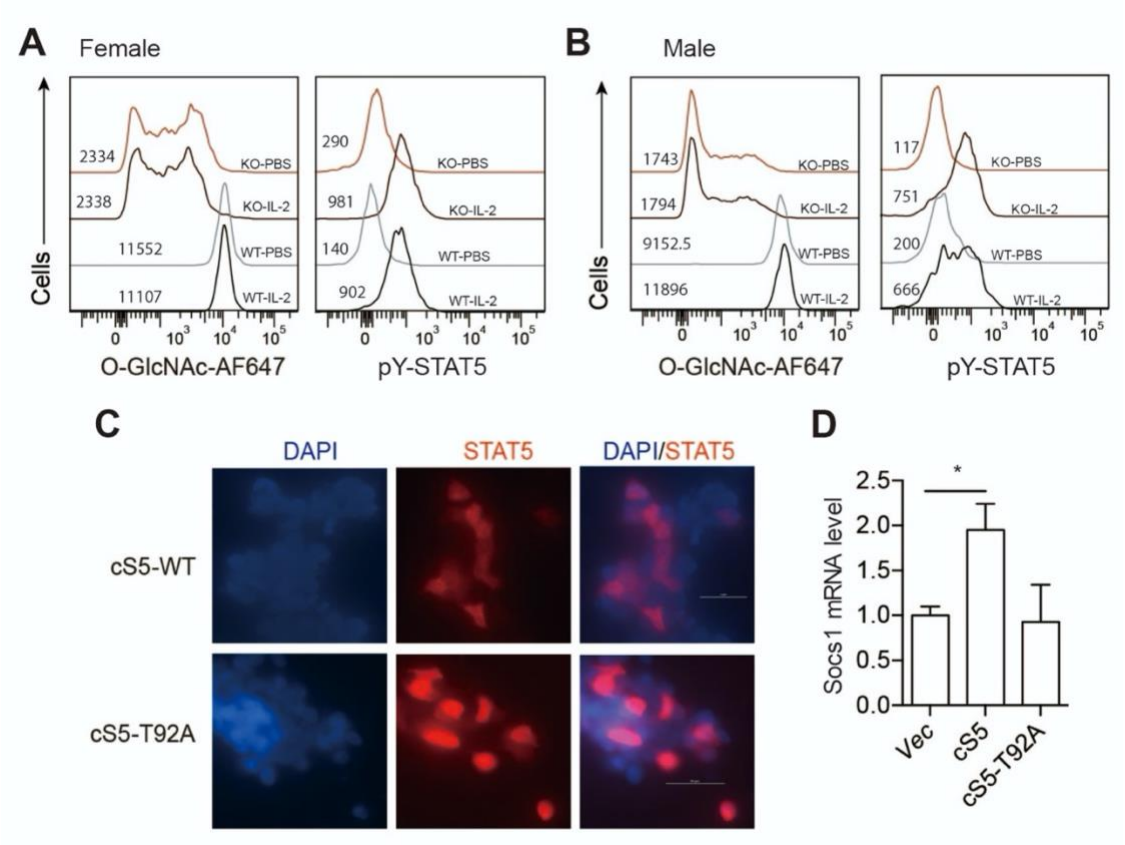

Figure 2.14. IL-2-activated tyrosine phosphorylation of STAT5 (pY-STAT5) in Treg cells was not affected by the loss of OGT.

(A, B) MFI of O-GlcNAcylation and pY-STAT5 among YFP^{+}CD25^{+} Treg cells in the LNs from *Foxp3*$^{YFP\text{-}Cre/wt}$ *Ogt*$^{wt/fl}$ and *Foxp3*$^{YFP\text{-}Cre/wt}$ *Ogt*$^{fl/fl}$ female mice (A) and *Foxp3*$^{YFP\text{-}Cre/Y}$ *Ogt*$^{wt/Y}$ and *Foxp3*$^{YFP\text{-}Cre/Y}$ *Ogt*$^{fl/Y}$ male mice (B) stimulated with IL-2 in vitro, PBS incubation was used as control. (C) Representative images of STAT5 nuclear translocation in HEK 293 cells transfected with cS5 or cS5-T92A. (D) mRNA levels of *Socs1* in OGT-deficient Treg cells after retrovirus infection as indicated, n = 3. Data are shown as mean ± s.e.m. *, p<0.05 by one-way ANOVA.

2.2.6 Constitutive activation of STAT5 partially rescues Treg-cell dysfunction

Treg cell-specific deletion of OGT resulted in a scurfy phenotype with comparable early onset and disease severity to those observed upon IL-2R or STAT5 ablation [121]. Expression of a constitutively active form of STAT5B-CA partially rescues IL-2R deficient Treg function [121]. We next sought to determine whether STAT5 activation could restore Treg cell function in *Foxp3*$^{YFP\text{-}Cre/Y}$ *Ogt*$^{fl/Y}$ mice by crossing them to a Cre-inducible line overexpressing STAT5B-CA at the *Rosa26* locus (*Rosa26*$^{Stat5b\text{-}}$

^{CA}) [121]. Remarkably, the *Foxp3*$^{YFP\text{-}Cre/Y}$*Ogt*$^{fl/Y}$*Rosa26*$^{Stat5b\text{-}CA/wt}$ mice with STAT5B-CA overexpression specifically in OGT-deficient Treg cells alleviated skin inflammation (Fig. 2.15A), reduced size of the LNs and spleen (Fig. 2.15B), and prolonged lifespan (Fig. 2.15C), when compared to *Foxp3*$^{YFP\text{-}Cre/Y}$*Ogt*$^{fl/Y}$ mice. Consistent with the role of STAT5 in regulating *Foxp3* transcription and Treg-cell development [107,121,142], FOXP3 protein expression was restored to a level comparable to wildtype mice and the frequency of Treg cells was further increased when STAT5B-CA was present (Fig. 2.15D, E, and Fig. 2.16A). Meanwhile, the eTreg cell population was significantly boosted to a level comparable to wildtype mice, shown as CD44^{hi}CD62L^{lo} (Fig. 2.15F and Fig. 2.16B) and CD44^{+}KLRG1^{+} subsets (Fig. 2.15G and Fig. 2.16C). However, the expression levels of CD73 and PD-1 on a per-cell basis did not change (Fig. 2.16D), suggesting a partial rescue in the suppressive function of Treg cells by STAT5B-CA. Moreover, the fraction of YFP^{+} OGT-deficient Treg cells that lost FOXP3 expression as a result of protein instability was substantially inhibited by the presence of STAT5B-CA (Fig. 2.15H and Fig. 2.16E), indicating that STAT5B-CA also restored Treg lineage stability.

Accordingly, STAT5B-CA overexpression reduced the number of total CD4^{+} and CD8^{+} T cells (Fig. 2.15I and J) and the frequency of memory/effector CD4^{+} and CD8^{+} T cells in *Foxp3*$^{YFP\text{-}Cre/Y}$*Ogt*$^{fl/Y}$*Rosa26*$^{Stat5b\text{-}CA/wt}$ mice (Fig. 2.15K, L, and Fig. 2.16F). In addition, STAT5B-CA overexpression prevented the increase in Th1 and Th2 cells caused by loss of O-GlcNAcylation in Treg cells (Fig. 2.15M-O and Fig. 2.16G) and reduced the production of IFNγ by CD4^{+} and CD8^{+} T cells (Fig. 2.15P and Fig. 2.16H and I). Collectively, these data show that restoring STAT5 signaling in OGT-deficient Treg cells improves lineage stability and suppressive function, thereby delaying the autoimmune responses in mice.

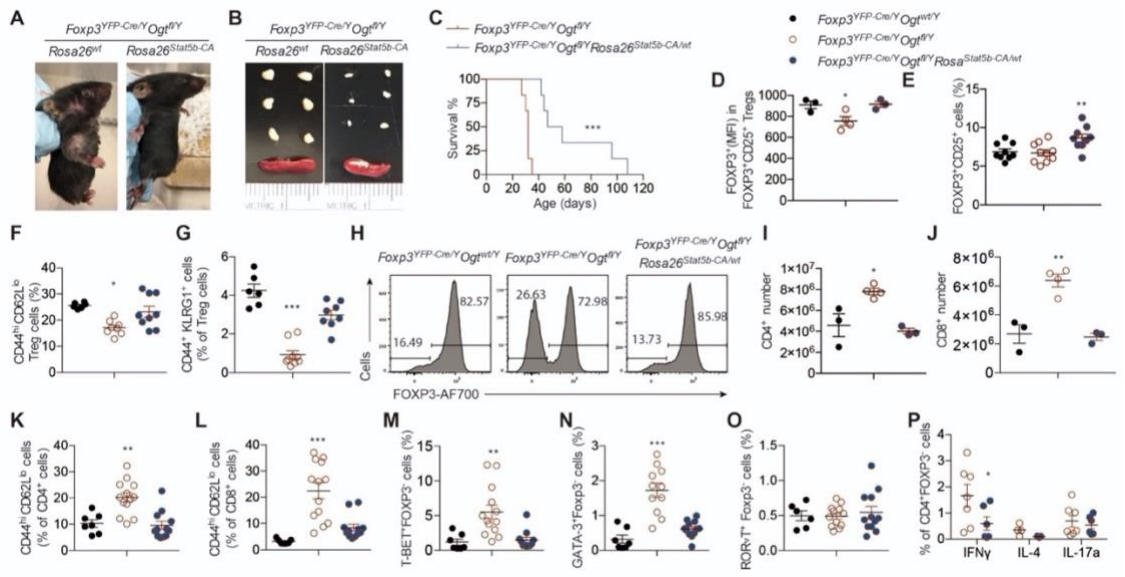

Figure 2.15. Constitutive activation of STAT5 partially rescues Treg cell dysfunction.

(A, B) Representative images of mice (A) and peripheral LNs and spleen (B) from 2-week-old *Foxp3*$^{YFP\text{-}Cre/Y}$ *Ogt*$^{fl/Y}$ and *Foxp3*$^{YFP\text{-}Cre/Y}$*Ogt*$^{fl/Y}$ *Rosa26*$^{Stat5b\text{-}CA/wt}$ mice. (C) Survival curve of *Foxp3*$^{YFP\text{-}Cre/Y}$ *Ogt*$^{fl/Y}$ and *Foxp3*$^{YFP\text{-}Cre/Y}$*Ogt*$^{fl/Y}$ *Rosa26*$^{Stat5b\text{-}CA/wt}$ mice (n = 6). (D) MFI of FOXP3 in FOXP3^{+}CD25^{+} Treg cells in the LNs from 2-week-old *Foxp3*$^{YFP\text{-}Cre/Y}$ *Ogt*$^{wt/Y}$, *Foxp3*$^{YFP\text{-}Cre/Y}$ *Ogt*$^{fl/Y}$ and *Foxp3*$^{YFP\text{-}Cre/Y}$*Ogt*$^{fl/Y}$ *Rosa26*$^{Stat5b\text{-}CA/wt}$ mice, at least n = 3 each group. (E) Frequencies of FOXP3^{+}CD25^{+} Treg cells among CD4^{+} T cells, at least n = 9 each group. (F-G) Frequencies of CD44^{hi}CD62L^{lo} (F) and CD44^{+}KLRG1^{+} (G) eTreg cells among FOXP3^{+}CD25^{+} Treg cells in the LNs from 2-week-old *Foxp3*$^{YFP\text{-}Cre/Y}$ *Ogt*$^{wt/Y}$, *Foxp3*$^{YFP\text{-}Cre/Y}$ *Ogt*$^{fl/Y}$ and *Foxp3*$^{YFP\text{-}Cre/Y}$*Ogt*$^{fl/Y}$ *Rosa26*$^{Stat5b\text{-}CA/wt}$ mice, at least n = 6 each group. (H) Histogram of FOXP3 expression in CD4^{+}CD25^{+}YFP^{+} Treg cells in the LNs from 2-week-old *Foxp3*$^{YFP\text{-}Cre/Y}$ *Ogt*$^{wt/Y}$, *Foxp3*$^{YFP\text{-}Cre/Y}$ *Ogt*$^{fl/Y}$ and *Foxp3*$^{YFP\text{-}Cre/Y}$*Ogt*$^{fl/Y}$ *Rosa26*$^{Stat5b\text{-}CA/wt}$ mice. (I, J) Absolute number of CD4^{+} (I) and CD8^{+} (J) T cells in the LNs, at least n = 3 each group. (K, L) Frequencies of CD44^{hi}CD62L^{lo} effector T cells in CD4^{+} (K) and CD8^{+} cells (L), at least n = 7 each group. (M-O) Frequencies of T-BET^{+} (M), GATA3^{+} (N) and RORγT^{+} (O) populations among CD4^{+}FOXP3^{-} cells in the LNs, at least n = 6 each group. (P) Frequencies of INFγ, IL-4 and IL-17A-producing CD4^{+}FOXP3^{-} cells from *Foxp3*$^{YFP\text{-}Cre/Y}$ *Ogt*$^{fl/Y}$ and *Foxp3*$^{YFP\text{-}Cre/Y}$*Ogt*$^{fl/Y}$ *Rosa26*$^{Stat5b\text{-}CA/wt}$ mice, at least n = 3 each group. Data are shown as mean ± s.e.m. **p* < 0.05; ***p* < 0.01; ****p* < 0.001 by Kaplan-Meier Analysis (C), unpaired student's t-test (P) and one-way ANOVA (D–G, I–O).

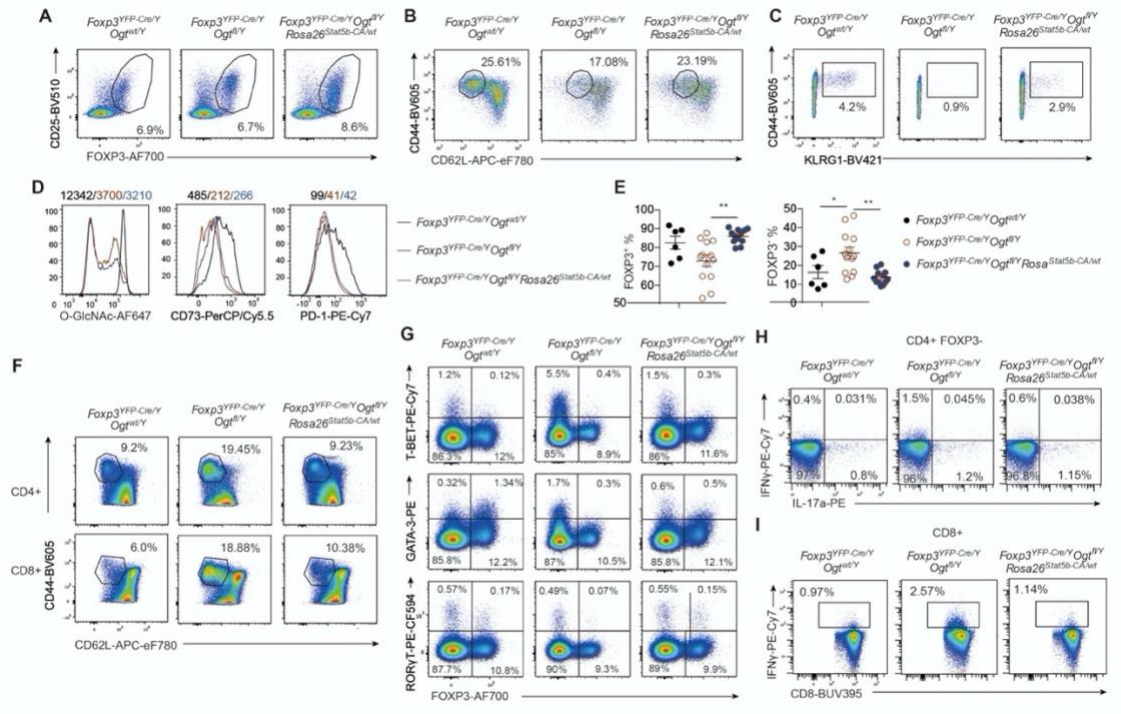

Figure 2.16. Characterization of *Foxp3*$^{YFP\text{-}Cre/Y}$*Ogt*$^{fl/Y}$*Rosa26*$^{Stat5b\text{-}CA/wt}$ mice.

(A) Flow cytometry of FOXP3$^+$CD25$^+$ Treg cells among CD4$^+$ T cells in the LNs from *Foxp3*$^{YFP\text{-}Cre/Y}$ *Ogt*$^{wt/Y}$, *Foxp3*$^{YFP\text{-}Cre/Y}$ *Ogt*$^{fl/Y}$ and *Foxp3*$^{YFP\text{-}Cre/Y}$*Ogt*$^{fl/Y}$*Rosa26*$^{Stat5b\text{-}CA/wt}$ mice. (B, C) Flow cytometry of CD44^{hi}CD62L^{lo} eTreg cells (B) and CD44$^+$KLRG1$^+$ eTreg cells (C) among FOXP3$^+$CD25$^+$ Treg cells in the LNs from *Foxp3*$^{YFP\text{-}Cre/Y}$ *Ogt*$^{wt/Y}$, *Foxp3*$^{YFP\text{-}Cre/Y}$ *Ogt*$^{fl/Y}$ and *Foxp3*$^{YFP\text{-}Cre/Y}$*Ogt*$^{fl/Y}$*Rosa26*$^{Stat5b\text{-}CA/wt}$ mice. (D) MFI of O-GlcNAcylation, CD73 and PD-1 among FOXP3$^+$CD25$^+$ Treg cells. (E) Frequencies of FOXP3$^+$ and FOXP3$^-$ cells among CD4$^+$CD25$^+$YFP$^+$ Treg cells in the LNs, at least n = 6 each group. (F) Flow cytometry of CD44^{hi}CD62L^{lo} cells among CD4$^+$ and CD8$^+$ T cells in the LNs. (G) Flow cytometry of T-BET$^+$, GATA3$^+$ and RORγT$^+$ population among CD4$^+$FOXP3$^-$ cells in the LNs. (H, I) Flow cytometry of IFNγ-expressing cells among CD4$^+$FOXP3$^-$ (H) and CD8$^+$ T cells (I) in the LNs. Data are shown as mean ± s.e.m. **p*<0.05; ***p*<0.01 by one-way ANOVA.

2.2.7 Activating O-GlcNAcylation promotes the suppressive program of Treg cells

The therapeutic potential of Treg cells for autoimmune disorders and graft-versus-host disease (GVHD) has been well characterized in preclinical and early clinical studies [143,144]. We then asked whether enhancing protein O-GlcNAcylation could augment the suppressive function of Treg cells. We first treated mouse Treg cells with TMG to inhibit OGA (Fig. 2.17A), the enzyme removing O-GlcNAc moieties from proteins [145], and found that elevating protein O-GlcNAcylation by TMG increased the

level of FOXP3 protein on a per cell basis (Fig. 2.17B and C) and the number of $CD4^+FOXP3^+$ Treg cells (Fig. 2.18A), again demonstrating that O-GlcNAcylation stabilizes FOXP3 and Treg cell lineage. In addition, TMG treatment enhanced the expression of STAT5-target genes *Socs1* and *Socs3* (Fig. 2.17D, E), and the expression of activation markers including *Klrg1*, *Pd-1* and, to a lesser extent, *Cd73* and *Cd44* in mouse Treg cells (Fig. 2.17F).

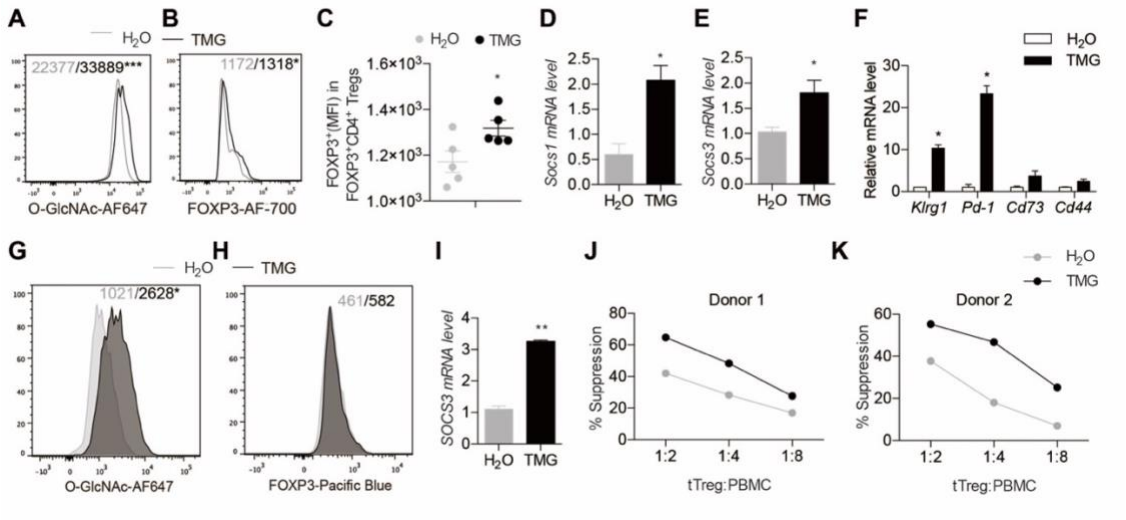

Figure 2.17. Activating O-GlcNAcylation promotes Treg-cell suppressive function.

(A-C) MFI of protein O-GlcNAcylation (A), FOXP3 (B, C) in mouse $CD4^+FOXP3^+$ Treg cells treated with TMG, H_2O treatment was used as a control (n = 5). (D, E) mRNA levels of *Socs1*(D) and *Socs3* (E) in mouse Treg cells treated with TMG, H_2O treatment was used as a control (n = 3). (F) Gene expression in iTreg cells treated with TMG, H_2O treatment was used as a control (n = 2). (G, H) MFI of protein O-GlcNAcylation (G) and FOXP3 (H) in human tTreg cells treated with TMG for 7 days (n = 3), H_2O treatment was used as a control. (I) mRNA levels of *SOCS3* in human tTreg cells treated with TMG, H_2O treatment was used as a control (n = 3). (J, K) Suppression activity of human tTreg cells treated with TMG for 7 days, H_2O treatment was used as a control. Data are shown as mean ± s.e.m. **p*<0.05 by unpaired student's *t*-test.

Finally, we purified $CD4^+CD25^+CD127^-CD45RA^+$ naïve human thymus Treg (tTreg) cells from peripheral blood mononuclear cells (PBMNCs) as previously described [146]. OGA inhibition by TMG significantly increased intracellular O-GlcNAc levels (Fig. 2.17G) but had no effect on FOXP3 expression or tTreg-cell expansion (Fig. 2.17H and Fig. 2.18B), indicating that the endogenous O-GlcNAcylation was sufficient to maintain human FOXP3 stability. Nevertheless, we observed a significant increase in the expression of *SOCS3* gene (Fig. 2.17I) and the suppressive activity of human Treg cells when treated with TMG (Fig. 2.17J, K, and Fig. 2.18C). Collectively,

these results reveal a fundamental role for O-GlcNAc signaling in supporting the suppressive program of mouse and human Treg cells.

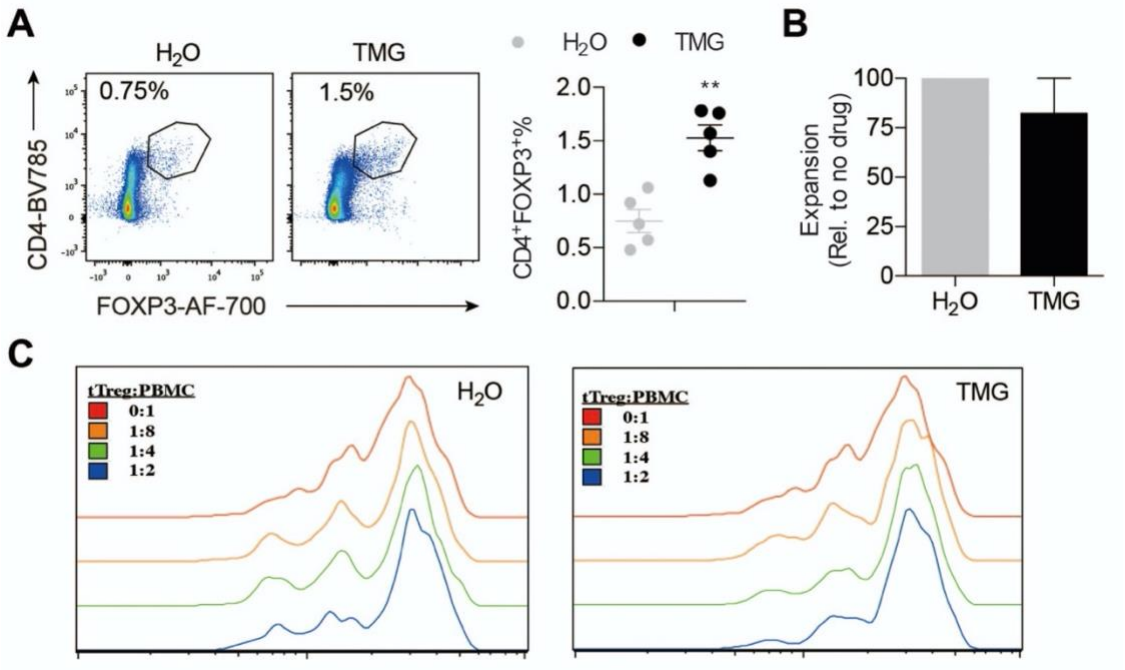

Figure 2.18. TMG treatment of mouse and human Tregs.

(A) Flow cytometry and quantification of the frequencies of mouse $CD4^+FOXP3^+$ Treg cells treated with TMG, H_2O treatment was used as a control, n = 5 each group. (B) Frequencies of human tTreg cells expansion treated with or without TMG for 7 days, n=3. (C) Representative plots showing the cell proliferation of $CD8^+$ cells labeled with CFSE. Data are shown as mean ± s.e.m. ***p*<0.01 by unpaired student's *t*-test.

2.3 Discussion

In mature Treg cells, FOXP3 expression and signals from TCR and IL-2R are continuously required for Treg lineage stability and suppressive function [113,114,119–121,147]. In this study, we have demonstrated that, in response to TCR activation, protein O-GlcNAcylation stabilizes FOXP3 and activates STAT5, thus integrating critical signaling nodes for Treg-cell homeostasis and function.

Our data suggest that O-GlcNAcylation promotes FOXP3 stability by counteracting with ubiquitination. Prior studies have demonstrated that polyubiquitination marks FOXP3 for protein degradation via the proteasome [148–150]. Treatment of Treg cells with a pan-deubiquitinase inhibitor reduces FOXP3 protein levels and decreases suppressive activity [132]. Ubiquitination dynamics of FOXP3 is dictated by the ubiquitin ligase STUB1 and the deubiquitinase USP7 [131,132]. We postulate that O-GlcNAcylation inhibits STUB1-mediated polyubiquitination and/or facilitates USP7-mediated deubiquitination to stabilize FOXP3. By identifying and mutating O-GlcNAc sites on the FOXP3 protein, we were able to show reduced FOXP3 stability when O-GlcNAcylation was ablated (Fig. 2.4), suggesting a potential direct interplay between O-GlcNAcylation and ubiquitination. Nonetheless, O-GlcNAc signaling can modulate proteasome activity and other posttranslational modifications to indirectly control FOXP3 protein abundance [127].

Foxp3$^{YFP\text{-}Cre/Y}$*Ogt*$^{fl/Y}$ mice developed a scurfy phenotype at a similar pace as observed in mice with germline *Foxp3* deficiency [110–112]. When OGT was absent, FOXP3 stability was only modestly reduced ex vivo and in vivo (Fig. 2.4 and 2.7). Thus, FOXP3 instability is only one of the contributors to Treg-cell dysfunction observed in *Foxp3*$^{YFP\text{-}Cre/Y}$*Ogt*$^{fl/Y}$ mice. In Treg cells with TCR ablation, there was also a slight reduction in FOXP3 protein expression, without affecting *Foxp3* transcription [119,120]. It would be interesting to determine whether TCR signaling controls FOXP3 stability through protein O-GlcNAcylation.

In conventional T (Tconv) cells, O-GlcNAcylated proteins are abundant and dynamically regulated by TCR activation [151–153]. These proteins are involved in many biological processes, including TCR signaling (LCK, ZAP70, STAT3, c-JUN, NFAT, etc), transcriptional and translational processes, and mRNA processing. Compared to Tconv cells, Treg cells possess a unique proteomic signature to accommodate specific

metabolic requirements and regulatory function [154,155]. It is unclear if O-GlcNAcylated proteins identified in Tconv cells can be modified in Treg cells. Future O-GlcNAc proteomics is needed to not only profile O-GlcNAcylated proteins in response to TCR activation but also identify other potential targets that could regulate Treg-cell function. Nevertheless, it is unlikely that TCR signaling is a major pathway that mediates the effect of O-GlcNAcylation, as the activation of immune system in Treg-specific TCR deletion mice was much milder than we observed in *Foxp3*$^{YFP\text{-}Cre/Y}$*Ogt*$^{fl/Y}$ mice [119,120].

Through gene expression profiling, we predicted that the IL-2/STAT5 signaling pathway was inhibited in OGT-deficient Treg cells. In accordance with the prediction, we found that eTreg cells failed to expand in response to IL-2 immune complexes when OGT was ablated and the scurfy phenotype in *Foxp3*$^{YFP\text{-}Cre/Y}$*Ogt*$^{fl/Y}$ mice could be partially ameliorated by a constitutive-active form of STAT5B. In OGT-deficient Treg cells, even though the expression of STAT5 target genes was significantly downregulated, we did not observe any change in levels of pY-STAT5, suggesting O-GlcNAcylation can function independently of tyrosine phosphorylation. This is consistent with a recent study showing that O-GlcNAcylation and tyrosine phosphorylation act together to activate STAT5-depedent malignancies [141]. Although O-GlcNAcylation at threonine 92 is required for strong pY-STAT5A upon IL-3 stimulation, erythropoietin-activated pY-STAT5A and IL-2-stimulated T-cell proliferation were comparable between cells expressing constitutively active STAT5A (cS5) and cS5-T92A that lacks O-GlcNAcylation. In addition, there was no significant change in pY-STAT5B when introducing the T92A mutant to human STAT5B or the hyperactive N642H derivative [141]. These findings indicate that O-GlcNAcylation and IL-2-induced pY-STAT5 have separate but additive effects on STAT5 function.

In TCR-triggered naïve T cells, glucose and glutamine flux into the hexosamine biosynthetic pathway (HBP) to generate UDP-GlcNAc, which fuels the protein O-GlcNAcylation [130]. O-GlcNAcylation is critical for self-renewal and malignant transformation of T cell progenitors, thymocyte positive selection, and clonal expansion of peripheral T cells [130]. It is still unclear how TCR-activation promotes the HBP flux. In addition, Treg cells and CD4^{+} Tconv cells program distinct cellular metabolism [156]. Tconv cells are dependent on aerobic glycolysis and glutaminolysis to fulfill their bioenergetic and biosynthetic demand of proliferation [157]. However, Treg cells couple

TCR and IL-2R signals with mTORC1-dependent lipid biosynthesis to establish their functional program [134]. It is thus unlike that TCR-activated protein O-GlcNAcylation in Treg cells is a result of increased glucose flux. Recently, our findings in hepatocytes have indicated that Ca^{2+}-dependent CaMKII phosphorylates and activates OGT [158]. Ca^{2+} release is induced downstream of TCR signaling and the Ca^{2+}-dependent serine-threonine phosphatase Calcineurin, by dephosphorylating and mediating nuclear translocation of NFAT, is crucial for Treg cell development [159,160]. It is warranted to test whether Ca^{2+} signaling mediates TCR-activated O-GlcNAcylation via modulating OGT activity.

Treg cells restrain autoimmune disease, suppress inflammation, prevent organ transplant rejection, and contribute to immune dysfunctions in some infections and cancers [161,162]. However, challenges for Treg cell immunotherapy exist as Treg cells display functional instability and heterogeneity. Our study has identified OGT and protein O-GlcNAcylation as a regulatory hub connecting TCR, FOXP3, and IL-2R to support Treg-cell lineage stability and suppressive function. More importantly, pharmacological elevation of O-GlcNAcylation by inhibiting OGA augments the suppressive activity of human Treg cells, thus targeting O-GlcNAcylation can facilitate the translation of Treg cell therapy into the clinic to treat diseases such as autoimmune disorders, inflammation, and GVHD.

2.4 Methods

2.4.1 Mice

Foxp3$^{YFP\text{-}cre}$ mice (stock number 016959) and *Foxp3*$^{eGFP\text{-}Cre\text{-}ERT2}$ mice (stock number 016961) were purchased from the Jackson Laboratory. *Rosa26*$^{Stat5b\text{-}CA}$ mice were provided by Dr. Alexander Rudensky at Memorial Sloan Kettering Cancer Center [121]. *Ogt*$^{fl/fl}$ Mice (Jackson Laboratory stock number 004860) were kindly provided by Dr. Xiaoyong Yang at Yale University. *Rosa26*^{tdTomato} reporter mice (Jackson Laboratory stock number 007909) were kindly provided by Dr. Jop van Berlo at University of Minnesota. *Ubc*$^{CreER+}$ mice (Jackson Laboratory stock number 007001) were kindly provided by Dr. Doug Mashek at University of Minnesota. All mice were on C57BL/6 background. *Foxp3*$^{YFP\text{-}Cre/Y}$ *Ogt*$^{fl/Y}$ male mice were used at 2-week-old unless specific noted, with the same age *Foxp3*$^{YFP\text{-}Cre/Y}$ *Ogt*$^{wt/Y}$ as control. Other mice were used at 6-12 weeks old unless specific noted. Mice were free to access water and fed on a regular chow or Tamoxifen food (Teklad, TD.130860) as indicated. All procedures were approved by the Institutional Animal Care and Use Committee at the University of Minnesota.

For IL-2-immune complex administration, IL-2 (eBioscience, catalog no. 14-8021-64) and JES6-1A12 (eBioscience, catalog no. 16-7022-81) were incubated at a molar ratio of 2 to 1 in PBS at room temperature for 30 min followed by 3 consecutive days i.p. injections. For female mice, each mouse received 1 μg of IL-2 and 5 μg of JES6-1A12 in 200ul PBS at 6-week-old. For male mice, each mouse received 0.5 μg of IL-2 and 2.5 μg JES6-1A12 in 100ul PBS at 2-week-old.

For histology, mouse tissues were dissected and fixed in 10% buffered formalin. Sectioning and haematoxylin & eosin (H&E) staining were performed by the Comparative Pathology Shared Resource of UMN.

2.4.2 Human participants

Nonmobilized PB leukapheresis products were collected from normal adult volunteers with Food and Drug Administration (FDA)–approved/cleared apheresis instruments at Memorial Blood Center (St. Paul, MN) as previously described [146].

Written informed consent was obtained from all subjects with approval from the University of Minnesota Institutional Review Board.

2.4.3 Naïve T cell isolation and *in vitro* Treg cell induction.

Naïve $CD4^+$ T cells were purified from lymph nodes and spleen according to the protocol provided by the manufacturer (Invitrogen, catalog no. 11461D). Plates were coated with 10 μg/ml of anti-mouse CD3ε antibody (BioLegend catalog no. 100314) for 4h at 37°C. Before plating the cells, plates were washed once with PBS. Naïve $CD4^+$ T cells were suspended at the concentration of 2 x 10^6/ml in X-Vivo15 serum-free medium (Fisher Scientific, catalog no. 04-744Q) with 2 μg/ml anti-mouse CD28 antibody (BioLegend catalog no. 102112) in the presence or absence of mouse TGF-β (BioLegend catalog no. 763102). Cells were cultured for 5 days before the collection for RNA and immunoblot analysis [163].

2.4.4 Treg cell purification and expansion.

$CD4^+CD25^+$ Treg cells were purified from mouse lymph nodes and spleen according to the protocol provided by the manufacturer (Invitrogen, catalog no. 11463D). Treg cells were expanded according to the Treg Expansion Kit protocol (Miltenyi Biotec, catalog no. 130-095-925). Treg cells were treated with 0.5 μM 4-Hydroxytamoxifen (4-OHT) (Millipore Sigma, catalog no. H7904) for 3 days and 100 μg/ml cycloheximide (CHX) (Millipore Sigma, catalog no. C7698) as indicated. To determine the purity, Treg cells were assessed by flow cytometry and immunoblot analysis.

2.4.5 Flow cytometry

For surface markers, cells were stained in PBS containing 0.5% (wt/vol) BSA with relevant antibodies at 4 °C for 30 min. For analysis of intra- cellular markers, cells were first fixed with Fixation/Permeabilization buffer (ThermoFisher, catalog no. 00–5123) at 4 °C for 30 min and then stained in Per- meabilization Buffer (ThermoFisher, catalog no. 00–8333) with relevant antibodies at 4 °C for 30 min. For detection of Annexin V population, cells were suspended in 100 μl 1× Annexin V binding buffer after surface staining, added 5ul APC-Annexin V at room temperature for 15 min, and then

added 400 µl 1× Annexin V binding buffer for flow cytometry measurement. For pY-STAT5 signaling detection, lym- phocytes were stimulated with IL-2 (0.5 ug/ml in PBS) (BioLegend, catalog no. 575402) at 37 °C for 20 min, fixed with 3% Paraformaldehyde (formaldehyde) aqueous solution (Electron Microscopy Sciences, catalog no. 15710) at 1:1 ratio at room temperature for 10 min, washed with PBS, resuspended in 100% cold methanol at 4 °C for 10 min and finally stained with antibodies for FACS. For intracellular cytokine staining, cells were stimulated with PMA (50 ng/ml, Sigma, catalog no. P1585) and Ionomycin (500 ng/ml, Sigma, catalog no. I3909), together with GolgiPlug (BD Biosciences, catalog no. 555029) for INFγ, IL-5, IL-13, and IL- 17A or GolgiStop (BD Biosciences, catalog no. 554724) for IL-4 at 37 °C for 5 h before being stained. Antibody information were shown in Supplementary Table 2. Flow cytometry data were acquired on BD Fortessa X-20 and analyzed with FlowJo (v10.5.3).

2.4.6 Suppression assay

Naïve human PB tTreg ($CD4^+CD25^+CD127^-CD45RA^+$) were sort-purified from PB mononuclear cells (PBMNCs) (Ficoll-Hypaque, Amersham Biosciences) in a two-step procedure in which $CD25^+$ cells were initially enriched from PBMNCs by AutoMACS (PosselD2) with GMP grade anti-CD25 microbeads (Miltenyi Biotec). $CD25^{high}$ cells were stained with CD4, CD8, CD25, CD127 and CD45RA and sorted via FACSAria as $CD4^+$, $CD8^-$, $CD25^{high}$, and $CD127^-CD45RA^+$. Note that the bead-bound and fluorochome-conjugated anti-CD25 antibodies recognize different epitopes (Miltenyi Biotec), followed by sorting on a FACSAria (BD Biosciences).

Purified naïve tTreg were stimulated with a K562 cell line engineered to express CD86 and the high-affinity Fc receptor (CD64) (37) (2:1 tTreg/KT), which had been irradiated with 10,000 cGy and incubated with anti-CD3 mAb (Miltenyi Biotec). In some experiments, tTregs were stimulated with KT64/86 cells that were preloaded, irradiated, and frozen (1:1 tTreg/KT). Naive tTreg were cultured in X-Vivo-15 (BioWhittaker, Walkersville, MD) media supplemented with 10% human AB serum (Valley Biomedical), Pen/Strep (Invitrogen), and n-acetyl cysteine (USP). Recombinant IL-2 (300 IU/mL; Chiron, Emeryville, CA) was added on day 2 and maintained for culture duration. Cultures were maintained at 0.25×10^6 to 0.5×10^6 viable nucleated cells/ml every 2 to 3 days. On day 14, tTreg and $CD4^+$ Teff were aliquoted and frozen.

When needed, frozen tTreg were thawed and re-stimulated with anti-CD3/CD28 mAb-coated Dynabeads (Life Technologies, Carlsbad, CA) at 1:3 (cell to bead) ratios in the presence of recombinant IL-2 (300U/ml). OGA inhibitor (10 μM) was added to re-stimulated tTreg cultures on day 0 and day 4. tTreg were cultured a total of 7 days following re-stimulation and were then harvested for flow phenotyping and suppressive function.

The in vitro suppressive capacity of expanded tTregs was assessed with a CFSE (Carboxyfluorescein succinimidyl ester) inhibition assay as previously published [164,165]. Briefly, PBMNCs were purified, labeled with CFSE (Invitrogen), and stimulated with anti-CD3 mAb-coated beads (Dynal) ± cultured tTreg (1:2 to 1:8 tTregs/PBMC). On day 4, cells were stained with antibodies to CD4 and CD8 and suppression was determined from the Division Index (FlowJo, TreeStar). tTregs suppressed CD4 and CD8 T cell responses equivalently and only CD8 data were presented.

2.4.7 Cell culture and transfection

HEK 293T cells were cultured in DMEM with 10% fetal bovine serum (FBS). TMG (CarboSynth, 10 μM), ST045849 (TimTec, 100 μM), MG132 (Cayman, 20 μM), and cycloheximide (Sigma, 100 μg/ml) were treated as indicated. The mouse FOXP3-Myc/DDK plasmid was purchased from OriGene (MR227205). Point mutants of FOXP3 were generated with the QuikChange XL II Site-Directed Mutagenesis Kit (Agilent). pCMV-Myc-human OGT and 3xFlag/2xMyc-OGA were kindly provided by Dr. Xiaochun Yu at University of Michigan and Dr. Xiaoyong Yang at Yale University, respectively. FOXP3-Myc/DDK was subcloned into the 3xFlag/2xMyc empty vector to construct the 3xFlag/2xMyc-FOXP3-Myc/DDK plasmid. IL-2 promoter luciferase (#12194) and pIS1 (#12179) were from Addgene. Cells were transfected with FuGENE HD (Promega) according to manufacturer's instructions.

2.4.8 FOXP3 protein purification, in-solution digestion, and mass spectrometry

3xFlag/2xMyc-FOXP3-Myc/DDK and Myc-OGT were co-transfected into 5x 15cm-dishes of 293T cells and purified by immunoprecipitation with M2 Flag beads (Sigma) followed by 3xFlag peptide (Sigma) elution according to established

procedures [126]. IP eluates were denatured in 0.2% Rapigest SF (Waters), reduced with 5 mM DTT, alkylated with 10 mM Iodoacetamide, and finally digested overnight at 37°C with 5% (w:w) sequencing grade Trypsin (Promega). Digests were acidified with formic acid for 30 mins to degrade the Rapigest and peptides were then recovered and desalted with C_{18} OMIX tips (Agilent).

Tryptic peptides were analyzed by on-line LC-MS/MS using an Orbitrap Fusion Lumos (Thermo) coupled with a NanoAcquity UPLC system (Waters). Peptides were separated over a 15 cm x 75 µm ID 3 µm C18 EASY-Spray column (Thermo). Precursor ions were measured from 350 to 1800 m/z in the Orbitrap analyzer (resolution: 120,000; AGC: 4.0e5). Ions charged 2+ to 8+ were isolated in the quadrupole (selection window: 1.6 m/z units; dynamic exclusion window: 30 s; MIPS Peptide filter enabled), fragmented by EThcD (Maximum Injection Time: 250ms, Normalized Collision Energy: 25%) and measured in the Orbitrap (resolution: 30,000; AGC; 5.0e4). The cycle time was 3 seconds.

Peaklists were generated using PAVA (UCSF) and searched using Protein Prospector 5.23.0 against the human SwissProt database (downloaded 9/6/2016) and a randomized concatenated database with the addition of the recombinant FoxP3 recombinant sequence. Cleavage specificity was set as Trypisn allowing 2 miscleavages. Carbamidomethylation of Cys was set as a constant modification and two of the following variable modifications were allowed per peptide: acetylation of protein N-termini, oxidation of Met, oxidation and acetylation of protein N-terminal Met, cyclization of N-terminal Gln, protein N-terminal Met loss, protein N-terminal Met loss and acetylation, acetylation of Lys, phosphorylation of Ser, Thr, Tyr, HexNAc on Asn within the N glycan motif (NXST), HexNAc on Ser, Thr, Tyr, and PhosphoHexNAc on Ser or Thr. Precursor mass tolerance was 20ppm and fragment mass tolerance was 30 ppm. Phosphorylated and HexNAcylated peptides were manually verified.

2.4.9 RNA and real-time PCR

Total RNA was extracted using RNeasy Plus Universal Kits (QIAGEN, catalog no. 73404). cDNA was reverse transcribed (BIO-RAD, catalog no. 170-8891) and amplified with SYBR Green Supermix (BIO-RAD, catalog no. 172-5124). All data were normalized to the expression of *18S.* Primer sequences are available on request.

2.4.10 Immunoprecipitation and Western blotting

Anti-O-GlcNAc (Abcam, catalog no. ab2739), anti-FOXP3 (eBioscience, catalog no. 56-7773-82), anti-c-Myc (SANTA CRUZ, catalog no. sc-40), anti-Flag (Millipore Sigma, catalog no. F3165), anti-β-Actin (Millipore Sigma, catalog no. A5441) antibodies were used. For Immunoprecipitation, whole-cell lysates were precipitated by anti-FLAG M2 Affinity Gel (Millipore Sigma, catalog no. A2220). Cells were lysed in buffer containing 1% Nonidet P-40, 50 mM Tris 3 HCl, 0.1 mM EDTA, 150 mM NaCl, proteinase inhibitors and TMG. Equal amounts of protein lysates or immunoprecipitation samples were electrophoresed on 8% SDS-PAGE gels and transferred to PVDF or Nitrocellulose membranes. Primary antibodies were incubated at 4 °C overnight. Western blotting was visualized by peroxidase conjugated secondary anti- bodies and ECL chemiluminescent substrate or by 800CW infrared fluorescent IgG secondary antibodies imaged on a Bio-Rad ChemiDoc Imaging System or a LI-COR Odyssey 9120 infrared imager, respectively.

2.4.11 Retroviral transduction

STAT5A, constitutively active (CA)- STAT5A, and O-GlcNAc-deficient CA-STAT5A-T92A retroviral expression plasmids were kindly provided by Dr. Richard Moriggl at University of Veterinary Medicine, Vienna. Wildtype and mutant FOXP3 were constructed into the pMSCV-IRES-eGFP retroviral vector. Retrovirus were packaged in 293FT cells and viral supernatants were harvested for use. Treg cells were cultured 48 h, then spin infected with viral supernatants (2500 rpm, room temperature for 2 h) in the presence of 8 μg/ml polybrene [166]. Cells were cultured for another 3 days.

2.4.12 RNA-seq

Treg cells were isolated from female *Foxp3*$^{YFP\text{-}Cre/wt}$*Ogt*$^{fl/fl}$ and *Foxp3*$^{YFP\text{-}Cre/wt}$*Ogt*$^{wt/fl}$ mice using CD4 selection beads (ThermoFisher, 11461D) followed by sorting on YFP expression. RNA was extracted using the RNeasy Plus Micro Kit (QIAGEN, catalog no. 74034) and subjected to library construction and 2x50 paired-end sequencing on a HiSeq 2500 (Illumina) at the University of Minnesota Genomics Center. Sequencing reads were trimmed (Trimmomatic v0.33), quality control checked

(FastQC), mapped (bowtie2 v2.2.4.0), and quantified for gene expression (Cuffquant). Differentially expressed genes were determined by EdgeR. Pathway analyses and upstream regulator analyses were performed using Ingenuity Pathway Analysis (Qiagen).

2.4.13 Data availability

RNA Sequence data that support the findings of this study have been deposited in Gene Expression Omnibus with the accession number GSE116758. Mass spectra data can be accessed on MS-Viewer [167] with the key: artnlq2gpq.

2.4.14 Statistical analyses

Results are shown as mean ± SEM. Comparisons were carried out using a two-tailed Student's *t*-test, one-way ANOVA followed by Tukey's multiple comparisons test or two-way ANOVA followed by Tukey's multiple comparisons test. Survival curves were done using the Kaplan-Meier method and compared with a logrank test. Statistical analyses were performed using GraphPad Prism 7.

2.5 Publication

This chapter has been modified (with permission) from the following article:

Liu B*, Salgado OC*, Singh S, Hippen KL, Maynard JC, Burlingame AL, Ball LE, Blazar BR, Farrar MA, Hogquist KA, Ruan HB. The lineage stability and suppressive program of regulatory T cells require protein O-GlcNAcylation. *Nat Commun*. 2019 Jan 21;10(1):354. doi: 10.1038/s41467-019-08300-3.

*These authors contributed equally

Chapter 3 AIRE drives early life thymic interferons and changes thymic self-antigen expression

3.1 Introduction

Interferons provide a robust first line of defense against invading pathogens. Specifically, Type I IFNs (IFN-I) are highly and transiently induced upon viral infection, during which they activate intracellular programs that promote innate immunity and activate adaptive immune responses [168]. We found in a previous work, that medullary thymocytes had a distinct interferon stimulated gene (ISG) signature [169], which suggests that interferons might be constitutively produced in the thymus. This ISG signature was abrogated in thymocytes lacking the IFN-I receptor gene, *Ifnar1*, showing a direct role of IFN-I signaling in the thymus. Indeed, there is evidence of IFN-β (a subtype of IFN-I) being produced in the thymus at low levels during the steady state [170,171].

While the evidence for thymic IFN-I is clear, other related aspects such as the IFN-I cellular source, the cell populations responding to IFN-I and their effect on the thymic microenvironment remain uncertain. Lienenklaus *et al.* showed that thymic IFN-β expression was dependent on Aire and indicated that mTEC were the main producers [171], whereas Otero *et al.* suggested that IFN-β regulated both the development of mTEC and their expression of Aire [170]. Thus, there is a need to precisely identify the source of IFN-β and determine whether IFN-β is essential for development, maintenance, and gene expression of other thymic antigen presenting cells.

Previous studies indicated that multiple cells in the thymic microenvironment may be responding to IFN-I. Transcriptional studies and mouse reporter experiments showed that thymocytes [169,172], mTEC [171] and thymic dendritic cells (DC) [71] express ISG. However, there is confusion about the fraction of the cell populations responding to IFN-I and their dependency on the IFN-I receptor. For instance, thymic *Ifnar1*-deficient DCs still displayed a strong ISG signature [71]. Thus, it is essential to examine in more detail which populations are receiving IFN signaling in the steady state and which receptors are employed by cells to receive those signals.

In this study, we used various cytokine expression and cytokine signaling reporter mice, as well as RNAseq to address these questions. We found that IFN-β

was mainly produced by a very small number of MHC-II^{+} mTEC (mTEC^{hi}) in an AIRE-dependent manner. Furthermore, we demonstrated that most cells in the thymic microenvironment respond to both IFN-I and IFN-III (IFNλ), and that these signals significantly reshape the thymic microenvironment by regulating the thymic APC composition and their overall gene expression. These findings have important implications for the role of APC activation in the development of T cell tolerance.

3.2 Results

3.2.1 Developing T cells respond to IFNβ produced by mTEChi cells

Transcriptional profiling by our lab and others showed that both thymocytes [169,172] and thymic dendritic cells [173] express a strong IFN-I signature. Here, we sought to characterize this phenomenon in more detail. In thymocytes, the expression of the cell surface proteins Qa2 and Ly6A was strongly dependent on IFN-I in both CD4SP and CD8SP thymocytes (Figure 3.1). This effect was largely attributable to IFN-β, as Qa2 and Ly6A expression was substantially reduced in *Ifnb1*$^{-/-}$ SP thymocytes, and even further so in *Ifnar1*$^{-/-}$ SP thymocytes. The absence of both *Ifnar1* and *Ifnlr1*, or the gene encoding the signal transducer *Stat1* completely abrogated the expression of Qa2 and Ly6A.

These observations are in line with two previous studies reporting expression of IFN-β in the thymus during the steady state [170,171]. To identify the cell source of this IFN-β, we used a published luciferase mouse reporter (*Ifnb*^{luc}) [171]. After magnetic sorting, luciferase activity was mostly detected in the fraction enriched for epithelial cells, specifically the fraction expressing CD80 (Figure 3.1b) —mTEC^{hi} cells. Endogenous *Ifnb1* expression measured by qPCR in FACS-sorted thymic cell populations confirmed the highest expression was present in mTEC^{hi} cells (Figure 3.1c).

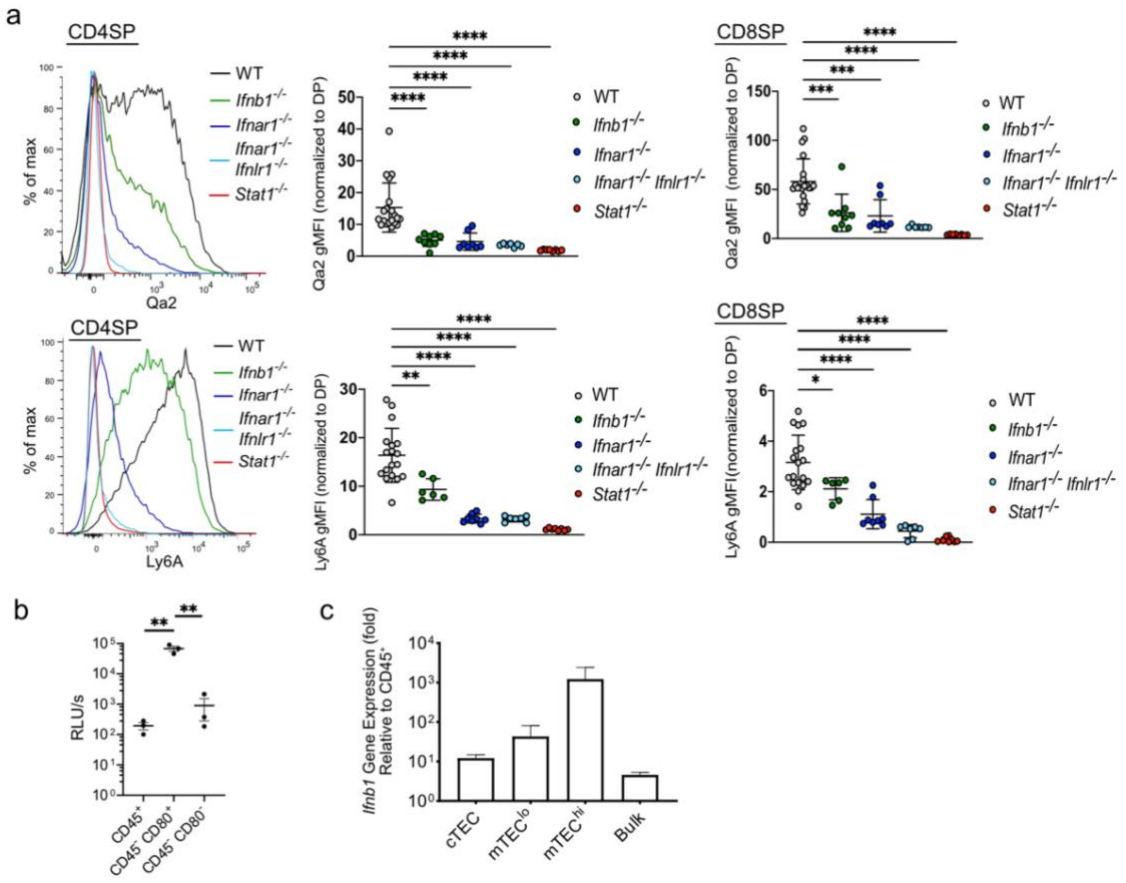

Figure 3.1. Developing T cells respond to IFNβ produced by mTEC^{hi} cells

(a) Representative expression and geometric mean fluorescence intensity (gMFI) of Qa2 and Ly6A on mature CD4SP (CD4$^+$ CD8$^-$ CD62L$^+$ CD69$^-$) thymocytes from WT, *Ifnar1*$^{-/-}$, *Ifnb1*$^{-/-}$, *Ifnar1*$^{-/-}$/*Ifnlr1*$^{-/-}$, and *Stat1*$^{-/-}$ mice (left). Qa2 and Ly6A gMFI of CD8SP (CD4$^-$ CD8$^+$ CD62L$^+$ CD69$^-$) (right) from 5-6-week-old mice. (b) Luminescence of indicated cell populations from thymi of *Ifnb*^{luc} mice) (c). *Ifnb1* expression by qPCR in sorted populations from wild-type C57BL/6 mice (n=4) presented relative to that of sorted CD45$^+$ cells from the same experiment. Data are shown as mean ± SD. *p<0.05, **p<0.01, ***p<0.001, ****p<0.0001 by ANOVA with multiple comparisons.

3.2.2 IFNβ expression is AIRE-dependent and expressed by a tiny fraction of mTEC

The two previous studies reporting IFN-β expression in the thymus came to contradictory conclusions about its activation. Otero *et al.* reported that RANKL induced *Ifnb1* expression in mTEC cells cultured *in vitro*, and concluded that RANKL could directly bind the *Ifnb1* gene and promote its expression, as it does in osteoclasts [170]. On the other hand, Lienenklaus *et al.* proposed that IFN-β expression is an Aire-dependent process [171]. We wanted to test if RANKL regulates *Ifnb1 in vivo*, but could

not examine RANKL deficient mice, as they have strongly impaired mTEC differentiation [174–177]. Rather, we performed short term RANKL blockade. Two days of anti-RANKL treatment resulted in a 2-fold decrease in *Ifnb1* expression in *Ifnb*^{luc} mice (Figure 3.2a) without decreasing the total number of TEC cells (Figure 3.2b). However, given the importance of RANK-RANKL signaling for mTEC differentiation, we examined Aire expression, and noted this RANKL blockade resulted in a 2-fold decrease in the number of mTEC cells expressing Aire as well (Figure 3.2c). Thus, we tested if *Ifnb1* expression was dependent on Aire. Indeed, as suggested by Lienenklaus *et al.* [171], *Ifnb1* expression was strongly dependent on Aire, being decreased more than 100-fold in mTECs from *Aire*$^{-/-}$ mice (Figure 3.3a). This was also reflected in the low levels of Qa2 and Ly6A expression in SP thymocytes from *Aire*$^{-/-}$ mice (Figure 3.3b and c).

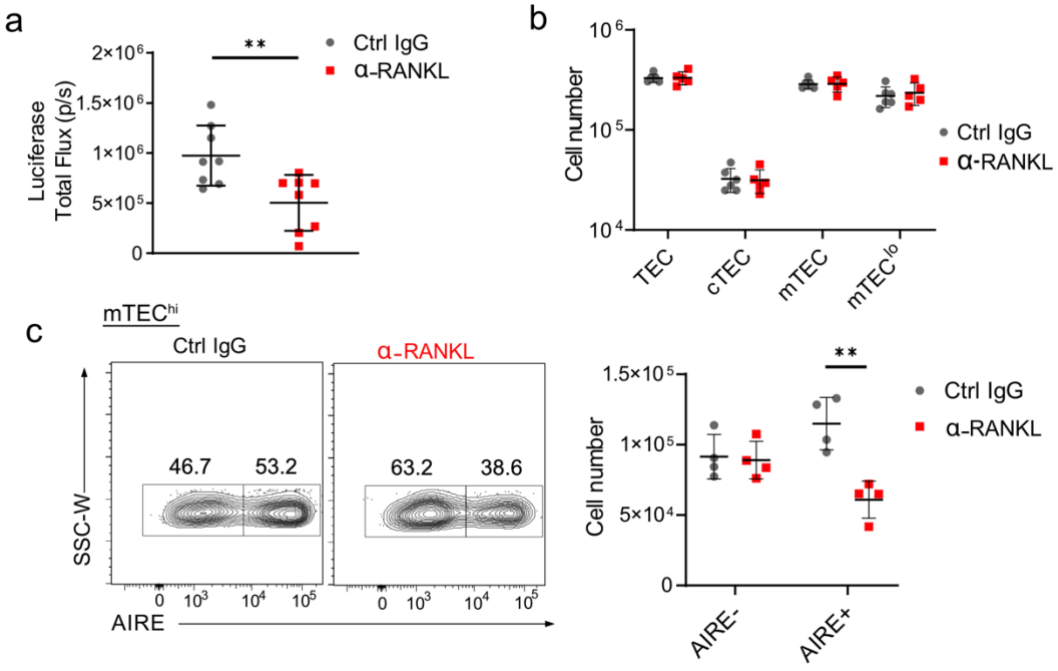

Figure 3.2. RANK-L blockade reduces the number of Aire-expressing mTECs.

Ifnb^{luc} mice were treated with a control IgG or α-RANKL antibody and 48 hours later (a) bioluminescence (as measured by average flux in photons/second) from *in vivo* imaging was measured. Data are pooled from 4 independent experiments. (b) Absolute cell numbers of indicated populations 48h after treatment. (c) Representative data of expression of Aire by flow cytometry in mTEC^{hi} 48h after treatment (left). Absolute cell number of Aire^{+} mTEC (right). Data are pooled from 2 independent experiments. Data are shown as mean ± SD. *p<0.05, **p<0.01 by unpaired t-test (a) and two-way ANOVA with multiple comparisons (d and c).

Since many Aire dependent genes are only expressed in a subset of Aire-positive mTEC [178,179] we wished to characterize *Ifnb1* expression at the single cell level. Thus, we obtained an *Ifnb1*-Tdtomato knock-in reporter (*Ifnb*^{tom}) mouse strain. Flow cytometric analysis of thymus of these animals revealed that only a very small fraction of mTEC^{hi} cells were Tdtomato^{+} (Figure 3.3d). We did not observe any Tdtomato^{+} cells in the hematopoietic compartment of the thymus (Figure 3.3e). Thus, we favor the conclusion that RANKL induces Aire expression in mTEC, a subset of which upregulates *Ifnb1*.

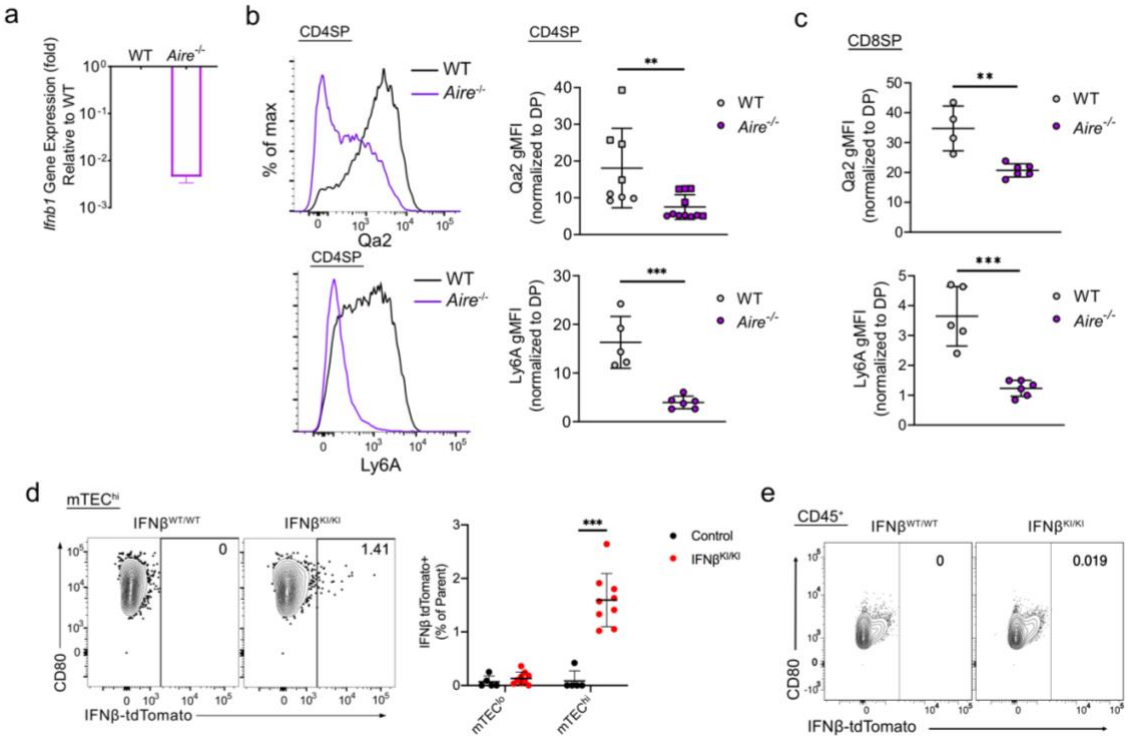

Figure 3.3. IFNβ expression is Aire-dependent and expressed by a tiny fraction of mTEC.

(a) *Ifnb1* expression by qPCR in sorted mTEC^{hi} from WT and *Aire*$^{-/-}$ mice (n=2) presented relative to WT mTEC^{hi} (b) Representative expression of Qa2 and Ly6A on CD4SP thymocytes from WT and *Aire-/-* mice (left); Qa2 and Ly6A gMFI of CD4SP normalized to mean of DP (right). (c) Qa2 and Ly6A gMFI of CD8SP normalized to mean of DP. (d) Expression of IFNβ-tdTomato in mTEC^{hi} (d) or CD45^{+} cells (e) from IFNβ$^{WT/WT}$ or IFNβ$^{KI/KI}$ mice. Data are shown as mean ± SD. *p<0.05, **p<0.01, ***p<0.001 by unpaired t-test (b and c) and two-way ANOVA with multiple comparisons (d).

3.2.3 IFNβ expression peaks at 3 weeks of age

To study the temporal dynamics of *Ifnb1* expression in the thymus, we evaluated luciferase expression in *Ifnb*^{luc} mice of different ages. Interestingly, luciferase

expression was the highest at around 2-3 weeks of age but remained expressed at low levels through adulthood (Figure 3.4a). This age dependence was closely correlated with the temporal abundance of Aire$^+$ cells within the thymus for (Figure 3.4b), even when corrected for the total number of cells in the thymus. This finding confirms the notion that Aire regulates the expression of IFN-β.

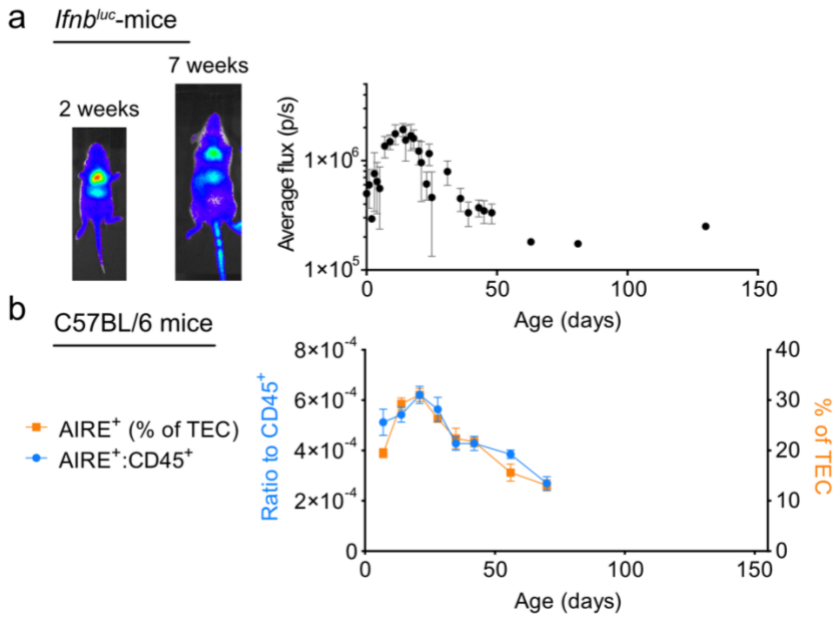

Figure 3.4. IFN-β expression changes with age.

(a) *Ifnb*^{luc} mice were injected with D-Luciferin at different ages and bioluminescence (average flux in photons/second) was measured. Between 1 to 8 mice per time point. Data are shown as mean ± SD. (b) AIRE$^+$ mTEC as a ratio to CD45$^+$ cells (left axis, circles) or as a proportion of TEC (right axis, squares) in various ages of WT C57BL/6 mice. Data are shown as mean ± SEM.

3.2.4 Most cells in the thymic microenvironment respond to interferons in the steady state

Given that IFN-β is produced constitutively in the thymus, we evaluated which cells in the thymic microenvironment are responding to it in the steady state. To do this we used a reporter mouse that expresses GFP under the control of the endogenous Mx1 locus (*Mx1*^{gfp}) [180]. Mx1 is an ISG induced by both IFN-α/β and IFN-λ [181]. We found that numerous cells, including DCs, B cells, other myeloid cells and thymocytes were GFP$^+$ in these mice, implying they respond constitutively to IFN (Figure 3.5). The percentage of GFP$^+$ cells and their mean fluorescence intensity (MFI) was notably

higher in the thymus than in the spleen, which indicates that the thymic IFN response is stronger than the systemic basal IFN response described previously [180,182,183]. This is also consistent with the strong luciferase signal in the thymus of *Ifnb*^{luc} mice.

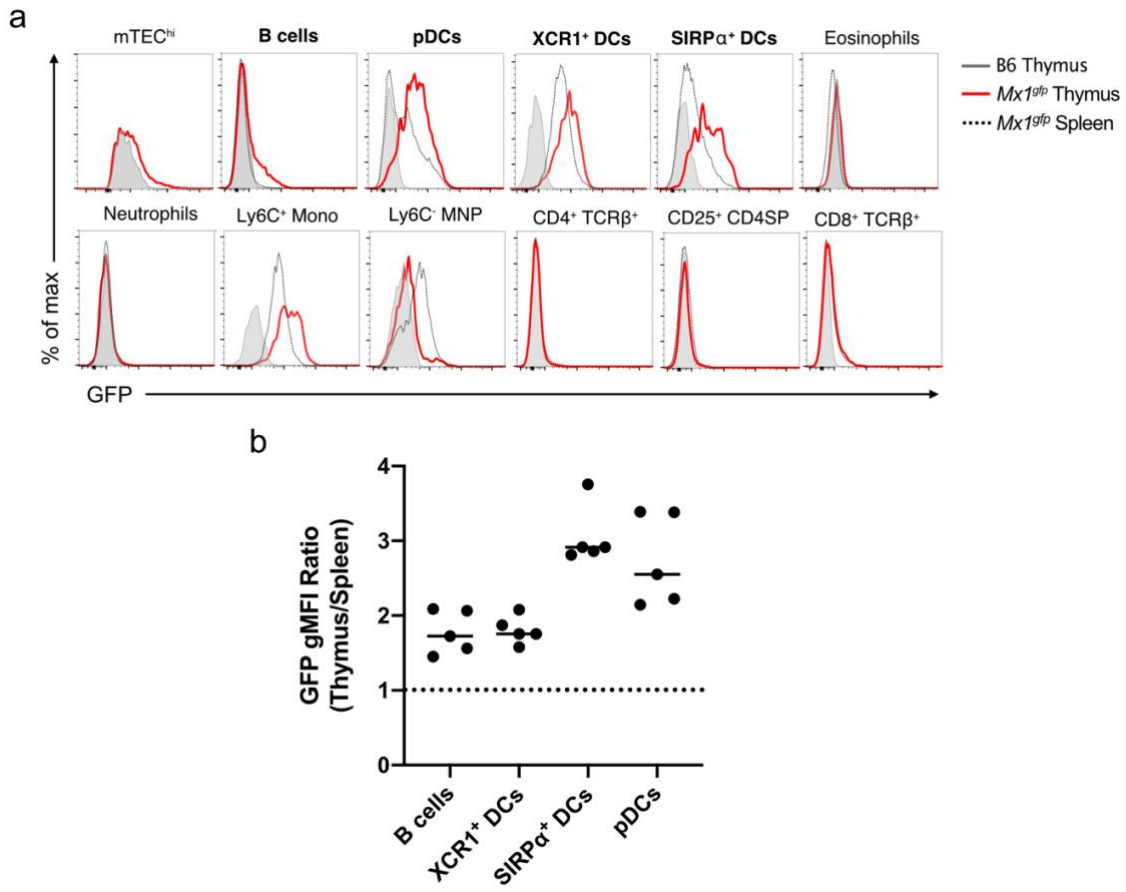

Figure 3.5. GFP expression of thymic and splenic cell populations from *Mx1^{gfp}* mice.

Thymus and spleen cells from B6 and *Mx1^{gfp}* mice were stained for the indicated populations and GFP expression was measured by flow cytometry. (a) Representative histograms showing GFP expression in indicated cell populations. (b) Ratio of geometric mean fluorescence (gMFI) of GFP in the thymus vs. spleen for the indicated populations.

To understand how different IFN signaling pathways are involved in the Mx1 response in the thymus, we crossed this reporter line to mice lacking *Ifnar1* or *Stat1* (a critical signal transducer of both IFNAR and IFNLR signaling pathways). We found that, contrary to what occurs in the spleen, where the basal IFN response is dependent on IFN-I [180], the intrathymic IFN response was more complex. GFP expression was absent in T cells, pDCs and some myeloid cells in *Mx1^{gfp}/Ifnar1$^{-/-}$* mice; however, the response

in thymic B cells and DCs was not abrogated unless *Stat1* was deficient, indicating that both IFN-I and IFN-III are inducing cellular responses constitutively in the thymus.

The percentage of GFP^+ B cells did not change in the absence of *Ifnar1* but was completely abolished in the absence of *Stat1*, which suggests a potential redundant role of IFN-III signaling in this cell population. The IFN response in DCs was more heterogeneous with the response being partially dependent on IFN-I in $SIRP\alpha^+$ DCs, and IFN-I-independent in $XCR1^+$ DCs. GFP expression in T cells confirmed their dependence on IFN-I for their IFN response in the steady state.

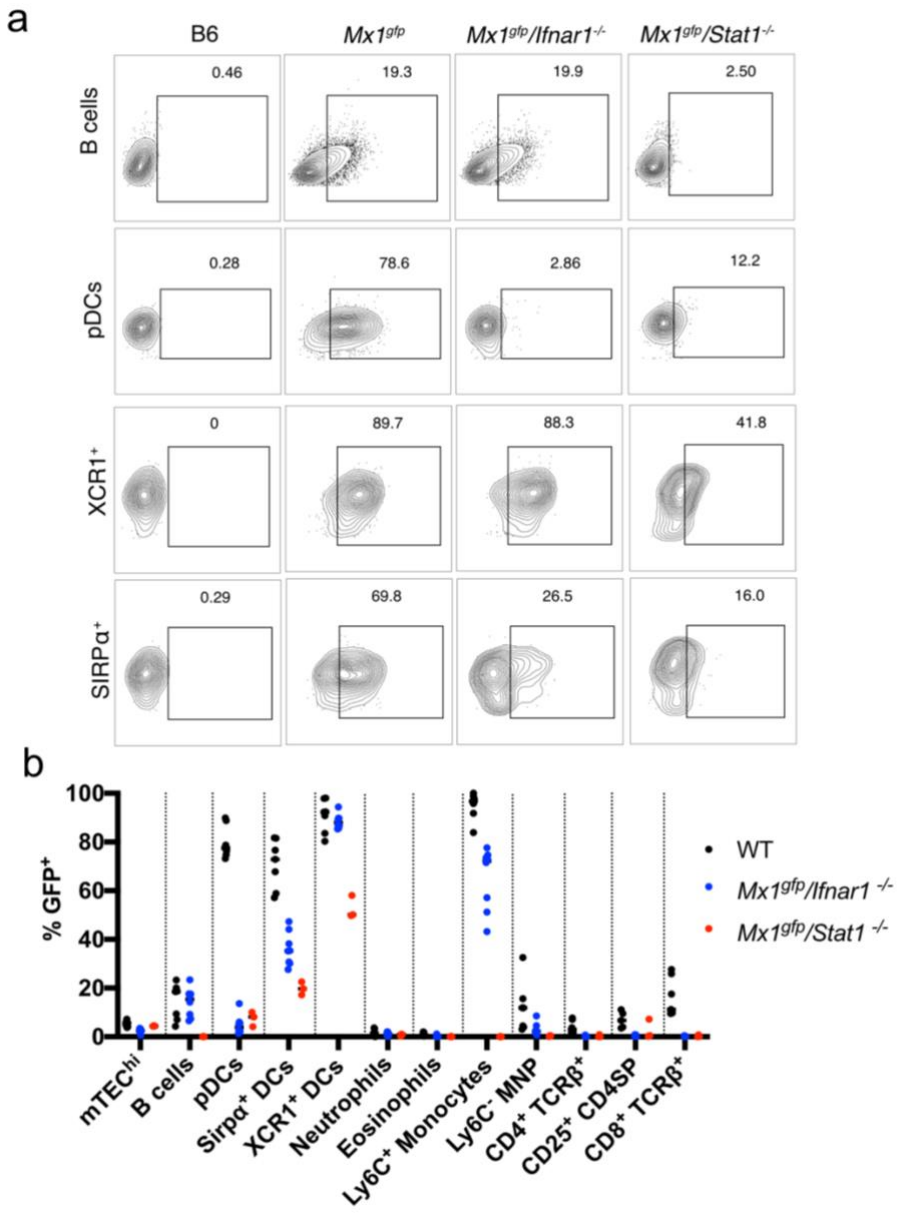

Figure 3.6. Thymic cell populations respond to both IFN-I and IFN-III in the steady state.

Thymus and spleen cells from B6 (WT), *Mx1*^{gfp}, *Mx1*^{gfp}*/Ifnar1*$^{-/-}$ and *Mx1*^{gfp}*/Stat1*$^{-/-}$ mice were stained for the indicated populations and GFP expression was measured by flow cytometry. (a) Representative plots for four of the main cell populations. (b) Summary of the percentage of GFP^{+} cells out of every cell population.

3.2.5 IFN impacts hematopoietic, but not stromal, APC composition and gene expression

With IFN-I and IFN-III regulating *Mx1*^{gfp} expression in the thymus, we wondered whether this expression had consequences for the population composition of the

thymic APC. To evaluate this, we quantified the number of thymic APCs from mice lacking IFN-I and/or IFN-III signaling. While the absence of IFNAR did reduce the number of pDCs and Ly6C$^+$ monocytes, the rest of the populations remained mostly unchanged. However, the absence of both IFNAR and IFNLR, or STAT1, also reduced drastically the number of B cells and DCs, as well as pDC and Ly6C$^+$ monocytes (Figure 3.7).

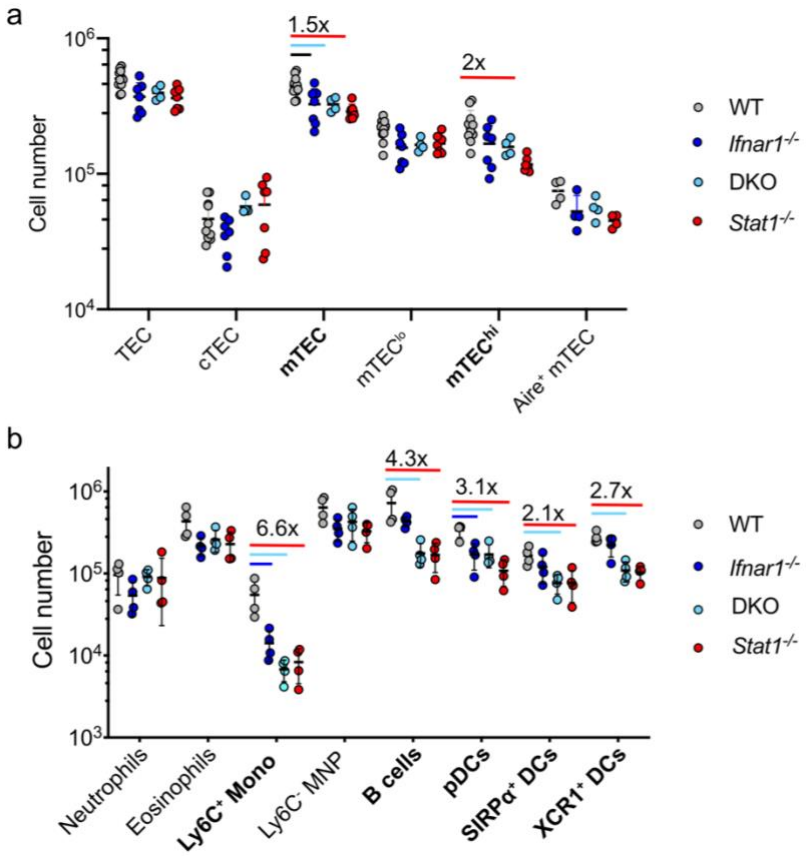

Figure 3.7. Interferon-dependent changes in thymic APC composition.

Thymus cells from the stromal (a) and hematopoietic (b) compartment B6 (WT), *Ifnar1*$^{-/-}$, *Ifnar1*$^{-/-}$ */Ifnlr1*$^{-/-}$ (DKO), and *Stat1*$^{-/-}$ mice were stained for the indicated populations and quantified by flow cytometry.

IFNs induce the expression of hundreds of genes that reshape the cellular response to infections [184]. Given that thymic APCs were responding to IFN in the *Mx1*^{gfp} reporter mice, we examined the broader gene expression changes associated with this response. To do this, we performed high-throughput RNA sequencing (RNAseq) on the major DC subsets (XCR1$^+$, SIRPα^+ CD301b$^-$, SIRPα^+ CD301b$^+$) from

wildtype, *Ifnar1*$^{-/-}$, *Ifnb1-/-*, *Ifnar1*$^{-/-}$*Ifnlr1*$^{-/-}$, and *Stat1*$^{-/-}$ mice (Figure 3.8). This transcriptome analysis revealed a few genes downregulated in the absence of IFNAR, which were also identified in the *Ifnb1*$^{-/-}$ DCs. This indicates that, just as in T cells (see Figure 1a), the IFN-I response in DCs is mainly mediated through IFN-β.

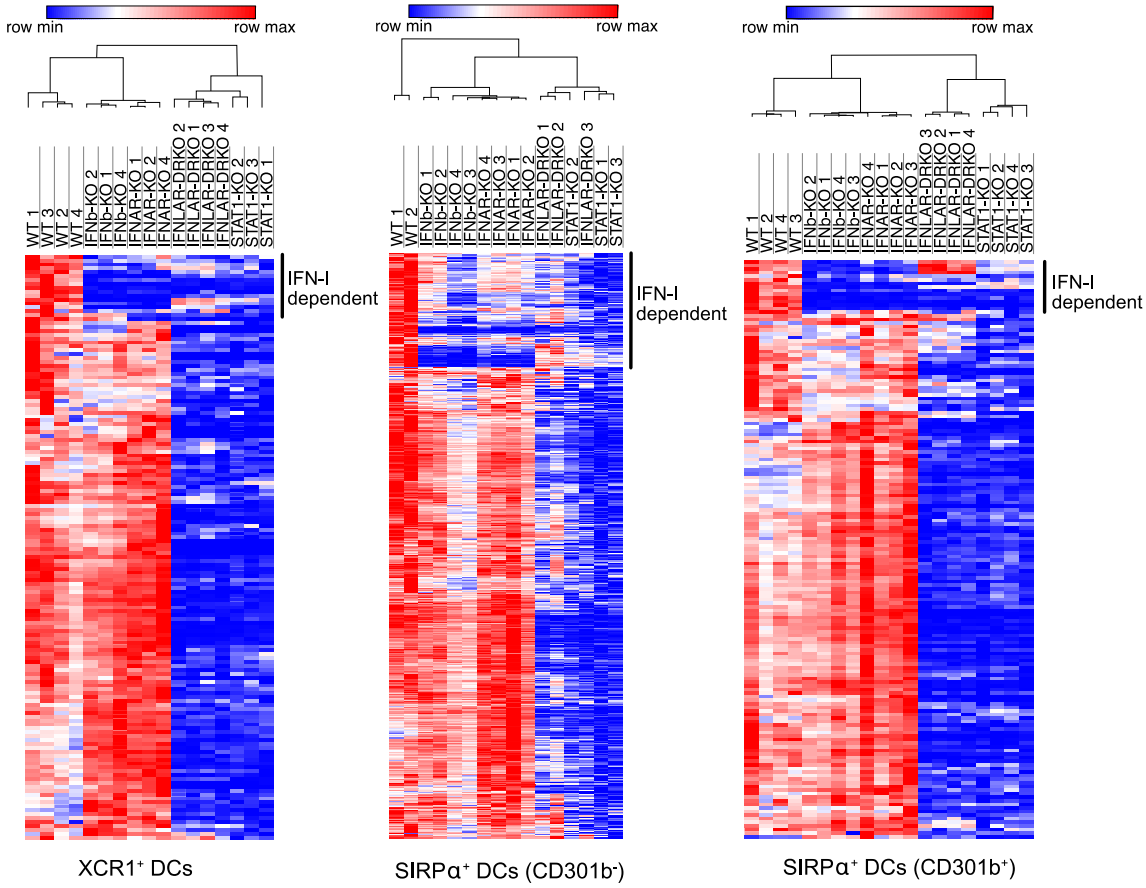

Figure 3.8. RNA-seq reveals profound changes in gene expression driven by IFNs.

Thymus cells from WT, *Ifnar1*$^{-/-}$, *Ifnb1*$^{-/-}$ (IFNb-KO), *Ifnar1*$^{-/-}$*Ifnlr1*$^{-/-}$ (IFNLAR-DRKO), and *Stat1*$^{-/-}$ mice were stained and FACS-sorted for the indicated populations of DCs and their transcriptome was examined with bulk RNA sequencing. Heatmaps display unsupervised clustering of the normalized expression of genes significantly downregulated in *Stat1*$^{-/-}$ compared to the WT in each DC population.

Furthermore, we found striking changes in the transcriptome of all DCs subsets in the absence of STAT1. The magnitude of these gene expression changes was significantly larger than the changes found in the absence of IFNAR alone (Figure 3.8).

Remarkably the changes in *Stat1*$^{-/-}$ APC were equivalent in mice that lacked both IFNAR and IFNLR, again suggesting that type I and III interferons are involved.

Given the significant effect of IFNs in DC gene expression, we decided to take a comprehensive approach to examine the effects of IFNs in all thymic APCs. To do this, we performed single-cell RNA sequencing (scRNA-seq) analysis on MHC class II-expressing thymic cells. We used cell hashing with barcoded antibodies [185], which allowed us to multiplex samples from WT, *Ifnar1*$^{-/-}$ and *Ifnar1*$^{-/-}$*/Ifnlr1*$^{-/-}$ mice and simultaneously analyze them in a single run. After processing and doublet removal, we obtained 10,743 individual cell transcriptomes with roughly equivalent cell numbers per genotype. Dimensionality reduction analysis was performed to visualize the expression data and allowed us to identify 14 cell clusters (Figure 3.9a), consistent with the cell heterogeneity of the sample. B cells and different subpopulations of conventional DCs were identified in the 5 most populated clusters (#0 - 4) and accounted for approximately 70% of the whole sample. Cluster 5 contained cells with monocyte/macrophage identity (*C1q* genes, *CD68, Mrc1, Mertk,* etc.). The remaining clusters (#6-13) were identified as apoptotic cells, T cells, eosinophils, neutrophils, pDC and TEC. These clusters were expected to be small due to either low expression levels of MHC-II (#6-10, 12-13) or inefficient cell recovery with the digestion protocol used (collagenase D) (#11).

When the analysis was broken down by cell hashtags, we found that the cells from WT and *Ifnar1*$^{-/-}$ mice tended to cluster together, whereas *Ifnar1*$^{-/-}$*/Ifnlr1*$^{-/-}$ cells clustered further from the other two genotypes, indicating their dissimilarity (Figure 3.9b). This was the case for all the main six clusters (#0-5), as well as #9 and #11. Indeed, consistent with the bulk RNA-seq analysis of DCs, the differentially expressed gene (DEG) analysis of all the main clusters found only a handful of DEGs between WT and *Ifnar1*$^{-/-}$, but an extensive list when WT and *Ifnar1*$^{-/-}$*/Ifnlr1*$^{-/-}$ were compared (Figure 3.10a). Not surprisingly, the majority of DEGs were ISG (discussed below). Representative genes from these two expression patterns are depicted in Figure 3.9c, with *Ifi27l2a* downregulated in the absence of IFNAR alone (except in the B cell cluster), and *Isg15* expression unchanged in the *Ifnar1*$^{-/-}$ but almost absent in all the clusters from the *Ifnar1*$^{-/-}$*/Ifnlr1*$^{-/-}$.

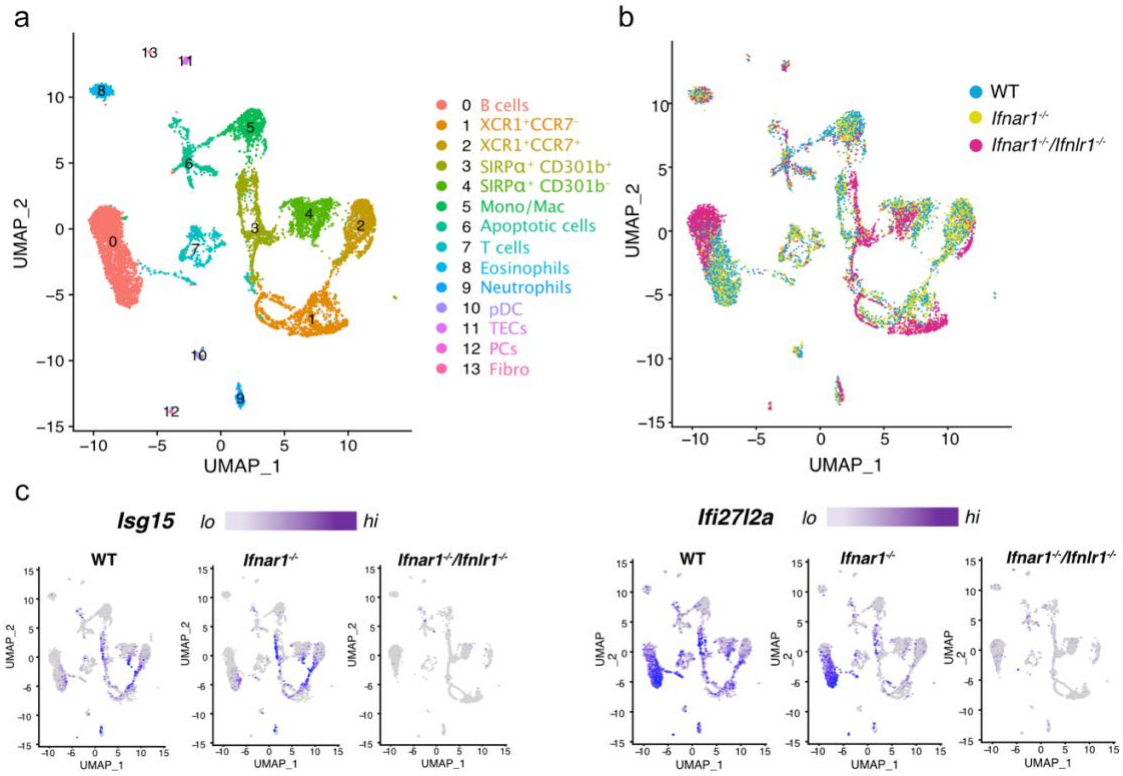

Figure 3.9. scRNA-seq profiling reveals profound changes in gene expression by IFN-I and IFN-III.

MHC class II-expressing thymus cells from WT, *Ifnar1*$^{-/-}$ and *Ifnar1*$^{-/-}$/*Ifnlr1*$^{-/-}$ were FACS-sorted, captured with a 3' Single Cell V5 chemistry platform, and sequenced. Cell hashing was used to distinguish the genotypes of origin. (a) UMAP plot from all 10,743 transcriptome events showing 14 clusters identified. (b) UMAP plot presented in a with information about the genotype of origin (c) Normalized expression of selected gene markers in the three different genotypes analyzed.

Finally, to further scrutinize these IFN-dependent gene expression changes, we created a heat map to visualize the normalized expression of the genes that were downregulated by the absence of both IFNAR and IFNLR in at least half of the main clusters. Interestingly, we found that in addition to the classic and universally expressed ISGs (*Stat1, Usp18, Bst2*, etc), there were many DEGs whose expression tended to be more cell-specific (Figure 3.10a). For example, the absence of *Ifnar1/Ifnlr1* in B cells resulted in the downregulation of genes involved in B cell maturation and activation, like *Igha* or *Iglc1*, and consequently relative upregulation of genes that promote memory formation over effector differentiation, like *Ets1* [186] and

Bach2 [187]. In DCs, we noticed many DEGs were associated with antigen processing and presentation (*Psmb8, Psmb9, Tap1, B2m*).

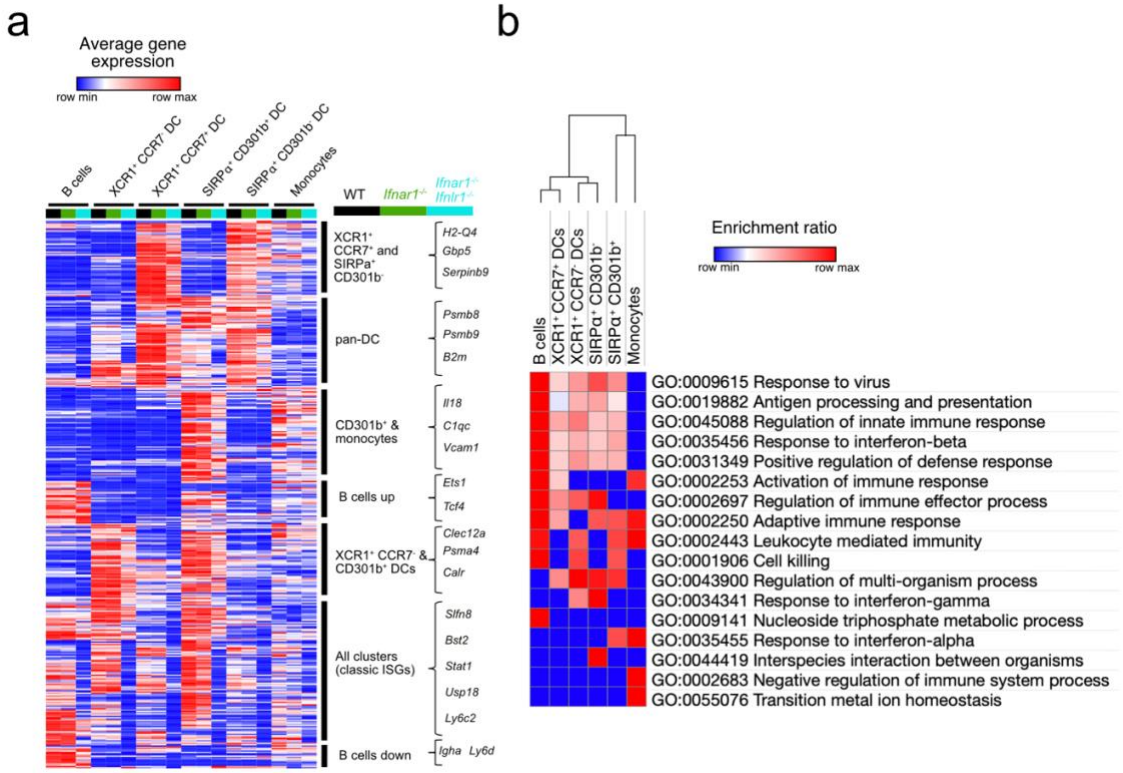

Figure 3.10. Thymic IFNs induce the expression of genes involved in antigen processing and presentation.

(a) Heat map displaying unsupervised clustering of the normalized expression of a subset of 427 genes that were downregulated in *Ifnar1*$^{-/-}$/*Ifnlr1*$^{-/-}$ cells compared to the WT in at least 3 of the 6 clusters shown. Exemplary genes of each group with similar gene expression pattern. (b) Over-representation analyses against the Gene Ontology database were performed on the lists of differentially expressed genes (WT vs. *Ifnar1*$^{-/-}$/*Ifnlr1*$^{-/-}$) of each cluster and the heat map displays the enrichment ratios of the gene sets with FDR<0.05.

Nevertheless, when we did analysis to identify gene sets that were enriched in the lists of DEGs of each cluster, we found that most clusters shared the biological processes affected by the absence of IFN-I and IFN-III signaling (Figure 3.10b). Of note, besides the highly inducible ISGs involved in IFN response, the IFN response in B cells and DCs, but not in monocyte/macrophages, was enriched in genes involved in antigen processing and presentation.

Taken together, these data suggest that IFN-I and, likely IFN-III [188], are constitutively being produced in the thymus and drive the expression of hundreds of genes in APCs that reshape the thymic microenvironment during T cell development. Moreover, thymic IFN signaling plays a vital role in the regulation of antigen processing and presentation, which seems likely to promote qualitative changes in the repertoire of displayed self-peptides and impact T cell tolerance development (Figure 3.11).

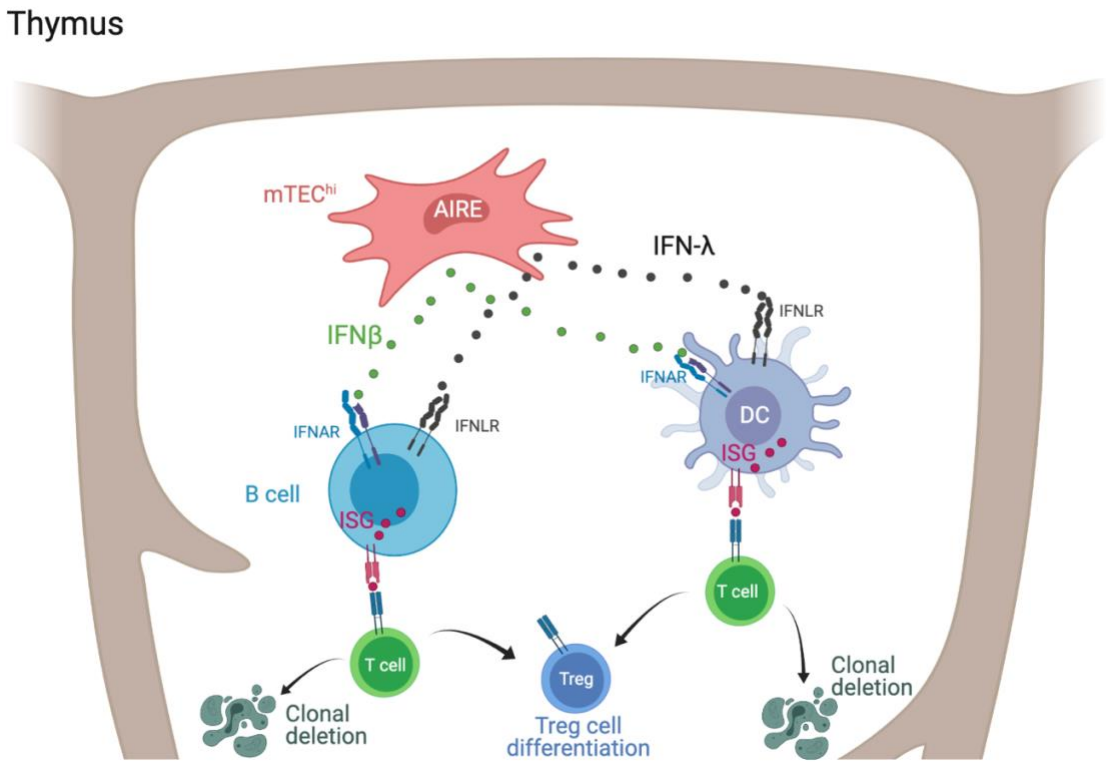

Figure 3.11. Proposed model of thymic IFNs during development.

In our model, a small number of mTEC^{hi} cells express both IFN-β and IFN-λ in an Aire-dependent manner. These IFNs induce the expression of ISGs on thymic APCs like B cells or DCs. IFNs also modify antigen processing and presentation, which regulates the repertoire of self-peptide displayed to developing thymocytes. ISG-self-reactive and other self-reactive clones are negatively selected by clonal deletion or induction of Treg cell differentiation. Created in Biorender.com.

3.3 Discussion

The presence of IFN-I and, more recently IFN-III [188], in the thymus has been described but the consequences of this expression on the thymic microenvironment are still not clearly defined. In this study, we characterized the expression of IFN-β in the thymus and found that it was constitutively expressed by a small number of mTEChi cells in an Aire-dependent manner. Importantly, we discovered that thymic APCs respond not only to IFN-I but also to IFN-III and that signaling through these molecules induces profound gene expression changes that alter the thymic microenvironment.

Our results agree with the notion that RANKL signaling can induce the expression of IFN-β, however, contrary to published data, we propose that it does so indirectly through the upregulation of Aire. The expression pattern of IFN-β resembles that of an Aire-regulated gene, with only a reduced number of $mTEC^{hi}$ cells producing it at any given moment. Notably, although we observed significant changes in the thymic hematopoietic APC composition in mice lacking both *Ifnar1* and *Ifnlr1*, the absence of IFN signaling (in *Ifnar1* or *Ifnar1-/-/Ifnlr1-/-*) did not dramatically change the TEC population composition (Figure 3.7), showing that TEC differentiation is largely independent of IFN-I/IFN-III. We did not observe significant gene expression changes in the TEC population by scRNA-seq either, but the tissue digestion protocol we used did not provide sufficient cell numbers to make conclusions with statistical power. That GFP expression was low in TECs in the $Mx1^{gfp}$ mice suggests that, although they are the main IFN producers, their IFN responses are not strong. This could be due to increased ligand-induced IFNAR internalization as a result of autocrine signaling [189], or enhanced expression of negative feedback loop mediators. Indeed, transcriptomics data from the ImmGen Consortium show an increased expression of *Socs1, Socs3,* and *Usp18* in mTECs compared to thymic DCs—genes that encode negative regulators of IFNAR signaling. However, detailed studies that allow for fair comparisons between the stromal and the hematopoietic compartments are needed.

The lower expression of MHC-I in TECs from $Ifnlr1^{-/-}$ (but not $Ifnar1^{-/-}$) mice suggests that TECs are constitutively responding to IFN-III [188]. Our results suggest that thymic B cells and DCs are also responding to IFN-III. This is an interesting finding

given the confusing current body of knowledge about the impact of IFN-III on non-epithelial cell populations (reviewed by Hemann *et al.* [190]). Furthermore, the role of IFN-III in B cell responses is unclear and thought to occur in humans but not in mice [190], but our data argue for a role of IFN-III in murine thymic B cell homeostasis.

The lack of IFN-I/III signaling caused reductions in several thymic hematopoietic APC subsets—notably monocytes, B cells, and pDCs. It is not clear if the absence of IFN resulted in poor recruitment of these APCs or affected their homoeostatic proliferation and survival. From the gene expression changes, we did not see evident downregulation of chemokine or cytokine levels, but we did see reduced maturation signals in some of the clusters. Whether these signals impacted cell proliferation or survival remains to be established.

The broad changes in gene expression driven by IFNs, and the fact that genes involved in antigen processing and presentation were altered, suggest that IFNs are likely modifying the repertoire of self-peptides displayed by thymic APCs. We found that IFN drives the expression of hundreds of ISG in most of the APC populations in the thymus, and it is reasonable to think that the proteins encoded by those ISGs will be processed and their epitopes presented by MHC molecules, as described for virally infected cells [106]. Besides, those processes of antigen degradation and loading into MHC molecules are themselves stimulated by IFNs, which would result in more and different peptides being displayed on their surface. This would have profound implications for the establishment of a tolerant repertoire of T cells. Proteomics studies addressing this issue are needed to understand how the immunopeptidome of thymic APC varies in the presence of constitutive IFN-I and IFN-III. Presumably, the interaction of thymocytes with IFN-stimulated APCs would lead to tolerance to the IFN-dependent changes that occur during some types of inflammation, like a viral infection, in the periphery.

3.4 Methods

3.4.1 Mice

C57BL/6NCrl (C57BL/6) were purchased from the National Cancer Institute. B6.129S2-*Ifnar1*^{tm1Agt}/Mmjax (*Ifnar1*$^{-/-}$), B6.129S(Cg)-*Stat1*^{tm1Dlv}/J (*Stat1*$^{-/-}$), and B6.129S2-*Aire*$^{tm1.1Doi}$/J (*Aire*$^{-/-}$) were obtained from Jackson Laboratories. B6.129P2-*Ifnb1*^{tm1Acgp} mice (*Ifnb1*$^{-/-}$) were kindly provided by E. Fish and have been described previously [191]. IFNβ^{tdTomato} (IFNβ$^{KI/KI}$) were kindly provided by D. B. Stetson (University of Washington). B6.Cg-*Mx1*$^{tm1.1Agsa}$/J (Mx1^{GFP}) were kindly provided by A. García-Sastre (Icahn School of Medicine at Mount Sinai) and have been described previously [180]. IFN-β$^{+/Δβ\text{-luc}}$ (Δβ-luc) were kindly provided by S. David (University of Minnesota) and have been described previously [171]. Unless noted, mice were used at approximately 5 weeks of age. All animal experiments were approved by the Institutional Animal Care and Use Committee of the University of Minnesota. All animals were maintained under specific pathogen-free conditions at the University of Minnesota.

3.4.2 Flow Cytometry

For all cell populations, except thymic epithelial cells (TEC), tissues were first injected with 500μL Collagenase D (1mg/mL; Roche), then finely chopped in 1mL Collagenase D, and incubated for 30 minutes at 37°C. The digestion was stopped by adding EDTA (Sigma) for a final concentration of 5mM. The suspensions were passed through 70μM cell strainers and washed with 5% FBS in RPMI. Single cell suspensions in 2% FBS in PBS were blocked with Fc block (anti-CD16/CD32; 2.4G2, Tonbo Biosciences) for 15 minutes at 4°C and then stained for 30 minutes at 4°C with the indicated antibodies (below). Samples were acquired with BD LSR Fortessa™ (BD Biosciences) and analyzed with FlowJo version X (FlowJo LLC).
Thymic epithelial cells were isolated using Liberase TH (Roche) digestion as previously described [192]. TECs were enriched by panning (also described [192]) prior to cell sorting, but not for direct flow cytometric analysis. Cells were sorted on a FACSAria (Becton Dickinson) and populations were reliably >90% of the target population.

3.4.3 Antibodies

Antibodies purchased from BioLegend: CD4 (RM4-5), CD11c (N418), CD19 (6D5), CD25 (PC61), CD80 (16-10A1), CD45 (30-F11), CD45.2 (104), CD64 (X54-5/7.1), CD45R (B220; RA3-6B2), CD90.2 (30-H12), CX3CR1 (SA011F11), CD172a (SIRPα; P84), CD301b (MGL2; URA-1), CD317 (PDCA-1, BST2; 129C1), F4/80 (BM8), TCRβ (H57-597), XCR1 (ZET) Ly-6A/E (Sca-1; [D7]), Ly-51 (6C3), Ly6G (1A8)
Antibodies purchased from BD Biosciences: CD4 (GK1.5), CD8a (53-6.7), CD69 (H1.2F3), TCRβ (H57-597), CD86 (GL1), CD90.2 (30-H12), Siglec F (E50-2440), EpCAM (G8.8).
Antibodies purchased from Thermo Fischer: MHC Class II– I-A/I-E (M5/114.15.2), Ly6C (HK1.4), FOXP3 (NRRF-30 and FJK-16s), Aire (5H12).

3.4.4 Cell Isolation and RNA preparation

Thymic epithelial cells and thymic dendritic cell (DCs) subsets were isolated from mice of the indicated genotypes. Briefly, for thymic DCs, thymus digested with Collagenase D was stained with Biotin-CD90.2 and was negatively enriched using anti-streptavidin microbeads (Miltenyi Biotec) according to the manufacturer's instructions. CD90.2$^-$ thymocytes were surface stained with indicated antibodies and were separated into three subsets with a FACSAria (BD Biosciences). An RNeasy micro kit (Qiagen) was used to isolate RNA obtained from each sample per the manufacturer's instructions.

3.4.5 Bulk RNA sequencing and analysis

RNA sequencing was performed by the University of Minnesota Genomics Center. Total RNA was quantified using a RiboGreen assay. RNA quality was assessed via Agilent BioAnalyzer (Agilent Biotechnologies). Library creation was performed using the SMARTer Stranded Total RNA Pico Mammalian v2 kit (Takara Bio), according to manufacturer's instruction. Sequencing was performed on a NovaSeq6000 using paired-end 150-base chemistry at the University of Minnesota Genomics Center.

3.4.6 scRNA-sequencing and analysis

Sequencing and initial analyses were done at the UMGC of the University of Minnesota. MHC-II-expressing thymic cells were captured using the 10x Genomics 3' Single Cell V3 chemistry platform and sequenced in a NovaSeq. Raw sequencing data were processed using CellRanger (v 4.0.0). Cellranger 'count' was used to obtain gene and protein count data for all cells. Count tables were generated for the mRNA and HTO data.

Raw count data were loaded into R (v 4.0.0) and analyzed with the Seurat R package (v 3.2.2). The mRNA expression data were normalized using a log normalization method in which feature counts for each cell were divided by the total count for that cell and multiplied by a scale factor. A subset of 2000 highly variable features (that is, genes that are highly expressed in some cells and lowly expressed in others) was identified using the 'FindVariableFeatures' function from the Seurat package. The HTO count data were added into the dataset and normalized using a centered-log ratio method. The Seurat function 'HTODemux" was used to identify 'doublet' cells.

Principal components analysis was performed using the Seurat function 'RunPCA' and a two-dimensional representation of the data was generated using the RunUMAP Seurat function. Cells were clustered using the Seurat 'FindNeighbors' and 'FindClusters' functions. In the 'FindClusters' function, different resolution values were tested and resolution value of 0.1, which identified 14 clusters, was chosen. Differentially expressed genes were identified between treatment groups within the six largest clusters identified above. A Wilcoxon Rank Sum test was implemented in the 'FindMarkers' function in Seurat to identify differentially expressed genes.

3.4.7 Luciferase assays

For *ex vivo* luciferase measurement of populations from *Ifnb*^{luc} mice, MACS separation columns were used (Miltenyi Biotech): depletion with CD45 microbeads was followed by CD80 enrichment (labeling with PE conjugated CD80, anti-PE microbeads). Samples were treated with cell culture lysis buffer (Promega), and luciferase activity was measured in a luminometer (Berthold) using the luciferase assay system following the manufacturer's protocol (Promega).

For *in vivo* imaging, mice were injected i.p. with D-luciferin in PBS (Goldbio), anesthetized using Isoflurane (Piramal) and analyzed using a Xenogen IVIS 100 imaging system (Caliper, a PerkinElmer company). Photon flux was quantified using Living Image (Caliper).

3.4.8 Quantitative RT-PCR (qPCR)

RNA from sorted cells was extracted using an RNeasy mini kit (Qiagen). cDNA was produced using SuperScript III First Strand Synthesis SuperMix (Invitrogen). FastStart Universal SYBR Green Master (Roche) and an ABI PRISM 7900HT sequence detection system (Applied Bioscience) were used for amplification and detection. *Gapdh* was used for normalization of samples. Primers for *Ifnb1* were forward: CCC TAT GGA GAT GAC GGA GA, reverse: CTG TCT GCT GGT GGA GTT CA.

3.4.9 Statistical Analysis

Comparisons of two data sets were carried out using a two-tailed unpaired Student's *t*-test. For comparison of three or more data sets, ordinary one-way ANOVA with Tukey’s multiple comparisons test was used. P-values less than 0.05 were considered significant. Sample size, experimental replicates, and additional details are provided in the figure legends. Statistical analyses were performed using GraphPad Prism 8.0.

References

1. Xing, Y. & Hogquist, K. A. T-Cell tolerance: Central and peripheral. *Cold Spring Harb. Perspect. Biol.* (2012) doi:10.1101/cshperspect.a006957.
2. Breed, E. R., Watanabe, M. & Hogquist, K. A. Measuring Thymic Clonal Deletion at the Population Level. *J. Immunol.* (2019) doi:10.4049/jimmunol.1900191.
3. Anderson, M. S. *et al.* Projection of an immunological self shadow within the thymus by the aire protein. *Science (80-.).* (2002) doi:10.1126/science.1075958.
4. Takaba, H. *et al.* Fezf2 Orchestrates a Thymic Program of Self-Antigen Expression for Immune Tolerance. *Cell* (2015) doi:10.1016/j.cell.2015.10.013.
5. Perry, J. S. A. *et al.* Distinct contributions of Aire and antigen-presenting-cell subsets to the generation of self-tolerance in the thymus. *Immunity* (2014) doi:10.1016/j.immuni.2014.08.007.
6. Li, J., Park, J., Foss, D. & Goldschneider, I. Thymus-homing peripheral dendritic cells constitute two of the three major subsets of dendritic cells in the steady-state thymus. *J. Exp. Med.* (2009) doi:10.1084/jem.20082232.
7. Fujihara, C. *et al.* T Cell–B Cell Thymic Cross-Talk: Maintenance and Function of Thymic B Cells Requires Cognate CD40–CD40 Ligand Interaction. *J. Immunol.* (2014) doi:10.4049/jimmunol.1401655.
8. Frommer, F. & Waisman, A. B cells participate in thymic negative selection of murine auto-reactive CD4+ T cells. *PLoS One* (2010) doi:10.1371/journal.pone.0015372.
9. Kleindienst, P., Chretien, I., Winkler, T. & Brocker, T. Functional comparison of thymic B cells and dendritic cells in vivo. *Blood* (2000) doi:10.1182/blood.v95.8.2610.
10. Yamano, T. *et al.* Thymic B Cells Are Licensed to Present Self Antigens for Central T Cell Tolerance Induction. *Immunity* (2015) doi:10.1016/j.immuni.2015.05.013.
11. Perera, J., Meng, L., Meng, F. & Huang, H. Autoreactive thymic B cells are efficient antigen-presenting cells of cognate self-antigens for T cell negative selection. *Proc. Natl. Acad. Sci. U. S. A.* (2013) doi:10.1073/pnas.1313001110.
12. Josefowicz, S. Z., Lu, L. F. & Rudensky, A. Y. Regulatory T cells: Mechanisms of differentiation and function. *Annual Review of Immunology* (2012) doi:10.1146/annurev.immunol.25.022106.141623.
13. Sakaguchi, S., Yamaguchi, T., Nomura, T. & Ono, M. Regulatory T Cells and Immune Tolerance. *Cell* (2008) doi:10.1016/j.cell.2008.05.009.
14. Aschenbrenner, K. *et al.* Selection of Foxp3+ regulatory T cells specific for self antigen expressed and presented by Aire+ medullary thymic epithelial cells. *Nat. Immunol.* (2007) doi:10.1038/ni1444.
15. Atibalentja, D. F., Byersdorfer, C. A. & Unanue, E. R. Thymus-Blood Protein Interactions Are Highly Effective in Negative Selection and Regulatory T Cell Induction. *J. Immunol.* (2009) doi:10.4049/jimmunol.0902632.
16. Proietto, A. I. *et al.* Dendritic cells in the thymus contribute to T-regulatory cell induction. *Proc. Natl. Acad. Sci. U. S. A.* (2008) doi:10.1073/pnas.0810268105.
17. Walters, S. N., Webster, K. E., Daley, S. & Grey, S. T. A Role for Intrathymic B Cells in the Generation of Natural Regulatory T Cells. *J. Immunol.* (2014) doi:10.4049/jimmunol.1302519.
18. Lu, F. T. *et al.* Thymic B cells promote thymus-derived regulatory T cell development and proliferation. *J. Autoimmun.* (2015)

doi:10.1016/j.jaut.2015.05.008.
19. ElTanbouly, M. A. & Noelle, R. J. Rethinking peripheral T cell tolerance: checkpoints across a T cell's journey. *Nat. Rev. Immunol.* (2020) doi:10.1038/s41577-020-00454-2.
20. Zhang, S. *et al.* Newly Generated CD4 + T Cells Acquire Metabolic Quiescence after Thymic Egress . *J. Immunol.* (2018) doi:10.4049/jimmunol.1700721.
21. Chapman, N. M., Boothby, M. R. & Chi, H. Metabolic coordination of T cell quiescence and activation. *Nature Reviews Immunology* (2020) doi:10.1038/s41577-019-0203-y.
22. Hamilton, S. E. & Jameson, S. C. CD8 T cell quiescence revisited. *Trends in Immunology* (2012) doi:10.1016/j.it.2012.01.007.
23. Parish, I. A. & Heath, W. R. Too dangerous to ignore: Self-tolerance and the control of ignorant autoreactive T cells. *Immunology and Cell Biology* (2008) doi:10.1038/sj.icb.7100161.
24. Mueller, D. L. Mechanisms maintaining peripheral tolerance. *Nature Immunology* (2010) doi:10.1038/ni.1817.
25. Bandyopadhyay, S. *et al.* Interleukin 2 gene transcription is regulated by Ikaros-induced changes in histone acetylation in anergic T cells. *Blood* (2007) doi:10.1182/blood-2006-07-037754.
26. Villarino, A. V. *et al.* Posttranscriptional Silencing of Effector Cytokine mRNA Underlies the Anergic Phenotype of Self-Reactive T Cells. *Immunity* (2011) doi:10.1016/j.immuni.2010.12.014.
27. Rocha, B., Tanchot, C. & Von Boehmer, H. Clonal anergy blocks in vivo growth of mature T cells and can be reversed in the absence of antigen. *J. Exp. Med.* (1993) doi:10.1084/jem.177.5.1517.
28. Pape, K. A., Merica, R., Mondino, A., Khoruts, A. & Jenkins, M. K. Direct evidence that functionally impaired CD4+ T cells persist in vivo following induction of peripheral tolerance. *J. Immunol.* (1998).
29. Kahan, S. M., Wherry, E. J. & Zajac, A. J. T cell exhaustion during persistent viral infections. *Virology* (2015) doi:10.1016/j.virol.2014.12.033.
30. Wherry, E. J. T cell exhaustion. *Nature Immunology* (2011) doi:10.1038/ni.2035.
31. Reed, J. R. *et al.* Telomere erosion in memory T cells induced by telomerase inhibition at the site of antigenic challenge in vivo. *J. Exp. Med.* (2004) doi:10.1084/jem.20040178.
32. P. Chou, J. & B. Effros, R. T Cell Replicative Senescence in Human Aging. *Curr. Pharm. Des.* (2013) doi:10.2174/138161213805219711.
33. Hasegawa, H. & Matsumoto, T. Mechanisms of tolerance induction by dendritic cells in vivo. *Frontiers in Immunology* (2018) doi:10.3389/fimmu.2018.00350.
34. McBride, J. M., Jung, T., De Vries, J. E. & Aversa, G. IL-10 alters DC function via modulation of cell surface molecules resulting in impaired T-cell responses. *Cell. Immunol.* (2002) doi:10.1016/S0008-8749(02)00007-2.
35. Tuettenberg, A. *et al.* The Role of ICOS in Directing T Cell Responses: ICOS-Dependent Induction of T Cell Anergy by Tolerogenic Dendritic Cells. *J. Immunol.* (2009) doi:10.4049/jimmunol.0802733.
36. Torres-Aguilar, H. *et al.* Tolerogenic Dendritic Cells Generated with Different Immunosuppressive Cytokines Induce Antigen-Specific Anergy and Regulatory Properties in Memory CD4 + T Cells . *J. Immunol.* (2010) doi:10.4049/jimmunol.0902133.
37. Bar-On, L., Birnberg, T., Kim, K. wook & Jung, S. Dendritic cell-restricted

CD80/86 deficiency results in peripheral regulatory T-cell reduction but is not associated with lymphocyte hyperactivation. *Eur. J. Immunol.* (2011) doi:10.1002/eji.201041169.
38. Akbari, O. *et al.* Antigen-specific regulatory T cells develop via the ICOS-ICOS-ligand pathway and inhibit allergen-induced airway hyperreactivity. *Nat. Med.* (2002) doi:10.1038/nm745.
39. Wang, L. *et al.* Programmed death 1 ligand signaling regulates the generation of adaptive Foxp3+CD4+ regulatory T cells. *Proc. Natl. Acad. Sci. U. S. A.* (2008) doi:10.1073/pnas.0710441105.
40. Fife, B. T. *et al.* Interactions between PD-1 and PD-L1 promote tolerance by blocking the TCR-induced stop signal. *Nat. Immunol.* (2009) doi:10.1038/ni.1790.
41. Sharma, A. & Rudra, D. Emerging functions of regulatory T cells in tissue homeostasis. *Frontiers in Immunology* (2018) doi:10.3389/fimmu.2018.00883.
42. Teh, P. P., Vasanthakumar, A. & Kallies, A. Development and Function of Effector Regulatory T Cells. in *Progress in Molecular Biology and Translational Science* (2015). doi:10.1016/bs.pmbts.2015.08.005.
43. Klein, L., Robey, E. A. & Hsieh, C. S. Central CD4 + T cell tolerance: deletion versus regulatory T cell differentiation. *Nature Reviews Immunology* (2019) doi:10.1038/s41577-018-0083-6.
44. Ebert, P. J. R., Ehrlich, L. I. R. & Davis, M. M. Low Ligand Requirement for Deletion and Lack of Synapses in Positive Selection Enforce the Gauntlet of Thymic T Cell Maturation. *Immunity* (2008) doi:10.1016/j.immuni.2008.09.014.
45. Peterson, D. A., DiPaolo, R. J., Kanagawa, O. & Unanue, E. R. Cutting edge: Negative selection of immature thymocytes by a few peptide-MHC complexes: Differential sensitivity of immature and mature T cells. *J. Immunol.* (1999).
46. Malhotra, D. *et al.* Tolerance is established in polyclonal CD4 + T cells by distinct mechanisms, according to self-peptide expression patterns. *Nat. Immunol.* (2016) doi:10.1038/ni.3327.
47. Legoux, F. P. *et al.* CD4+ T Cell Tolerance to Tissue-Restricted Self Antigens Is Mediated by Antigen-Specific Regulatory T Cells Rather Than Deletion. *Immunity* (2015) doi:10.1016/j.immuni.2015.10.011.
48. Malchow, S. *et al.* Aire Enforces Immune Tolerance by Directing Autoreactive T Cells into the Regulatory T Cell Lineage. *Immunity* (2016) doi:10.1016/j.immuni.2016.02.009.
49. Owen, D. L., Sjaastad, L. E. & Farrar, M. A. Regulatory T Cell Development in the Thymus. *J. Immunol.* (2019) doi:10.4049/jimmunol.1900662.
50. Owen, D. L. *et al.* Identification of Cellular Sources of IL-2 Needed for Regulatory T Cell Development and Homeostasis. *J. Immunol.* (2018) doi:10.4049/jimmunol.1800097.
51. Thiault, N. *et al.* Peripheral regulatory T lymphocytes recirculating to the thymus suppress the development of their precursors. *Nat. Immunol.* (2015) doi:10.1038/ni.3150.
52. Salomon, B. *et al.* B7/CD28 costimulation is essential for the homeostasis of the CD4+CD25+ immunoregulatory T cells that control autoimmune diabetes. *Immunity* (2000) doi:10.1016/S1074-7613(00)80195-8.
53. Tai, X., Cowan, M., Feigenbaum, L. & Singer, A. CD28 costimulation of developing thymocytes induces Foxp3 expression and regulatory T cell differentiation independently of interleukin 2. *Nat. Immunol.* (2005)

doi:10.1038/ni1160.
54. Lio, C.-W. J., Dodson, L. F., Deppong, C. M., Hsieh, C.-S. & Green, J. M. CD28 Facilitates the Generation of Foxp3 − Cytokine Responsive Regulatory T Cell Precursors . *J. Immunol.* (2010) doi:10.4049/jimmunol.1000019.
55. Kishimoto, H. & Sprent, J. Several different cell surface molecules control negative selection of medullary thymocytes. *J. Exp. Med.* (1999) doi:10.1084/jem.190.1.65.
56. Pobezinsky, L. A. *et al.* Clonal deletion and the fate of autoreactive thymocytes that survive negative selection. *Nat. Immunol.* (2012) doi:10.1038/ni.2292.
57. Watanabe, M., Lu, Y., Breen, M. & Hodes, R. J. B7-CD28 co-stimulation modulates central tolerance via thymic clonal deletion and Treg generation through distinct mechanisms. *Nat. Commun.* (2020) doi:10.1038/s41467-020-20070-x.
58. Mahmud, S. A. *et al.* Costimulation via the tumor-necrosis factor receptor superfamily couples TCR signal strength to the thymic differentiation of regulatory T cells. *Nat. Immunol.* (2014) doi:10.1038/ni.2849.
59. van Loosdregt, J. & Coffer, P. J. Post-translational modification networks regulating FOXP3 function. *Trends in Immunology* (2014) doi:10.1016/j.it.2014.06.005.
60. Yang, X. & Qian, K. Protein O-GlcNAcylation: Emerging mechanisms and functions. *Nature Reviews Molecular Cell Biology* (2017) doi:10.1038/nrm.2017.22.
61. Breed, E. R., Lee, S. T. & Hogquist, K. A. Directing T cell fate: How thymic antigen presenting cells coordinate thymocyte selection. *Seminars in Cell and Developmental Biology* (2018) doi:10.1016/j.semcdb.2017.07.045.
62. Anderson, M. S. & Su, M. A. AIRE expands: New roles in immune tolerance and beyond. *Nature Reviews Immunology* (2016) doi:10.1038/nri.2016.9.
63. Hu, Z., Lancaster, J. N. & Ehrlich, L. I. R. The contribution of chemokines and migration to the induction of central tolerance in the thymus. *Frontiers in Immunology* (2015) doi:10.3389/fimmu.2015.00398.
64. Lei, Y. *et al.* Aire-dependent production of XCL1 mediates medullary accumulation of thymic dendritic cells and contributes to regulatory T cell development. *J. Exp. Med.* (2011) doi:10.1084/jem.20102327.
65. Baba, T., Nakamoto, Y. & Mukaida, N. Crucial Contribution of Thymic Sirpα + Conventional Dendritic Cells to Central Tolerance against Blood-Borne Antigens in a CCR2-Dependent Manner . *J. Immunol.* (2009) doi:10.4049/jimmunol.0900438.
66. Perera, J. *et al.* Self-Antigen-Driven Thymic B Cell Class Switching Promotes T Cell Central Tolerance. *Cell Rep.* (2016) doi:10.1016/j.celrep.2016.09.011.
67. Esashi, E., Sekiguchi, T., Ito, H., Koyasu, S. & Miyajima, A. Cutting Edge: A Possible Role for CD4 + Thymic Macrophages as Professional Scavengers of Apoptotic Thymocytes . *J. Immunol.* (2003) doi:10.4049/jimmunol.171.6.2773.
68. Tacke, R. *et al.* The transcription factor NR4A1 is essential for the development of a novel macrophage subset in the thymus. *Sci. Rep.* (2015) doi:10.1038/srep10055.
69. Guilliams, M. *et al.* Dendritic cells, monocytes and macrophages: A unified nomenclature based on ontogeny. *Nature Reviews Immunology* (2014) doi:10.1038/nri3712.
70. Vobořil, M. *et al.* Toll-like receptor signaling in thymic epithelium controls

monocyte-derived dendritic cell recruitment and Treg generation. *Nat. Commun.* (2020) doi:10.1038/s41467-020-16081-3.
71. Ardouin, L. *et al.* Broad and Largely Concordant Molecular Changes Characterize Tolerogenic and Immunogenic Dendritic Cell Maturation in Thymus and Periphery. *Immunity* (2016) doi:10.1016/j.immuni.2016.07.019.
72. Watanabe, N. *et al.* Hassall's corpuscles instruct dendritic cells to induce CD4 +CD25+ regulatory T cells in human thymus. *Nature* (2005) doi:10.1038/nature03886.
73. Hanabuchi, S. *et al.* Thymic Stromal Lymphopoietin-Activated Plasmacytoid Dendritic Cells Induce the Generation of FOXP3 + Regulatory T Cells in Human Thymus . *J. Immunol.* (2010) doi:10.4049/jimmunol.0804106.
74. Park, J. E. *et al.* A cell atlas of human thymic development defines T cell repertoire formation. *Science (80-.).* (2020) doi:10.1126/science.aay3224.
75. Roche, P. A. & Furuta, K. The ins and outs of MHC class II-mediated antigen processing and presentation. *Nature Reviews Immunology* (2015) doi:10.1038/nri3818.
76. Steimle, V., Siegrist, C. A., Mottet, A., Lisowska-Grospierre, B. & Mach, B. Regulation of MHC class II expression by interferon-γ mediated by the transactivator gene CIITA. *Science (80-.).* (1994) doi:10.1126/science.8016643.
77. Meissner, T. B., Li, A. & Kobayashi, K. S. NLRC5: A newly discovered MHC class I transactivator (CITA). *Microbes and Infection* (2012) doi:10.1016/j.micinf.2011.12.007.
78. Schmid, D., Pypaert, M. & Münz, C. Antigen-Loading Compartments for Major Histocompatibility Complex Class II Molecules Continuously Receive Input from Autophagosomes. *Immunity* (2007) doi:10.1016/j.immuni.2006.10.018.
79. Deretic, V. & Levine, B. Autophagy balances inflammation in innate immunity. *Autophagy* (2018) doi:10.1080/15548627.2017.1402992.
80. Früh, K. & Yang, Y. Antigen presentation by MHC class I and its regulation by interferon γ. *Curr. Opin. Immunol.* (1999) doi:10.1016/S0952-7915(99)80014-4.
81. Vyas, J. M., Van Der Veen, A. G. & Ploegh, H. L. The known unknowns of antigen processing and presentation. *Nature Reviews Immunology* (2008) doi:10.1038/nri2368.
82. Blum, J. S., Wearsch, P. A. & Cresswell, P. Pathways of antigen processing. *Annual Review of Immunology* (2013) doi:10.1146/annurev-immunol-032712-095910.
83. Ito, T. *et al.* Differential Regulation of Human Blood Dendritic Cell Subsets by IFNs. *J. Immunol.* (2001) doi:10.4049/jimmunol.166.5.2961.
84. Montoya, M. *et al.* Type I interferons produced by dendritic cells promote their phenotypic and functional activation. *Blood* (2002) doi:10.1182/blood.V99.9.3263.
85. Paquette, R. L. *et al.* Interferon-α and granulocyte-macrophage colony-stimulating factor differentiate peripheral blood monocytes into potent antigen-presenting cells. *J. Leukoc. Biol.* (1998) doi:10.1002/jlb.64.3.358.
86. Schiavoni, G., Mattei, F. & Gabriele, L. Type I interferons as stimulators of DC-mediated cross-priming: Impact on anti-tumor response. *Frontiers in Immunology* (2013) doi:10.3389/fimmu.2013.00483.
87. Diamond, M. S. *et al.* Type I interferon is selectively required by dendritic cells for immune rejection of tumors. *J. Exp. Med.* (2011) doi:10.1084/jem.20101158.
88. Spadaro, F. *et al.* IFN-α enhances cross-presentation in human dendritic cells by

modulating antigen survival, endocytic routing, and processing. *Blood* (2012) doi:10.1182/blood-2011-06-363564.
89. Le Bon, A. & Tough, D. F. Type I interferon as a stimulus for cross-priming. *Cytokine Growth Factor Rev.* (2008) doi:10.1016/j.cytogfr.2007.10.007.
90. Le Bon, A. *et al.* Cross-priming of CD8+ T cells stimulated by virus-induced type I interferon. *Nat. Immunol.* (2003) doi:10.1038/ni978.
91. Le Bon, A. *et al.* Direct Stimulation of T Cells by Type I IFN Enhances the CD8 + T Cell Response during Cross-Priming . *J. Immunol.* (2006) doi:10.4049/jimmunol.176.8.4682.
92. Freudenburg, W., Gautam, M. & Chakraborty, P. Immunoproteasome Activation During Early Antiviral Response in Mouse Pancreatic β-cells: New Insights into Auto-antigen Generation in Type I Diabetes? *J. Clin. Cell. Immunol.* (2013) doi:10.4172/2155-9899.1000141.
93. Ebstein, F. *et al.* Maturation of human dendritic cells is accompanied by functional remodelling of the ubiquitin-proteasome system. *Int. J. Biochem. Cell Biol.* (2009) doi:10.1016/j.biocel.2008.10.023.
94. Yao, Y. & Qian, Y. Expression regulation and function of NLRC5. *Protein and Cell* (2013) doi:10.1007/s13238-012-2109-3.
95. Simmons, D. P. *et al.* Type I IFN Drives a Distinctive Dendritic Cell Maturation Phenotype That Allows Continued Class II MHC Synthesis and Antigen Processing. *J. Immunol.* (2012) doi:10.4049/jimmunol.1101313.
96. Padovan, E., Spagnoli, G. C., Ferrantini, M. & Heberer, M. IFN-alpha2a induces IP-10/CXCL10 and MIG/CXCL9 production in monocyte-derived dendritic cells and enhances their capacity to attract and stimulate CD8+ effector T cells. *J. Leukoc. Biol.* (2002) doi:10.1189/jlb.71.4.669.
97. Schmeisser, H., Bekisz, J. & Zoon, K. C. New function of Type i IFN: Induction of autophagy. *Journal of Interferon and Cytokine Research* (2014) doi:10.1089/jir.2013.0128.
98. Xu, D. *et al.* Modification of BECN1 by ISG15 plays a crucial role in autophagy regulation by type I IFN/ interferon. *Autophagy* (2015) doi:10.1080/15548627.2015.1023982.
99. Le Bon, A. *et al.* Type I interferons potently enhance humoral immunity and can promote isotype switching by stimulating dendritic cells in vivo. *Immunity* (2001) doi:10.1016/S1074-7613(01)00126-1.
100. Litinskiy, M. B. *et al.* DCs induce CD40-independent immunoglobulin class switching through BLyS and APRIL. *Nat. Immunol.* (2002) doi:10.1038/ni829.
101. Le Bon, A. *et al.* Cutting Edge: Enhancement of Antibody Responses Through Direct Stimulation of B and T Cells by Type I IFN. *J. Immunol.* (2006) doi:10.4049/jimmunol.176.4.2074.
102. Lazear, H. M., Schoggins, J. W. & Diamond, M. S. Shared and Distinct Functions of Type I and Type III Interferons. *Immunity* (2019) doi:10.1016/j.immuni.2019.03.025.
103. Ye, L., Schnepf, D. & Staeheli, P. Interferon-λ orchestrates innate and adaptive mucosal immune responses. *Nature Reviews Immunology* (2019) doi:10.1038/s41577-019-0182-z.
104. Hemann, E. A. *et al.* Interferon-λ modulates dendritic cells to facilitate T cell immunity during infection with influenza A virus. *Nat. Immunol.* (2019) doi:10.1038/s41590-019-0408-z.
105. Makjaroen, J. *et al.* Comprehensive proteomics identification of IFNλ3-regulated

antiviral proteins in HBV-transfected cells. *Mol. Cell. Proteomics* (2018) doi:10.1074/mcp.RA118.000735.
106. Spencer, C. T. *et al.* Viral infection causes a shift in the self peptide repertoire presented by human MHC class I molecules. *Proteomics - Clin. Appl.* (2015) doi:10.1002/prca.201500106.
107. Burchill, M. A., Yang, J., Vogtenhuber, C., Blazar, B. R. & Farrar, M. A. IL-2 Receptor β-Dependent STAT5 Activation Is Required for the Development of Foxp3 + Regulatory T Cells . *J. Immunol.* (2007) doi:10.4049/jimmunol.178.1.280.
108. Burchill, M. A. *et al.* Linked T Cell Receptor and Cytokine Signaling Govern the Development of the Regulatory T Cell Repertoire. *Immunity* (2008) doi:10.1016/j.immuni.2007.11.022.
109. Lio, C. W. J. & Hsieh, C. S. A Two-Step Process for Thymic Regulatory T Cell Development. *Immunity* (2008) doi:10.1016/j.immuni.2007.11.021.
110. Fontenot, J. D., Gavin, M. A. & Rudensky, A. Y. Foxp3 programs the development and function of CD4+CD25+ regulatory T cells. *J. Immunol.* (2017) doi:10.1038/ni904.
111. Hori, S., Nomura, T. & Sakaguchi, S. Control of regulatory T cell development by the transcription factor Foxp3. *J. Immunol.* (2017) doi:10.1126/science.1079490.
112. Khattri, R., Cox, T., Yasayko, S. A. & Ramsdell, F. An essential role for Scurfin in CD4+CD25+T regulatory cells. *J. Immunol.* (2017) doi:10.1038/ni909.
113. Wan, Y. Y. & Flavell, R. A. Regulatory T-cell functions are subverted and converted owing to attenuated Foxp3 expression. *Nature* (2007) doi:10.1038/nature05479.
114. Williams, L. M. & Rudensky, A. Y. Maintenance of the Foxp3-dependent developmental program in mature regulatory T cells requires continued expression of Foxp3. *Nat. Immunol.* (2007) doi:10.1038/ni1437.
115. Bailey-Bucktrout, S. L. & Bluestone, J. A. Regulatory T cells: Stability revisited. *Trends in Immunology* (2011) doi:10.1016/j.it.2011.04.002.
116. Hori, S. Lineage stability and phenotypic plasticity of Foxp3+ regulatory T cells. *Immunol. Rev.* (2014) doi:10.1111/imr.12175.
117. Li, X. & Zheng, Y. Regulatory T cell identity: Formation and maintenance. *Trends in Immunology* (2015) doi:10.1016/j.it.2015.04.006.
118. Cretney, E., Kallies, A. & Nutt, S. L. Differentiation and function of Foxp3+ effector regulatory T cells. *Trends in Immunology* (2013) doi:10.1016/j.it.2012.11.002.
119. Levine, A. G., Arvey, A., Jin, W. & Rudensky, A. Y. Continuous requirement for the TCR in regulatory T cell function. *Nat. Immunol.* (2014) doi:10.1038/ni.3004.
120. Vahl, J. C. *et al.* Continuous T Cell Receptor Signals Maintain a Functional Regulatory T Cell Pool. *Immunity* (2014) doi:10.1016/j.immuni.2014.10.012.
121. Chinen, T. *et al.* An essential role for the IL-2 receptor in T reg cell function. *Nat. Immunol.* (2016) doi:10.1038/ni.3540.
122. Hart, G. W., Housley, M. P. & Slawson, C. Cycling of O-linked β-N-acetylglucosamine on nucleocytoplasmic proteins. *Nature* (2007) doi:10.1038/nature05815.
123. Ruan, H. Bin, Singh, J. P., Li, M. D., Wu, J. & Yang, X. Cracking the O-GlcNAc code in metabolism. *Trends in Endocrinology and Metabolism* (2013) doi:10.1016/j.tem.2013.02.002.
124. Hanover, J. A., Krause, M. W. & Love, D. C. Bittersweet memories: Linking

metabolism to epigenetics through O-GlcNAcylation. *Nature Reviews Molecular Cell Biology* (2012) doi:10.1038/nrm3334.
125. Ruan, H. Bin *et al.* O-GlcNAc transferase enables AgRP neurons to suppress browning of white fat. *Cell* (2014) doi:10.1016/j.cell.2014.09.010.
126. Ruan, H. Bin *et al.* O-GlcNAc transferase/host cell factor C1 complex regulates gluconeogenesis by modulating PGC-1α stability. *Cell Metab.* (2012) doi:10.1016/j.cmet.2012.07.006.
127. Ruan, H. Bin, Nie, Y. & Yang, X. Regulation of protein degradation by O-GlcNAcylation: Crosstalk with ubiquitination. *Molecular and Cellular Proteomics* (2013) doi:10.1074/mcp.R113.029751.
128. Kearse, K. P. & Hart, G. W. Lymphocyte activation induces rapid changes in nuclear and cytoplasmic glycoproteins. *Proc. Natl. Acad. Sci. U. S. A.* (1991) doi:10.1073/pnas.88.5.1701.
129. O'Donnell, N., Zachara, N. E., Hart, G. W. & Marth, J. D. Ogt-Dependent X-Chromosome-Linked Protein Glycosylation Is a Requisite Modification in Somatic Cell Function and Embryo Viability. *Mol. Cell. Biol.* (2004) doi:10.1128/mcb.24.4.1680-1690.2004.
130. Swamy, M. *et al.* Glucose and glutamine fuel protein O-GlcNAcylation to control T cell self-renewal and malignancy. *Nat. Immunol.* (2016) doi:10.1038/ni.3439.
131. Chen, Z. *et al.* The ubiquitin ligase stub1 negatively modulates regulatory T cell suppressive activity by promoting degradation of the transcription factor Foxp3. *Immunity* (2013) doi:10.1016/j.immuni.2013.08.006.
132. vanLoosdregt, J. *et al.* Stabilization of the transcription factor Foxp3 by the deubiquitinase USP7 increases treg-cell-suppressive capacity. *Immunity* (2013) doi:10.1016/j.immuni.2013.05.018.
133. Madisen, L. *et al.* A robust and high-throughput Cre reporting and characterization system for the whole mouse brain. *Nat. Neurosci.* (2010) doi:10.1038/nn.2467.
134. Zeng, H. *et al.* MTORC1 couples immune signals and metabolic programming to establish T reg-cell function. *Nature* (2013) doi:10.1038/nature12297.
135. Cheng, G. *et al.* IL-2 Receptor Signaling Is Essential for the Development of Klrg1 + Terminally Differentiated T Regulatory Cells . *J. Immunol.* (2012) doi:10.4049/jimmunol.1103768.
136. Francisco, L. M., Sage, P. T. & Sharpe, A. H. The PD-1 pathway in tolerance and autoimmunity. *Immunological Reviews* (2010) doi:10.1111/j.1600-065X.2010.00923.x.
137. Antonioli, L., Pacher, P., Vizi, E. S. & Haskó, G. CD39 and CD73 in immunity and inflammation. *Trends in Molecular Medicine* (2013) doi:10.1016/j.molmed.2013.03.005.
138. Arvey, A. *et al.* Inflammation-induced repression of chromatin bound by the transcription factor Foxp3 in regulatory T cells. *Nat. Immunol.* (2014) doi:10.1038/ni.2868.
139. Cretney, E. *et al.* The transcription factors Blimp-1 and IRF4 jointly control the differentiation and function of effector regulatory T cells. *Nat. Immunol.* (2011) doi:10.1038/ni.2006.
140. Boyman, O., Kovar, M., Rubinstein, M. P., Surh, C. D. & Sprent, J. Selective stimulation of T cell subsets with antibody-cytokine immune complexes. *Science (80-.).* (2006) doi:10.1126/science.1122927.
141. Freund, P. *et al.* O-GlcNAcylation of STAT5 controls tyrosine phosphorylation

and oncogenic transcription in STAT5-dependent malignancies. *Leukemia* (2017) doi:10.1038/leu.2017.4.
142. Yao, Z. *et al.* Nonredundant roles for Stat5a/b in directly regulating Foxp. *Blood* (2007) doi:10.1182/blood-2006-11-055756.
143. Singer, B. D., King, L. S. & D'Alessio, F. R. Regulatory T cells as immunotherapy. *Frontiers in Immunology* (2014) doi:10.3389/fimmu.2014.00046.
144. Blazar, B. R., MacDonald, K. P. A. & Hill, G. R. Immune regulatory cell infusion for graft-versus-host disease prevention and therapy. *Blood* (2018) doi:10.1182/blood-2017-11-785865.
145. Yuzwa, S. A. *et al.* A potent mechanism-inspired O-GlcNAcase inhibitor that blocks phosphorylation of tau in vivo. *Nat. Chem. Biol.* (2008) doi:10.1038/nchembio.96.
146. Hippen, K. L. *et al.* Massive ex vivo expansion of human natural regulatory T cells (T regs) with minimal loss of in vivo functional activity. *Sci. Transl. Med.* (2011) doi:10.1126/scitranslmed.3001809.
147. Lin, W. *et al.* Regulatory T cell development in the absence of functional Foxp3. *Nat. Immunol.* (2007) doi:10.1038/ni1445.
148. Van Loosdregt, J. *et al.* Regulation of Treg functionality by acetylation-mediated Foxp3 protein stabilization. *Blood* (2010) doi:10.1182/blood-2009-02-207118.
149. van Loosdregt, J. *et al.* Rapid temporal control of foxp3 protein degradation by sirtuin-1. *PLoS One* (2011) doi:10.1371/journal.pone.0019047.
150. Dang, E. V. *et al.* Control of TH17/Treg balance by hypoxia-inducible factor 1. *Cell* (2011) doi:10.1016/j.cell.2011.07.033.
151. Lund, P. J., Elias, J. E. & Davis, M. M. Global Analysis of O -GlcNAc Glycoproteins in Activated Human T Cells . *J. Immunol.* (2016) doi:10.4049/jimmunol.1502031.
152. Woo, C. M. *et al.* Mapping and quantification of over 2000 O-linked glycopeptides in activated human T cells with isotope-targeted glycoproteomics (Isotag). *Mol. Cell. Proteomics* (2018) doi:10.1074/mcp.RA117.000261.
153. Lopez Aguilar, A. *et al.* Profiling of Protein O-GlcNAcylation in Murine CD8+ Effector- and Memory-like T Cells. *ACS Chem. Biol.* (2017) doi:10.1021/acschembio.7b00869.
154. Procaccini, C. *et al.* The Proteomic Landscape of Human Ex Vivo Regulatory and Conventional T Cells Reveals Specific Metabolic Requirements. *Immunity* (2016) doi:10.1016/j.immuni.2016.01.028.
155. Duguet, F. *et al.* Proteomic analysis of regulatory T cells reveals the importance of Themis1 in the control of their suppressive function. *Mol. Cell. Proteomics* (2017) doi:10.1074/mcp.M116.062745.
156. Galgani, M., De Rosa, V., La Cava, A. & Matarese, G. Role of Metabolism in the Immunobiology of Regulatory T Cells. *J. Immunol.* (2016) doi:10.4049/jimmunol.1600242.
157. Wang, R. *et al.* The Transcription Factor Myc Controls Metabolic Reprogramming upon T Lymphocyte Activation. *Immunity* (2011) doi:10.1016/j.immuni.2011.09.021.
158. Ruan, H. Bin *et al.* Calcium-dependent O-GlcNAc signaling drives liver autophagy in adaptation to starvation. *Genes Dev.* (2017) doi:10.1101/gad.305441.117.
159. Marson, A. *et al.* Foxp3 occupancy and regulation of key target genes during T-cell stimulation. *Nature* (2007) doi:10.1038/nature05478.

160. Chen, C., Rowell, E. A., Thomas, R. M., Hancock, W. W. & Wells, A. D. Transcriptional regulation by Foxp3 is associated with direct promoter occupancy and modulation of histone acetylation. *J. Biol. Chem.* (2006) doi:10.1074/jbc.M608848200.
161. Taams, L. S. *et al.* Regulatory T cells in human disease and their potential for therapeutic manipulation. *Immunology* (2006) doi:10.1111/j.1365-2567.2006.02348.x.
162. Cools, N., Ponsaerts, P., Van Tendeloo, V. F. I. & Berneman, Z. N. Regulatory T cells and human disease. *Clinical and Developmental Immunology* (2007) doi:10.1155/2007/89195.
163. Fantini, M. C., Dominitzki, S., Rizzo, A., Neurath, M. F. & Becker, C. In vitro generation of cd4+cd25+ regulatory cells from murine naive t cells. *Nat. Protoc.* (2007) doi:10.1038/nprot.2007.258.
164. Hippen, K. L. *et al.* Umbilical cord blood regulatory T-cell expansion and functional effects of tumor necrosis factor receptor family members OX40 and 4-1BB expressed on artificial antigen-presenting cells. *Blood* (2008) doi:10.1182/blood-2008-01-132951.
165. Hippen, K. L. *et al.* In Vitro Induction of Human Regulatory T Cells Using Conditions of Low Tryptophan Plus Kynurenines. *Am. J. Transplant.* (2017) doi:10.1111/ajt.14338.
166. Liu, G. *et al.* The receptor S1P1 overrides regulatory T cell-mediated immune suppression through Akt-mTOR. *Nat. Immunol.* (2009) doi:10.1038/ni.1743.
167. Baker, P. R. & Chalkley, R. J. MS-Viewer: A web-based spectral viewer for proteomics results. *Mol. Cell. Proteomics* (2014) doi:10.1074/mcp.O113.037200.
168. Ivashkiv, L. B. & Donlin, L. T. Regulation of type i interferon responses. *Nature Reviews Immunology* (2014) doi:10.1038/nri3581.
169. Xing, Y., Wang, X., Jameson, S. C. & Hogquist, K. a. Late stages of T cell maturation in the thymus involve NF-κB and tonic type I interferon signaling. *Nat. Immunol.* **9**, 1–10 (2016).
170. Otero, D. C., Baker, D. P. & David, M. IRF7-Dependent IFN-β Production in Response to RANKL Promotes Medullary Thymic Epithelial Cell Development. *J. Immunol.* (2013) doi:10.4049/jimmunol.1203086.
171. Lienenklaus, S. *et al.* Novel Reporter Mouse Reveals Constitutive and Inflammatory Expression of IFN-β In Vivo. *J. Immunol.* (2009) doi:10.4049/jimmunol.0804277.
172. Hemmers, S. *et al.* IL-2 production by self-reactive CD4 thymocytes scales regulatory T cell generation in the thymus. *J. Exp. Med.* (2019) doi:10.1084/jem.20190993.
173. Ardouin, L. *et al.* Broad and Largely Concordant Molecular Changes Characterize Tolerogenic and Immunogenic Dendritic Cell Maturation in Thymus and Periphery. *Immunity* (2016) doi:10.1016/j.immuni.2016.07.019.
174. Rossi, S. W. *et al.* RANK signals from CD4+3- inducer cells regulate development of Aire-expressing epithelial cells in the thymic medulla. *J. Exp. Med.* (2007) doi:10.1084/jem.20062497.
175. Hikosaka, Y. *et al.* The Cytokine RANKL Produced by Positively Selected Thymocytes Fosters Medullary Thymic Epithelial Cells that Express Autoimmune Regulator. *Immunity* (2008) doi:10.1016/j.immuni.2008.06.018.
176. Akiyama, T. *et al.* The Tumor Necrosis Factor Family Receptors RANK and CD40 Cooperatively Establish the Thymic Medullary Microenvironment and Self-

Tolerance. *Immunity* (2008) doi:10.1016/j.immuni.2008.06.015.
177. Desanti, G. E. *et al.* Developmentally Regulated Availability of RANKL and CD40 Ligand Reveals Distinct Mechanisms of Fetal and Adult Cross-Talk in the Thymus Medulla. *J. Immunol.* (2012) doi:10.4049/jimmunol.1201815.
178. Derbinski, J., Pinto, S., Rösch, S., Hexel, K. & Kyewski, B. Promiscuous gene expression patterns in single medullary thymic epithelial cells argue for a stochastic mechanism. *Proc. Natl. Acad. Sci. U. S. A.* (2008) doi:10.1073/pnas.0707486105.
179. Villaseñor, J., Besse, W., Benoist, C. & Mathis, D. Ectopic expression of peripheral-tissue antigens in the thymic epithelium: Probabilistic, monoallelic, misinitiated. *Proc. Natl. Acad. Sci. U. S. A.* (2008) doi:10.1073/pnas.0808069105.
180. Uccellini, M. B. & García-Sastre, A. ISRE-Reporter Mouse Reveals High Basal and Induced Type I IFN Responses in Inflammatory Monocytes. *Cell Rep.* (2018) doi:10.1016/j.celrep.2018.11.030.
181. Mordstein, M. *et al.* Interferon-λ contributes to innate immunity of mice against influenza A virus but not against hepatotropic viruses. *PLoS Pathog.* (2008) doi:10.1371/journal.ppat.1000151.
182. Mostafavi, S. *et al.* Parsing the Interferon Transcriptional Network and Its Disease Associations. *Cell* **164**, 564–578 (2016).
183. Gough, D. J., Messina, N. L., Clarke, C. J. P., Johnstone, R. W. & Levy, D. E. Constitutive Type I Interferon Modulates Homeostatic Balance through Tonic Signaling. *Immunity* vol. 36 166–174 (2012).
184. McNab, F., Mayer-Barber, K., Sher, A., Wack, A. & O'Garra, A. Type I interferons in infectious disease. *Nature Reviews Immunology* (2015) doi:10.1038/nri3787.
185. Stoeckius, M. *et al.* Cell Hashing with barcoded antibodies enables multiplexing and doublet detection for single cell genomics. *Genome Biol.* (2018) doi:10.1186/s13059-018-1603-1.
186. Sunshine, A. *et al.* Ets1 Controls the Development of B Cell Autoimmune Responses in a Cell-Intrinsic Manner. *ImmunoHorizons* (2019) doi:10.4049/immunohorizons.1900033.
187. Sidwell, T. & Kallies, A. Bach2 is required for B cell and T cell memory differentiation. *Nature Immunology* (2016) doi:10.1038/ni.3493.
188. Benhammadi, M. *et al.* IFN-λ Enhances Constitutive Expression of MHC Class I Molecules on Thymic Epithelial Cells. *J. Immunol.* (2020) doi:10.4049/jimmunol.2000225.
189. Fuchs, S. Y. Hope and fear for interferon: The receptor-centric outlook on the future of interferon therapy. *Journal of Interferon and Cytokine Research* (2013) doi:10.1089/jir.2012.0117.
190. Hemann, E. A., Gale, M. & Savan, R. Interferon lambda genetics and biology in regulation of viral control. *Front. Immunol.* (2017) doi:10.3389/fimmu.2017.01707.
191. Deonarain, R. *et al.* Impaired Antiviral Response and Alpha/Beta Interferon Induction in Mice Lacking Beta Interferon. *J. Virol.* (2000) doi:10.1128/jvi.74.7.3404-3409.2000.
192. Xing, Y. & Hogquist, K. A. Isolation, identification, and purification of murine thymic epithelial cells. *J. Vis. Exp.* (2014) doi:10.3791/51780.